SYNTHESIS AND CHARACTERIZATION OF COBALT AND COPPER SULFIDE NANOPARTICLES WITH REPRODUCIBLE STOICHIOMETRY USING SULFUR CONTAINING SINGLE-SOURCE PRECURSORS

BY

SIMON BONGINKOSI SIBOKOZA

DISSERTATION SUBMITTED IN PARTIAL FULFILMENT OF THE REQUIREMENT FOR THE DEGREE MAGISTER TECHNOLOGIAE IN THE FACULTY OF APPLIED AND COMPUTER SCIENCES AT VAAL UNIVERSITY OF TECHNOLOGY

SUPERVISOR: PROF M.J. MOLOTO

CO-SUPERVISOR: DR N. MOLOTO

ACADEMICYEAR 2012

DECLARATION STATEMENT

I hereby declare that the work on "Synthesis and characterization of cobalt and copper sulfide nanoparticles with reproducible stoichiometry using sulfur containing single-source precursors" is my work and all sources used are acknowledged by referencing.

S.B. SIBOKOZA (211080837)

……Date:……...

Supervisor: Prof M.J. Moloto

……Date:…….

ACKNOWLEDGEMENTS

I would like to pass my gratitude to my supervisors Prof M.J. and Dr N. Moloto for their guidance, motivation and support. I would also like to thank them for the opportunities they presented to me, that helped me in so many ways. As supervisors, you believed in me even when I don`t believe in myself. A special thanks goes to the group members: Dr. P.M. Shumbula, Ms. Nobathembu Faleni, Mr. Mbuso Mlambo, Mr. Ben Rakgalakane, Mr. Manuel Mashavhela, Ms. Thandeka Mthethwa, Ms. Phindile Khoza, and Ms. Maulusi Nelwamondo.

My heartfelt gratitude goes to my family; parents Mr. Sikhumbuzo (father), and Mrs. Nomziwakhe (mother) Sibokoza; brothers: Luthando, Luvuko, Zibele, and Enzokuhle; sisters: Nolizwi, Ncebakazi and Liza. I cannot find words that can express how important you are to my life. A special thanks to my academic friends: Zolile Mtumela, Bhekisa Mzimkulu, Lamla Thungatha, Lungisa Bitsha, Siyasanga Mpelane, Kwindla Nobaza, and Mzekelo Loyilane. You all shape my life one way or another to be a success.

I am grateful of Vaal University of Technology and University of Johannesburg for allowing me to do my studies at your premises. A sincere thanks to CSIR (National Centre for Nanostructured Materials), Wits University, and Tshwane University of Technology, for allowing me to use their facilities for characterization of the samples of the study. My thanks also go to VUT (Hub and Spokes funding) and NRF for their generous financial support. I would like to thank everyone who has interacted with me one way or another during my academic development. Above all, I would like to thank infinite that provided me with everything.

TABLE OF CONTENTS

TITLE PAGE ……..i

DECLARATION STATEMENT…….……ii

ACKNOWLEDGEMENTS…….…...iii

TABLE OF CONTENTS…….....iv-vii

LIST OF TABLES…….....…viii-ix

LIST OF FIGURES…….x-xii

LIST OF ABBREVIATIONS…….……....xiii-xiv

ABSTRACT…….....xv

PRESENTATION AND PUBLICATIONS……...……..…xvi

CHAPTER ONE: LITERATURE REVIEW OF NANOPARTICLES...……...……...……1

1.1 General background of nanoparticles……...…….……2

1.2 Properties of semiconductor nanoparticles…….…...3

1.2.1 Optical properties of semiconductor nanoparticles……...3

1.3 Synthesis of semiconductor nanoparticles…….…6

1.3.1 Chemical precipitation method…….…...6

1.3.2 Synthesis in confined matrices…….8

1.3.3 Metal-organic routes……...10

1.3.4 Hydrothermal and solvothermalmethods……....12

1.3.5 Single-source precursor method……14

1.4 Applications of semiconductor nanoparticles……..…....15

1.5 Aim and objectives of the thesis…….…...17

CHAPTER TWO: SYNTHESIS AND CHARACTERIZATION OF DIETHYLDITHIOCARBAMATE AND TETRAMETHYLTHIURAM DISULFIDE COMPLEXES OF COBALT AND COPPER……..…..…..…19

2.1 General background……...…….…….…....20

2.2 Experimental section……..……...24

2.2.1 Materials…….…….…….24

2.2.2 Instrumentation…….....…….....25

2.2.2 (a) Thermogravimetry……...…….…….25

2.2.2 (b) NMR spectroscopy……..…….…..……24

2.2.2 (c) FT-IR spectroscopy……..25

2.2.2 (d) Microanalysis.……25

2.2.3 Preparation of the complexes…….25

2.2.3 (a) $[CoCl_2((CH_3)_2NCS(S)SC(S)N(CH_3)_2)_2]$ I……...……...…26

2.2.3 (b) $[Co(CH_3CH_2)_2NCS(S))_2]$ II……...……26

2.2.3 (c) $CuCl_2((CH_3)_2NCS(S)SC(S)N(CH_3)_2)_2]$ III……...…….…27

2.2.3 (d) $[Co(CH_3CH_2)_2NCS(S))_2]$ IV...…….…..27

2.3 Results and discussion……...…….....28

2.3.1 Synthesis of the complexes…….…….……28

2.3.2 Spectroscopic studies…….……..29

2.3.3 Thermogravimetric studies…….32

2.4 Conclusion..……...……....33

CHAPTER THREE: SYNTHESIS AND CHARACTERIZATION OF COBALT SULFIDE NANOPARTICLES USING TETRAMETHYLTHIURAM DISULFIDE AND DIETHYLDITHIOCARBAMATE COMPLEXES OF COBALT……...……...…….35

3.1 Background……...……...……..……..……..……..……36

3.2 Experimental section……..…..……..37

3.2.1 Materials……...37

3.2.2 Instrumentation……..……....37

3.2.2 (a) Optical characterization……....37

3.2.2(b) X-ray diffraction analysis…….....……....37

3.2.2 (c) Electron microscopy……...37

3.2.3 Preparation of the nanoparticles……....38

3.2.3 (a) Preparation of cobalt sulfide using complex I……38

3.2.3 (b) Preparation of cobalt sulfide using complex II……..….38

3.3 Results and discussions.……39

3.3.1 Effect of concentration.……...39

3.3.1 (a) Nanoparticles prepared from complex I…..……....39

3.3.1 (b) Nanoparticles prepared from complex II.……..….45

3.3.2 Effect of temperature.……49

3.3.2 (a) Nanoparticles prepared from complex I……..……....50

3.3.2 (b) Nanoparticles prepared from complex II.……...……....52

3.3.3 Effect of time……...……55

3.3.3 (a) Nanoparticles prepared from complex I.……....56

3.3.3 (b) Nanoparticles prepared from complex II…..……...…….……..59

3.3 Conclusion…….…….....60

CHAPTER FOUR: SYNTHESIS AND CHARACTERIZATION OF COPPER SULFIDE NANOPARTICLES USING TETRAMETHYLTHIURAM DISULFIDE AND DIETHYLDITHIOCARBAMATE COMPLEXES OF COPPER..……..……..……...……..62

4.1 Background.……..…...…….……...…….63

4.2 Experimental……..……..…..…64

4.2.1 Materials……..…64

4.2.2 Instrumentation…….……..64

4.2.3 Preparation of the nanoparticles……..……..64

4.2.3 (a) Preparation of copper sulfide using complex III……64

4.2.3 (b) Preparation of copper sulfide using complex IV……65

4.3 Results and discussions.……65

4.3.1 Effect of concentration…….……..65

4.3.1 (a) Nanoparticles prepared from complex III.…….……66

4.3.1 (b) Nanoparticles prepared from complex IV…….…….69

4.3.2 Effect of temperature.……74

4.3.2 (a) Nanoparticles prepared from complex III…….……..74

4.3.2 (b) Nanoparticles prepared from complex IV…….…….78

4.3.3 Effect of time……...82

4.3.3 (a) Nanoparticles prepared from complex III.…….…83

4.3.3 (b) Nanoparticles prepared using complex IV…….……85

4.4 Conclusion....……...87

CHAPTER FIVE: CONCLUSION AND FUTURE WORK.....…….....89

5.1 Conclusion..……...……..90

5.2 Future work…….92

5.3 References……93

LIST OF TABLES

Table 2.1: IR spectra for the complexes **I–IV**…..……**30**

Table 2.2: ^{1}HNMR spectra for complexes **I–IV**.....……...……..**31**

Table 3.3.1: Variation of amount of the precursor used in the the preparation of Co_xS_y nanoparticles from complex **I**……**40**

Table 3.3.2: Absorption band edges and emission maxima of the cobalt sulfide nanoparticles prepared by variation of the amount of the precursor complex **I**.……**43**

Table 3.3.3: Variation of amount of the precursor used for the preparation of Co_xS_y nanoparticles using complex **II**...…….....**46**

Table 3.3.4: Variation of temperature used for the preparation of Co_xS_y nanoparticles from complex **I**..……..**50**

Table 3.3.5: Variation of temperature used for the preparation of Co_xS_y nanoparticles from complex **II**...……...**53**

Table 3.3.6: Variation of time for the preparation of Co_xS_y nanoparticles using complex **I**..…..**56**

Table 3.3.7: Variation of time for the preparation of Co_xS_y nanoparticles using complex **II**..…**59**

Table 4.3.1: Variation of amount of the precursor in the the preparation of Cu_xS_y *n*anoparticles from complex **III**…..……..**66**

Table 4.3.2: Variation of amount of the precursor in the the preparation of Cu_xS_ynanoparticles from complex **IV**...…….**69**

Table 4.3.3: Variation of temperature used for the preparation of Cu_xS_y nanoparticles from complex **III**...……**74**

Table 4.3.4: Variation of temperature used for the preparation of Cu_xS_y nanoparticles from complex **IV**..……**79**

Table 4.3.5: Variation of time for the preparation of Cu_xS_y nanoparticles using complex **III.....83**

Table 4.3.6: Variation of time for the preparation of Cu_xS_y nanoparticles using complex**IV....86**

LIST FIGURES

Figure 1.1: Electronic state diagram of the bulk, and quantum dot……**4**

Figure 2.1: Resonance structures of dithiocarbamate ligand……**20**

Figure 2.2: Resonance structures of thiuramdisulfide ligand……....**21**

Figure 2.3: Chemical structure for bis(chloro,N,N,N',N'-tetramethylthiuram disulfide)cobalt(II)/copper(II)…….....……**24**

Figure2.4: Chemical structure for bis(diethyldithiocarbamato)cobalt(II)/copper(II) complexes……...……**24**

Figure 2.5: IR spectra for (a) $[(CH_3)_2NCSS_2SCN(CH_3)_2]$ and (b) its cobalt complex……..**30**

Figure 2.6: ^{1}HNMR spectra for (a) $CoCl_2[(CH_3)_2NCSS_2SCN(CH_3)_2]_2$ and (b) $[(CH_3)_2NCSS_2SCN(CH_3)_2]$……**32**

Figure 2.7: TGA spectra of the complex **I**, **II**, **III** and **IV**……..…….....**33**

Figure 3.3.1: The absorption spectra of cobalt sulfide prepared by using various amount of the complex **I**: 1.0, (b) 0.5, (c) 0.1 and (d) 0.05 g……**41**

Figure 3.3.2: The emission spectra of cobalt sulfide prepared by using various amount of the complex **II**: (a) 1.0, (b) 0.5, (c) 0.1 and (d) 0.05 g……**42**

Figure 3.3.3: TEM images of cobalt sulfide prepared at 130 °C for 30 minutes in 5.0 g HDA by using various amount of the complex: (a) 1.0, (b) 0.5, (c) 0.1 and (d) 0.05 g……....**44**

Figure 3.3.4: XRD patterns of cobalt sulfide nanoparticles prepared at 130 °C for 30 minutes in 5.0 g HDA by using various amount of the complex: (a) 1.0, (b) 0.5, (c) 0.1 and (d) 0.05 g…....**45**

Figure 3.3.5: The absorption spectra of cobalt sulfide prepared at 130 °C for 30 minutes in 5.0 g HDA by using various amount of the complex: (a) 1.0, (b) 0.5, (c) 0.25 and (d) 0.125 g……..**47**

Figure 3.3.6: XRD pattern of $Co_{1-x}S$ nanoparticles prepared at 130 °C for 30 minutes and various amount of the complex II in 5.0 g HDA: (a) 1.0 g and (b) 0.125 g……...**48**

Figure 3.3.7: TEM images of cobalt sulfide prepared at 130 °C for 30 minutes and various amount of the complex in 5.0 g HDA: (a) 1.0 g, (b) 0.5 g, (c) 0.25 g and (d) 0.125 g**…….49**

Figure 3.3.8: Absorption spectra of cobalt sulfide prepared by using 0.5 g of the complex, 5.0 g of HDA, for 30 minutes at different temperature: (a) 80, (b) 130 and (c) 200 °C**……51**

Figure 3.3.9:TEM images of cobalt sulfide prepared by using 0.5 g of the complex, 5.0 g of HDA, for 30 minutes at different temperature: (a) 80, (b) 130, (c) 200 and (d) 250 °C**……...52**

Figure 3.3.10: Absorption spectra of cobalt sulfide prepared by using 0.5 g of the complex, 5.0 g of HDA, for 30 minutes at different temperature: (a) 80, (b) 200 and (c) 250 °C**……54**

Figure 3.3.11:TEM images of cobalt sulfide prepared by using 0.5 g of the complex, 5.0 g of HDA, for 30 minutes at different temperature: (a) 80, (b) 130, (c) 200 and (d) 250 °C**……...55**

Figure 3.3.12: Absorption spectra of cobalt sulfide prepared using 0.5 g of the complex in HDA (5.0 g), 130 °C and at various time interval of 5 min (5 – 30)**……57**

Figure 3.3.13: XRD pattern of cobalt sulfide prepared using 0.5 g of the complex in HDA (5.0 g), 130 °C and at various time interval of 5 min (5 – 30)**……..58**

Figure 3.3.14: Absorption spectra of cobalt sulfide prepared using 0.5 g of the complex in HDA: (5.0g), 130 °C and at various time interval of 5 min (5 – 30)**……60**

Figure 4.3.1: The absorption spectra of copper sulfide prepared at 130 °C for 30 minutes in 5.0 g HDA by using various amount of the complex: (a) 1.0, (b) 0.5, (c) 0.25 and (d) 0.125 g**……67**

Figure 4.3.2: XRD pattern of copper sulfide prepared at 130 °C for 30 minutes in 5.0 g HDA by using various amount of the complex: (a) 1.0, (b) 0.5, (c) 0.25 and (d) 0.125 g**……...68**

Figure 4.3.3:TEM images of copper sulfide prepared at 130 °C for 30 minutes and various amount of the complex in 5.0 g HDA: (a) 1.0 g, (b) 0.5 g, (c) 0.25 g, (d) 0.125 g**……...69**

Figure 4.3.4: The absorption spectra of copper sulfide prepared at 130 °C for 30 minutes in 5.0 g HDA by using various amount of the complex: (a) 1.0, (b) 0.5, (c) 0.25 and (d) 0.125 g**……71**

Figure 4.3.5: XRD pattern of copper sulfide prepared at 130 °C for 30 minutes in 5.0 g HDA by using various amount of the complex: (a) 1.0, (b) 0.5, (c) 0.25 and (d) 0.125 g**……...72**

Figure 4.3.6:TEM images of copper sulfide prepared at 130 °C for 30 minutes and various amount of the complex in 5.0 g HDA: (a) 1.0 g, (b) 0.5 g, (c) 0.25 g and (d) 0.125 g**……..73**

Figure 4.3.7: Absorption spectra of copper sulfide prepared by using 0.5 g of the complex, 5.0 g of HDA, for 30 minutes at different temperature (a) 80, (b) 130, (c) 200 and (d) 250 °C**…….75**

Figure 4.3.8:XRD pattern copper sulfide prepared by using 0.5 g of the complex, 5.0 g of HDA, for 30 minutes at different temperature (a) 80, (b) 130 and (c) 200 and (d) 250 °C**……..76**

Figure 4.3.9: TEM images of Cu_xS_y prepared by using 0.5 g of the complex, 5.0 g of HDA, for 30 minutes at different temperature (a) 80, (b) 130 , (c) 200 and (d) 250 °C**…….78**

Figure 4.3.10: Absorption spectra of copper sulfide prepared by using 0.5 g of the complex, 5.0 g of HDA, for 30 minutes at different temperature (a) 80, (b) 130 and (c) 250 °C**……....80**

Figure 4.3.11:XRD pattern of copper sulfide prepared by using 0.5 g of the complex, 5.0 g of HDA, for 30 minutes at different temperature (a) 80, (b) 130, (c) 200 and (d) 250 °C**…….81**

Figure 4.3.12:TEM images of copper sulfide prepared by using 0.5 g of the complex, 5.0 g of HDA, for 30 minutes at different temperature: (a) 80, (b) 130, (c) 200, and (d) 250 °C**……...82**

Figure 4.3.13: Absorptionspectra of copper sulfide nanoparticles prepared using 0.5 g of the complex in 5.0 g HDA, 130 °C and at various time intervals (5 – 30 minute)**……..84**

Figure 4.3.14: XRD pattern of copper sulfide nanoparticles prepared using 0.5 g of the complex in 5.0 g HDA, 130 °C and at various time intervals (5 – 30 minute)**…….85**

Figure 4.3.15: Absorptionspectra of copper sulfide nanoparticles prepared using 0.5 g of the complex in 5.0 g HDA, 130 °C and at various time intervals (5 – 30 minute)**……87**

LIST OF ABBREVIATIONS

Symbols and constants

a	lattice spacing
a.u	arbitrary units
°C	degree celsius
cm	centimeter
d	diameter
e	elementary charge
E	energy
E_g	band gap
eV	electron volts
h	Planck`s constant
h	hour(s)
m^*	effective mass (e = electron, h = hole)
nm	nanometer
QDs	quantum dots
R	radius
s	seconds
T	temperature
t	time
a_B	Bohr radius
ε	dielectric constant
λ_{exc}	excitation wavelength
ν	frequency

Instrumentation

FT-IR	Fourier transform infrared
NMR	Nuclear magnetic resonance
PL	Photoluminescence
TEM	Transmission electron microscopy
TGA	Thermogravimetric analysis
XRD	X-ray diffraction

Chemical reagents

AACVD	aerosol-assisted chemical vapour deposition
CVD	chemical vapour deposition
DTC	dithiocarbamates
HDA	hexadecylamine
LED	light-emitting diodes
LP-MOCVD	low-pressure metal-organic chemical vapour deposition
R_4tms	tetraalkylthiurammonosulfides
TOP	tri-n-octylphosphine
TOPS	tri-n-octylphosphine sulfide
TOPO	tri-n-octylphosphine oxide

ABSTRACT

COmplexes of alkyldithiocarbamate and thiuram have been extensively explored for various applications in the medical field. Thiuram and dithiocarbamate ligands were used to prepared complexes of cobalt and copper. The high abundance of sulfur in these ligands has resulted to be the preferred complexes for the synthesis of metal sulfide nanoparticles. All the prepared complexes were characterized using techniques such as IR and ^{1}HNMR spectroscopy, elemental analysis, and thermogravimetric analysis. All the spectra data obtained were consistent with the coordination of the ligands through sulfur atom to the metal ion. The thermogravimetric analysis of all complexes decomposed to form metal sulfide, which really confirmed that all the complexes could be used to metal sulfide nanoparticles.

All the prepared complexes were used to synthesize M_xS_y nanoparticles. The metal sulfide nanoparticles were successful prepared by thermal decomposition of the single-source precursor in hexadecylamine solution. The reaction parameter such as the concentration (1.0, 0.5, 0.25 and 0.125 g), reaction temperature (80, 130, 200, 250 °C) and the time (5, 10, 15, 20, 25 and 30) of the reactionwere varied to see their effect on the preparation of the nanoparticles. The prepared metal sulfide nanoparticles were characterized using techniques such as UV spectroscopy, photoluminescence spectroscopy, X-ray diffraction analysis and transmission electron microscopy.

The concentration was found to have a profound effect in size and shape of the prepared nanoparticles. The nanoparticles prepared at various concentrations were dominated by sphere with an average size of 2-30 nm. The XRD pattern confirmed that the composition is not affected by the temperature. Thetemperature has a dramatic effect in size, shape and the stoichiometry of the reaction. This was confirmed by an increase in size as the temperature was increased, with the exception of cobalt sulfide nanoparticles that decrease in size while temperature was increase. The XRD pattern showed different composition as the temperature was varied. Time of the reaction was found to affect the particles size of the nanoparticle. The sizes of the nanoparticles were increase as the time of the reaction was prolonged.

PRESENTATIONS AND PUBLICATIONS

Presentations

- SAIP conference July 2011: Poster presentation: 'Synthesis and characterization of reproducible stoichiometry of cobalt sulfide nanoparticles using sulfur containing single-source precursors'.
- VUT Hub and Spoke`s conference July 2011: Oral presentation: 'Synthesis and characterization of reproducible stoichiometry of cobalt sulfide nanoparticles using sulfur containing single-source precursors'.
- SACI and SANI Symposium October 2011: Oral presentation: 'Synthesis and characterization of reproducible stoichiometry of cobalt sulfide nanoparticles using sulfur containing single-source precursors'.

Publications

- Synthesis and characterization of reproduciblestoichiometry of cobalt sulfide nanoparticles using sulfur containing single-source precursors, SB Sibokoza, MJ Moloto, N Moloto, SAIP 2011 Conference Proceedings, *Condensed Matter and Materials Science Division A,* **2011,** 296-301.

CHAPTER ONE

LITERATURE REVIEW OF NANOPARTICLES

1.1 General background of nanoparticles

Nanoscience is a multi-disciplinary field that combines the knowledge of several areas such as physics, chemistry, biology and engineering. Nanoscience is a science field that focuses in the study of materials, whose size is less than 100 nanometers. The nanoscience field is involved in observing the governing laws of the nanosized objects, developing the theoretical models to explain the features of these nanosized objects and investigating its properties. The characteristics of the objects are altered when it goes to a nanometer scale size, hence the material's physical, chemical and biological properties are different from the one`s of micrometer and larger scales particles.

Nanotechnology is the design, characterization, production and application of structures, devices and systems by controlling shape and size at nanometer scale. It deals with creation of functional materials, devices and systems through control of matter on the nanometer scale (1–100 nm) and exploitation of novel phenomena and properties (physical, biological, electronic, optical, electrical, magnetic, chemical and mechanical) at that length scale. It is the self-assembly of individual atoms, molecules, or molecular clusters into structures to create materials and devices with new or enhanced properties. By harnessing these new properties, researchers can develop materials, devices and systems that are superior to those in use today. The nanotechnology focuses on the diverse properties such as strength, thermal and electrical conductance, reactivity and buoyancy of the materials, using its nanoscale behavior, to design and manufacture useful products. Nanotechnology is said to be the engineering field, which involves the study of nano objects and its application in diverse fields. Nanotechnology is generally applied in many different areas which include health care, agricultural industries, automobile, IT.

A nanocrystal is a small amount of the particles (size of 1-100 nm), which have a finite number of atoms (~100 to ~10,000 atoms). They are considered important because of their new or enhanced properties. They are obtainable as dispersion of a solid in a liquid (colloidal sol). Metal sols possess fascinating colours and have long been used as dyes. In 1857, Faraday established that dyes consist of tiny metal chunkys [1]. Semiconductor nanocrystals were discovered a century later [2]. The colloidal particles display a remarkable tendency to remain single-crystalline and are hence named as nanocrystals. Nanocrystals possess high surface area, a large fraction of the atoms in a nanocrystal are on its surface. A small nanocrystal of 1 nm diameter will have as much as 30% of its atoms on the surface, while a larger nanocrystal of 10 nm (~1000 atoms) will have around 15% of its atoms on the surface [3]. An added aspect to research on nanocrystals is their size-dependent properties. The electronic, magnetic and optical properties of a nanocrystal depend on its size [3].

1.2 Properties of semiconductors nanoparticles

1.2.1 Optical properties of semiconductors nanoparticles

The main difference in optical properties of macrocrystalline semiconductors and nanocrystalline arise from the two fundamental factors, which are size related: the first one is associated to the large surface area to volume ratio of nanoparticles. The second one is related to the three-dimensional quantum confinement of their charge carriers. In the cases of semiconductors, quantum confinement occurs when the particles size of a nanocrystal is smaller than the exciton Bohr radius of the bulk semiconductor of the same compound.The energy levels of the excited carriers (exciton) will become discrete and approach the molecular behavior as the particle size decreases. The quantum dot can be treated like a spherical quantum box and will display an atomic like absorption spectrum. The consequence

of the three-dimension confinement isdue to the energy gap that separates the conduction from the valence energy bands **(**Figure. 1.1a, left**)**.In addition to increasing energy gap, quantum confinement leads to a collapse of the continuous energy bands of the bulk material into discrete, ‘‘atomic’’ energy levels. These well-separated QD states can be labeled using atomic like notations (1S, 1P, 1D.), as illustrated in Figure. 1.1a. The discrete structure of energy states leads to the discrete absorption spectrum of QDs (schematically shown by vertical bars in Figure. 1.1c), which is in contrast to the continuous absorption spectrum of a bulk semiconductor (Figure. 1.1c).

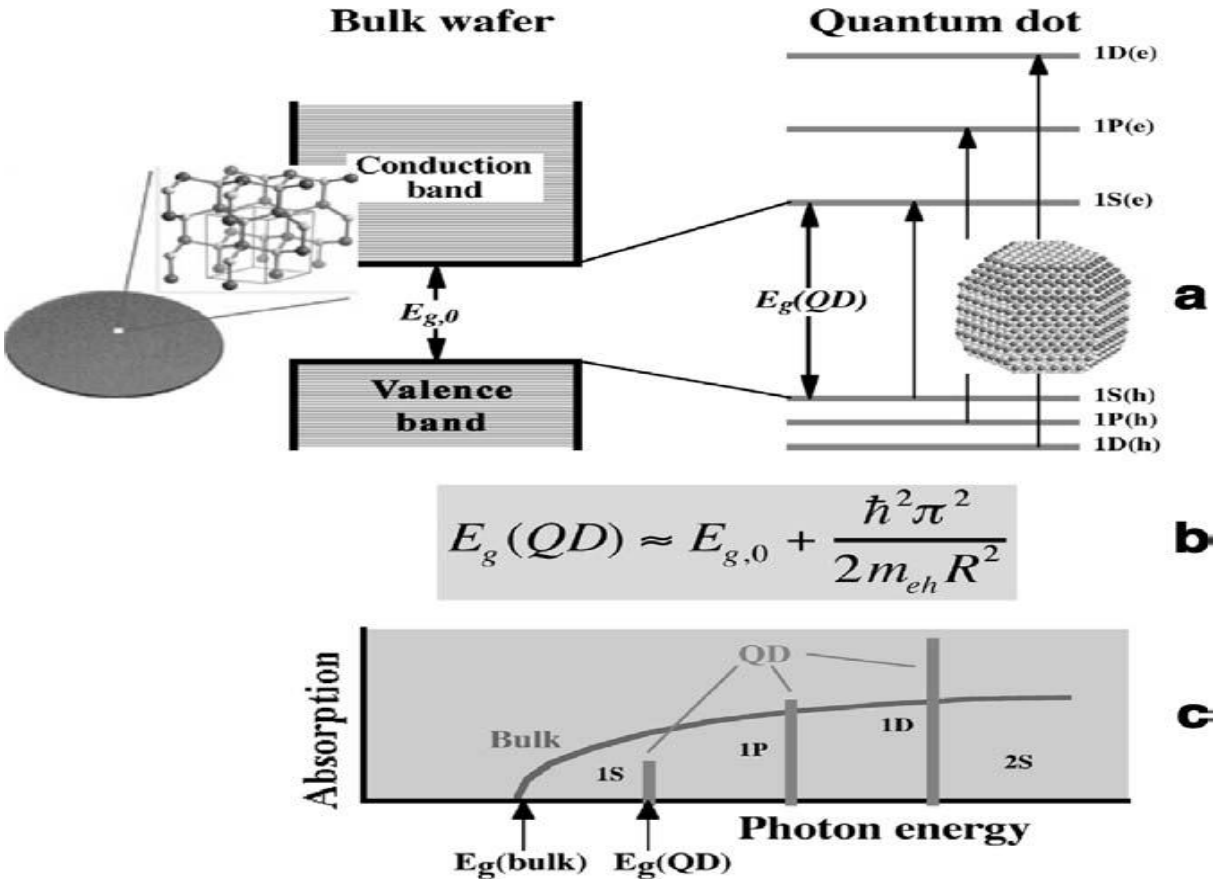

Figure 1.1: (a) The electronic state diagram of the bulk semiconductor (left) and of the quantum dot (QD) (right). (b) The expression for the size-dependent. (c) Absorption spectrum of a bulk semiconductor (curved line) and of the QD (vertical bars) [4].

Semiconductor QDs bridge the gap between cluster molecules and bulk materials. The boundaries among molecular, QD, and bulk regimes are not well defined and are strongly material dependent. However, a range from ~100 to ~10,000 atoms per particle can be considered as a crude estimate of sizes for which the nanocrystal regime occurs. The lower limit of this range is determined by the stability of the bulk crystalline structure with respect to isomerization into molecular structures. The upper limit corresponds to sizes for which the energy level spacing is approaching the thermal energy kT, meaning that carriers become mobile inside the QD [4].

Brus et al [2] use the equation (1) below to describe the electron-hole state E_{1S1s} for cadmium sulfide and selenide (CdS, CdSe).

$$E_{1S1s} = E_g + \frac{\pi^2 h^2}{2a^2 \mu} - 1.786\frac{e^2}{\varepsilon a} \ldots (1)$$

where a is the particle radius, μ the electron-hole reduced mass, e the electronic charge and ε the dielectric constant of the bulk semiconductor. The first term on the right, E_g, corresponds to the bulk band gap energy, the second represent the confinement energy and the third term represent the electron-hole Coulomb interaction.Equation (1) shows that, besides inducing energy quantization, decreasing the dots size makes the Coulomb term shift the total energy to lower values with a^{-1} dependence. Conversely, the confinement term adds to the total energy with an a^{-2} dependence. Hence, for smaller dot sizes, the confinement term becomes dominant and the optical spectrum shows a blue shift in the band edge energy when the QD's size is decreased below a_B. The smaller the dot the greater will be the blue shift observed relative to the typical $E_g$of the bulk semiconductor. Like in bulk semiconductors, the band edge energy determines the absorption onset and the luminescence peak emission (near band edge). Therefore, QDs will absorb any photon with energy $h\nu > E_{1S1s}$ and display an emission peak

around the same energy value. In this context, Equation (1) shows that QD technology allows band gap tuning by control of the nanoparticles size (a) or material type (ε) [5].

1.3 Synthesis of semiconductor nanocrystals

The synthesis of nanoparticles is very critical in order to produce materials of quality. The properties of the resulting particles determine its quality and thus a number of methods have been developed. The chemical methods for the production of nanoparticles are discussed from section 1.3.1-1.3.5.

1.3.1 Chemical precipitation method

The general method used to synthesize nanoparticles of quality and monodispersity entail controlled precipitation of colloidal solution. The method involves discrete nucleation that is followed by rapid growth of monomer concentration and finally slower growth by Ostwald ripening [6]. Small crystals (less stable) dissolve and recrystallise on larger crystals (more stable), a process called Ostwald ripening. The precursor is quickly injected to a hot coordinating solvent, this result in thermal decomposition of the precursor reagents and supersaturation of the formed "monomer" to generate nucleation.

Growth then proceeds by the addition of monomer from solution to the nanoparticle nuclei. Monomer concentrations are below the critical concentration for nucleation; thus, these species only add to existing particles, rather than form new nuclei [7]. Once monomer concentrations are sufficiently depleted, growth can proceed by Ostwald ripening. Here, sacrificial dissolution of smaller (higher-surface-energy) particles results in growth of larger particles and, thereby, fewer particles in the system [6]. This method is most favorable, when

nanoparticles have low solubility, which is normally achieved by choosing a good solvent, pH, temperature and stabilizers. The colloidal stability is improved by using solvent with low dielectric constant or by using stabilizers such as styrene or maleic acid copolymer. Brus and co-workers used aqueous solution of ammonium sulfide and cadmium sulfate to prepare CdS nanoparticles [8]. The stable CdS nanoparticles were achieve by using acetonitrile as the solvent in the presence of a styrene or maleic anhydride copolymer [8]. CdS and ZnS nanoparticles have also been synthesized from aqueous and methanolic solution with organic capping agent [8]. Henglein [9] and Weller et al [10] made significant progress using CdS colloids prepared by controlled precipitation methods.

Weller group [10] synthesized nanocrystallites of Zn_3P_2 and Cd_3P_2 by the injection of phosphine (PH_3) into solutions containing metal salts; control of particle size was achieved by varying the phosphine concentration and the temperature of the reaction. Samples of both Zn_3P_2 and Cd_3P_2 showed remarkable quantum size effects, as observed by changes in the color of the products. Hexametaphosphate was used as a stabilizer to prevent particle aggregation. The solubility of inorganic salts can be used to prepare more structures that are complex by such methods and examples include: CdS/ZnS [11], CdSe/AgS [12] HgS/CdS [13], PbS/CdS [14], CdS/HgS [15], ZnS/CdSe [16] and ZnSe/CdSeb[17] particles. The main constraints on the production of such structures involve the relative solubility of the solids and lattice mismatches between the phases. The preparation of ‘‘quantum dot quantum well systems’’ such as CdS/HgS/CdS [18] has also been reported in which an HgS quantum well of 1–3 monolayers is capped by 1–5 monolayers of CdS.

1.3.2 Synthesis in confined matrices

The use of a matrix to define the reaction space is an intrinsically attractive approach to the preparation of large amounts of material which could be deposited from solution or from the vapor phase. A number of matrices have been used including: zeolites [19], layered solids [20], molecular sieves [21], micelles/micro-emulsions [22], gels [23], polymers [24] and glasses [25]. The matrix provides a mesoscopic reaction chamber in which the crystal can only grow to a certain size. The properties of the nanocrystallites are determined, not only by the confinements of the host material, but also by the properties of the system, which can include a range of factors including the internal/external surface properties e.g. of the zeolite or the lability of a micelle. The particle size is controlled by the system chosen e.g. in zeolites the nanocrystallite diameter is limited by the pore size of the zeolite (typically smaller than 2 nm).

Wang and Herron [19] have studied the optical properties of both CdS and PbS clusters encapsulated in zeolites. The nanocrystallites were prepared in two different zeolites; modernite (uni-directional channels of 7 Å diameter) and zeolite Y (13 Å diameter channels with cages of tetrahedral symmetry interconnected by 8 Å windows, and 5 Å cages interconnected by 3 Å windows). For the preparation of CdS in zeolite Y, the sodium cations in the zeolite were first ion-exchanged with cadmium cations, by treatment with aqueous $Cd(NO_3)_2$ at pH 5. This was followed by passing hydrogen sulfide (H_2S) gas over the sample [19]. Depending on the loading level of cadmium ions within the zeolite, different sizes of CdS clusters could be obtained. At low loading levels (1:1 metal/sulfide) CdS clusters with an average size less than 13 Å were obtained. These gave an absorption peak at around 280 nm in their optical spectra. When an excess of cadmium was used the individual clusters aggregated into an extended structure, modulated by the internal cavities of the zeolite. These

produced optical spectra showing an excitonic shoulder near 350 nm corresponding to CdS clusters of approximately 28 Å in diameter. The small dimensions reported in this work are typical of nanoparticles obtained when zeolites are used as the host structure.

Stable, cubic phase, PbS nanoparticles were prepared in a polymeric matrix by exchanging Pb^{2+} ions in an ethylene – 15% methacrylic acid copolymer followed by reaction with H_2S [23]. The size of the PbS nanoparticles was dependent on the initial concentration of Pb^{2+} ions with diameters ranging from 13 to 125 Å. The smallest particles (13 Å) are reported to be molecular in nature and exhibit discrete absorption bands in their optical spectra. Two theoretical models, which take into account the effect of non-parabolicity, were proposed in order to explain the observed size-dependent optical shifts for PbSnanocrystallites. The authors reported that the effective mass approximation fails for PbSnanocrystallites. Steigerwald et al. prepared capped CdSe, ZnS, ZnS/CdSe and CdSe/ZnSnanocrystallites from inverse micellar solutions [25]. Silylchalcogenide reagents were added to micro-emulsions containing the appropriate metal ions. The particle surfaces were subsequently capped; for example with phenyl groups or with other semiconductor materials such as ZnS. Silylorganochalcogenides react readily with metal salts or simple metal alkyls to form metal–chalcogenide bonds [26]. Micelle stabilized CdSe nanocrystallites, with Cd^{2+} rich surfaces, react similarly with $[(CH_3)_3Si]_2Se$ to give larger CdSe crystallites encapsulated by a layer of organic ligands. These surface passivated crystallites can be isolated as powders, which are soluble in organic solvents such as pyridine. ^{77}Se NMR spectra of three size distributions of organic-capped CdSe were reported, with each giving different spectra [27], consisting of broad lines corresponding to bulk material along with additional peaks appearing at higher field and becoming more intense with decreasing particle size.

Several types of nanoparticles prepared from synthesis involving biologically related processes, bio-mimetic, have been reported [28]. For example, using empty polypeptide cages found in the iron storage protein ferritin; bio-inorganic nanocomposites of CdS–ferritin can be synthesized [29]. Another approach to nanocrystallite synthesis in a matrix was developed by Choi and Shea [23], who report using porous inorganic–organic xerogel (polysilsesquioxanes) to produce CdS (6 and 9 nm) [22] and chromium particles (1–10 nm) [23]. The chromium precursor used was a zero-valentarenetricarbonylchromium complex, introduced as a component of the xerogel matrix, which after heating under vacuum produced chromium nanoparticles. By first doping CdS into the starting material two different phases of chromium and CdS are reported to be obtained. Perhaps the most important use of a biological approach to nanoparticle growth is that taken in the commercial sector by Nanomagnetics Ltd [30]. They have used the 8 nm cavity of the iron storage protein ferritin to grow iron oxide for use in magnetic storage devices and hope to fully commercialize the process [31].

1.3.3 Metal-organic routes

The routine synthesis of well-defined semiconductor nanocrystallites was really opened up in a landmark paper by Murray, Norris and Bawendi [32]. They reacted solutions of dimethylcadmiumdispersed in tri-n-occtylphosphine and trin-octylphosphineselenide in hot tri-n-octylphosphine oxide (TOPO) at the temperature range of 120–300 °C. This reaction produced TOPO-capped nanocrystallites of CdSe. The size of the particles is controlled mainly by the temperature of reaction, with larger particles being obtained at higher temperatures. This TOPO method has advantages over previous synthetic methods, including, producing monodispersity ($\sigma \approx 5\%$) and the ability to produce hundreds of milligrams of materials in a single experiment. Aliv subsequently used higher temperatures for injection and growth to improve the quality of the material prepared [33]. In a series of recent

papersinteresting rod and tetrapodal structures have been grown especially in the CdSe system [34]. The method was readily adapted to the production of core–shell structures [35] with materials having high quantum efficiencies being prepared.

An early example was the synthesis of cubic PbS [36] and PbSe [37], this work has been emulated and developed for the production of various morphologies [38]. Clusters of the general formula $[M_{10}Se_4(SPh)_{16}]^{-4}$ (M = Zn or Cd and SPh = phenyl thiolate) have been used to great effect in the synthesis of nanoparticulates of both the simple and core–shell type [39]; dialkyl-diseleo and dithio-carbamates have also been used to prepare core shell nanoparticles [40]. In devising safer syntheses for nanoparticulates based on the original TOPO type of methodologies it has occurred to more than one group that the use of metal alkyls may not be required [41]. In early experiment cadmium chloride and TOPS were used to prepare CdS. More recently, Peng has produced a series of papers in which cadmium salts, especially the acetate, have been used to prepare good quality CdSe [41]. In the most recent report a blend of octadecene and oleic acid was used to produce CdS under conditions in which sulfur was the limiting reagent. Particle size control could be achieved by varying the amount of oleic acid in the reaction mixture. In related work, lead-containing materials have been prepared.

A review of the general area of the synthesis of nanodispersed semiconductors is available [42]. A TOPO-based method has been used by Alivisatos group [43] in the synthesis of InP nanocrystals (2–5 nm in diameter). The reaction used $InCl_3$ in TOPO followed by addition of $P(Si(CH_3)_3)_3$, with annealing of the resulting InP nanocrystals. InAs has been prepared by a similar method by the dehalosilylation reaction between $As[Si(CH_3)_3]_3$ and $InCl_3$, surface oxidation did not change the properties of the resulting particles [43]. III/V semiconductors are less ionic in character than their II/VI analogs and thus do not crystallise as readily [44]

used solid state metathesis involving the reaction of sodium pnictides with group III halides, at high temperatures, in a closed vessel, to produce III/V nanoparticles. A relatively low temperature method involving similar reactions in organic solvents has been reported for the preparation of GaP and GaAs nanoparticles, using gallium(III)halides and $(Na/K)_3E$ (E = P, As) [45]. This method avoids the use of hazardous phosphines or arsines. Nanocrystallites of InAs and InP were also synthesized [46] from the reaction of InX_3 (X = Cl, Br, I) with $As(SiMe_3)_3$ or $P(SiMe_3)_3$, respectively. Other analogous chemical routes to indium pnictides have also appeared in the literature [46].

GaAs nanocrystallites have been prepared by reacting $GaCl_3$ with $As(SiMe_3)_3$ in boiling quinoline, however, as yet unidentified species were found to mask the optical properties of the resulting particles and hence quantum size effects could not be properly determined [47]. The alcoholysis or thermolysis of silylated single molecule precursors is one of several processes used for nanoparticle synthesis of III/V and II/V semiconductor materials. Another preparative method for the syntheses of GaAs [48] and InP [49] is by the methanolysis of organometallic compounds such as $[Cp^*(Cl)In(\mu\text{-}P(SiMe_3)_2]_2$. The chemical route led [50] to bulk, amorphous, Cd_3P_2 after rapid flocculation of Cd_3P_2 nanoparticles.

1.3.4 Hydrothermal and solvothermal methods

An alternative approach to the use of high-temperature solvents, which can be both toxic and expensive, is to use more usual solvents conventionally limited by their rather low boiling points. However, solvents can be used well-above their boiling point at atmospheric pressure if heated in a sealed vessel (an autoclave or 'bomb') the autogenous pressure then far exceeds the ambient pressure raising the boiling point of the solvent. Such solvothermal reaction conditions are extensively used in the preparation of inorganic solids, especially zeolites [51].

Qian and coworkers [52] have reported wurtzite ZnSe nanoparticles with sizes in the 18 nm range starting from the elements in ethylenediamine (T = 120 °C, t = 6 h.). This reaction yields a complex with the formula ZnSe(en) where en is ethylenediamine. Seshadriet al has used toluene as the solvent in a neat preparation of CdSe from cadmium stearate and Se powder [53], tetralin(tetrahydronaphthalene) was added as a reducing agent. Tetralin is aromatized to naphthalene in the presence of Se, producing H_2Se in the process.

Cu_2Se particles were obtained by Qian and coworkers [54] starting from CuI, Se, and ethylenediamine, with T = 90 °C, t = 4 h. The particles are spherical and quite monodisperse. Qian and coworkers [55] have also reported a solvothermal preparation of $CuInSe_2$, obtaining 15 nm particles from $CuCl_2$, $InCl_3$ and Se in either ethylenediamine or diethylamine, at 180 °C for 15 h in ethylenediamine, and 36 h for diethylamine. $CuInSe_{2x}S_x$ also has been prepared by Qian and coworkers [56] using $InCl_3$, $CuCl_2$, S and Se with ethylenediamine as the solvent. Recently microwave-solvothermal reactions and flow-solvothermal reactions have been reported. These methods may be of particular interest in devising scalable synthesis of nanoparticles. Komarneni group [57] have prepared a number of oxide nanoparticles, including 5–20 nm $MnFe_2O_4$, $CoFe_2O_4$, $NiFe_2O_4$ and $ZnFe_2O_4$ ferrite particles, usually by the reaction of metal nitrates in suitable ammoniacal solution. These solutions are microwaved, typically for around 4 min. In flow hydrothermal techniques, a preheated solvent is mixed with the reactants just prior to introduction into a heated chamber with a back-pressure regulator. The reactants are pumped using a standard HPLC pump through the system. In this way Yoffe group[58] have prepared CeO_2ZrO_2. A residence time of 9 seconds at a (regulated) pressure of 25 MPa was sufficient to yield the product, which comprised nanoparticles with sizes as small as 4 nm. These two methods may well have great promise not only for scale-up, but also for good monodispersity.

1.3.5 Single-source precursor method

The use of single-molecule precursors in which the metal-chalcogenide bond is available has proven to be a very efficient route to high-quality nanoparticles. The other advantages of using this method include:

- Single-source method avoids the use of toxic, volatile and pyropholic precursors.
- Some nanoparticles are air sensitive. The precursors for those are synthesized under both aerobic and anaerobic conditions, with resulting precursor being air and moisture stable.
- The use of one involatile precursor minimise the chance of incorporating impurities into nanoparticles.
- The preparation of nanoparticles at low temperature is possible.

Original, single-molecular precursors have been use for the preparation of semiconductor thin films CVD techniques, but this method has proved problematic because of the low volatility of the precursors and lack of stoichiometric control of the resultant materials. Mohammad et al [59] deposited manganese and cobalt sulfide thin films using n-hexyldithiocarbamato complexes by hot-wall aerosol-assisted chemical vapour deposition (AACVD) technique. The deposition of the latter involves the use of $[M(S_2CNMe^n\text{-}Hex)_3$ (M = Co, Mn) complexes. Kemmler et al [60] reported copper sulfide and selenide thin films deposited using $[Cu(E_2CNMe^n\text{-}Hex)_3]$ (E = S, Se) complexes by low-pressure metal-organic chemical vapour deposition (LP-MOCVD) method. Trindade and O`Brien [61] first reported the use of bis(dialkyldithio/seleno-carbamato)cadmium(II)/ Zinc(II) complexes for the synthesis of zinc and cadmium sulfide selenium nanoparticles. Bis(dialkyldithio/seleno-carbamato)cadmium(II)/ zinc(II) complexes were thermolysed in TOPO or in 4-ethylpyridine to prepare MS and MSe nanoparticles(M = Cd, Zn).

1.4. Applications of semiconductor nanocrystals

Nanoparticles have been suggested recently for various potential applications in electronics where quantum confinement effects may be of advantage. When electrons are confined to a small domain such as a nanoparticle the system is called a “quantum dot” or zero-dimensional (0-D) structure. Then the electrons are behaving like “particles-in-a-box” and their resulting new energy levels are determined by quantum ‘confinement’effects. These new energy levels give rise to a modification of the optoelectronic properties as compared to the corresponding properties determined by the bulk material electronic structure [62]. As a result, discrete energy levels are needed to describe the electron excitation and transport in quantum dots. Quantum confinement effects lead for example to higher energy level transitions as compared to the bulk material observed as a shorter wavelength optical absorption edge, indicated by a spectral “blue shift”. Quantum dots can be used also to produce light emitters of various colors by “band-gap tuning” using particle size effects rather than the current complex techniques of synthesizing compound semiconductors [63]. Another advantage of 0-D semiconductor structures stem from the very long lifetime of electrons in the excited states, which is an important requirement in laser optical applications [64].

Alivisatos group produced light-emitting diodes (LED) with high conversion efficiencies (10%) by using quantum dots embedded in polymer matrices [61]. Moreover, quantum dots were employed in LEDs with a voltage-controlled, tunable output color by Colvin *et al.*[62], who assembled CdSe nanoparticles on the surface of an electroluminescent polymer (PPV). The LEDs emitted green light from the polymer and red light from the nanoparticle layer being also color tunable as a function of the applied voltage. Finally, lasers based upon such structures are expected to have a higher gain and to lose at much lower electrical threshold as compared to current available laser technologies [64]. Enhancement of the nonlinear optical

properties by quantum size effects are also of great interest today. This effect has been applied already commercially for producing optical cut-off color filters based on CdS_xSe_{1-x}nanoparticles embedded in silicate glasses. It is expected also that nanoparticles such as CdS, CdSe, GaAs and Si dispersed in glasses will have applications in fast optical switches and optical fibers based on the nonlinear optical behavior [58]. In nonlinear optical materials, the refractive index can be changed either by carrier injection or by applying electrical fields [66]. This change in the refractive index allows electronic modulation of light, enabling, for instance, faster electro-optical switching as compared to electronical switching.Another potential application of quantum dots is the fabrication of optical memories. A 3-D array of quantum dots that are addressed optically can pack in the same volume much larger amounts of information than current planar-based microelectronic memory devices. This can be done, for instance, by spectral hole burning [67]. In this method, a laser beam with tunable monochromatic wavelength irradiates a structure containing many quantum dots of different sizes thus having different quantum-confined absorption peaks. Only those quantum dots in resonance with the laser wavelength will be excited and thus "bleach". These bleached dots can then be detected again, enabling thus "writing" a "0" or a "1" memory "state", corresponding to specific wavelengths and with a resolution smaller than the size of the laser spot, defined by the particle size.

This is one of the main difficulty forms of producing electronic devices based on quantum dots. Since attaching electrical leads to an array of quantum dots is a formidable technological task, one way of making an efficient contact is by using a semiconductor structure consisting of an ensemble of quantum dots. The voltage-tunable LED described earlier is a successfully implemented example, which uses a matrix of quantum dots. Another example of efficient contacts can be found in photovoltaics. Hodes *et al*. [65] measured photocurrents arising from

a film consisting of CdSe nanoparticles on glass and reported quantum effects. To allow conversion of significant quantities of light into an electrical current for obtaining an efficient solar cell, a rather "thick" film up to 20 monolayers of particles had to be deposited. Increasing the contact area between nanoparticles and electrode to increase the signals is possible by depositing the nanoparticles on a very porous TiO_2 electrode [69].

In microelectronics, the need for faster switching times calls for a reduction in the size of the electronic components. At present, one switching cycle in a transistor gives rise to the movement of many thousands of electrons, requiring a considerable amount of switching energy and producing excessive heat, which can hardly be dissipated in high-frequency applications. This calls for developing single-electron devices, in which the switching occurs with the motion of only a single electron. Such a device may be realized by a quantum dot in which the charge of an added electron effectively blocks the flow of other electrons by the so-called "Coulomb blockade" both switching, which performs logic operations, and storage of information are possible with these devices.

1.5 Aim and objectives

The aim of this study is to synthesize mono-dispersed cobalt and copper sulfide nanoparticles from the single-source precursors.

Objectives of the study:

- To synthesize and characterize cobalt and copper complexes from tetramethylthiuram disulfide and sodium diethyldithiocarbamate ligands.
- To synthesize of HDA-capped copper and cobalt sulfide nanoparticles using the complexes as single source precursor.

- To investigate the influence of the precursor concentration, temperature of injection, growth time, and capping agent on the morphology and size of the nanoparticles.

CHAPTER TWO

SYNTHESIS AND CHARACTERIZATION OF DIETHYLDITHIOCARBAMATE AND TETRAMETHYLTHIURAM DISULFIDE COMPLEXES OF COBALT AND COPPER

2.1 General background

Dithiocarbamates (DTC) are the reduced forms of thiuramdisulfides with strong complexing properties [70]. They exhibit very rich coordination chemistry with a large variety of transition metals [71]. These ligands have both nitrogen (hard) and sulfur (soft) atoms, which can be used for co-ordination to the metal center. Dithiocarbamates and their derivatives are known to display both mono and bi-dentate co-ordination [72]. The dithiocarbamate anion has shown to form strong chelate complexes with wide range metals.

They are well known compounds to bind strongly and selectively to many metal ions through sulfur atom. DTC ligands readily form chelates with all transition metal ions through its two donor sulfur atoms. Although the sulfur atoms of dithiocarbamate and thiuram ligands possess δ-donor and π-back-donation characteristics of the same order of magnitude, these ligands have a special feature in that there is an additional π-electron flow from nitrogen to sulfur *via* a planar delocalised π-orbital system, as shown below (Figure 2.1 and 2.2):

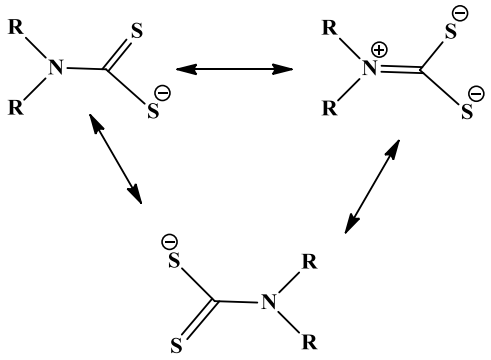

Figure 2.1: Resonance structures of dithiocarbamate ligand

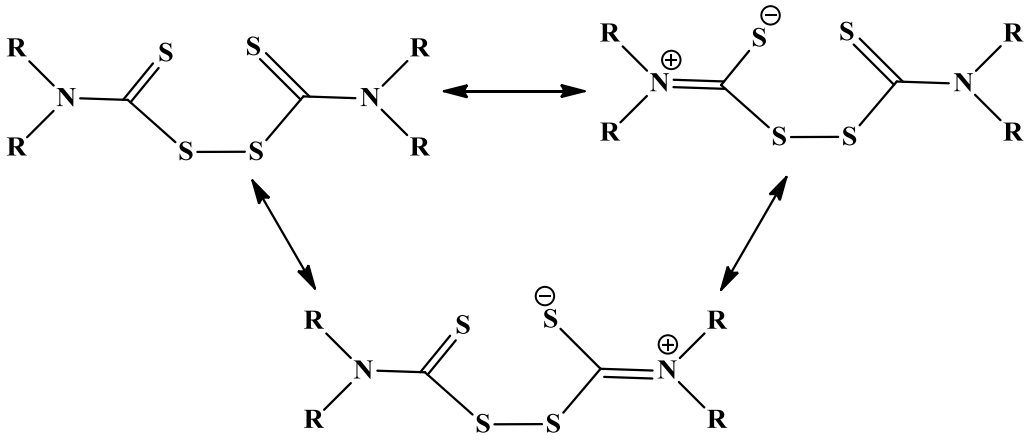

Figure 2.2: Resonance structures of thiuram disulfide ligand.

This effect results in strong electron donation and hence a high electron density on the metal leading to its next higher oxidation state [73]. However, while dithiocarbamate complexes have been known for over a century, with many thousands having been prepared, the vast majority of these contain only simple alkyl substituents such as methyl and ethyl. The continuing discovery of the many pivotal roles played by DTC and thiurams in chemical, biological and environmental processes has stimulated the construction of molecular host systems capable of complexing anionic guests. These widely diverse applications have been attributed to a combination of these factors:

(i) The capability to fit into a receptor site.

(ii) The capability to form complexes with most of the elements and able to stabilise transition metals in a variety of oxidation states. This property of stabilising high oxidation states in metal complexes reflects strong δ-bonding characteristic of these ligands.

(iii) The ability to undergo reversible redox reactions at suitable potentials. From this point of view, the equilibrium relating thiuram disulfides and dithiocarbamates is very relevant to the chemistry of the disulfides.

Coordination compounds containing ligands with sulfur atoms as donors have received great attention, because of metal sulfur bonds, which are analogues to proteins [74]. One of these ligands is dithiocarbamates, which have been used to synthesize model compounds for enzyme activity [75]. In addition, polynuclear metal dithiocarbamates may act as mineral analogues and thus as models of sulfide mineral degradation by microorganisms [76]. It must also be stated that one successful approach to the development of new metal sulfide catalysts involves thermolysis of discrete metal thio complexes containing co-ligands rich in sulfur, such as dithiocarbamates[77].

Tetraalkylthiuramdisulfides are sulfur rich compounds (contains four sulfur atoms), therefore good ligands for our single-source precursor. Thiuramdisulfides are unique among thiolato-type ligands, in that reductive scission of the S-S bond leads to chelating systems (dithiocarbamate anions) which are mostly well suited to stabilize high oxidation states [78].

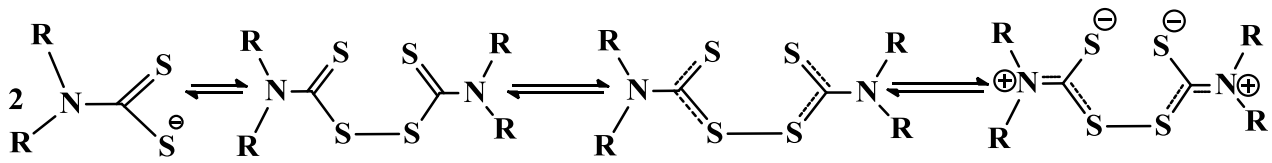

Dialkyldithiocarbamate Tetraalkylthiuramdisulfide

(dithiocarbamate) (thiuramdisulfide)

Scheme 2.1: Dithiocarbamates (reduced form) and thiuram disulfides (oxidized form).

A considerable body of literature exists on the preparation and structure of *N*,*N*-dialkyldithiocarbamato complexes of Group 12 [79]. These compounds are air and moisture stable and sufficiently volatile that they readily sublime. Recently, these properties have been

exploited to prepare II-VI semiconductor materials using *N*,*N*-dialkyldithiocarbamato complexes as single-source precursors. Thermolytic desulfurization of dialkyldithiocarbamato complexes of cadmium and zinc has become a method of choice for the synthesis of metal sulfide semiconductor materials by chemical vapor deposition [80]. In addition, nanoparticulate clusters of group 12 sulfides are prepared by thermolysis of $[M(S_2CNR_2)_2]$ precursors in high-boiling solvents [81].

The tetraalkylthiurammonosulfides (n = 1) R_4tms were less explored, because the lack application which are known for the disulfide. R_4tms are bidantateligands which forms simple coordination compounds. Tetraalkylthiurammonosulfide is known to form cationic complexes such as $[CrR_4tmsX_2]^{+1}$ and the neutral complexes of the type MR_4tmsX_2 (M = Zn [82], Hg [83], Ni and Co [84]) and MR_4tmsX (M = Cu and Ag [85]. The reaction of thiuramdisulfide and metal ions involves scission of the S-S bond and formation of dithiocarbamate complexes. This transformation has become the standard preparation of metal dithiocarbamate [86]. Monosulfide only have one example of metal dithiocarbamate ($Cu[Me_4dtc]_2$), which is formed by a reaction of Me_4tms and $CuCl_2$ in boiling ethanol [87].The sketch of the propose structure of tetramethylthiuram disulfide and diethyldithiocarbamate complexes of cobalt and copper sulfide.

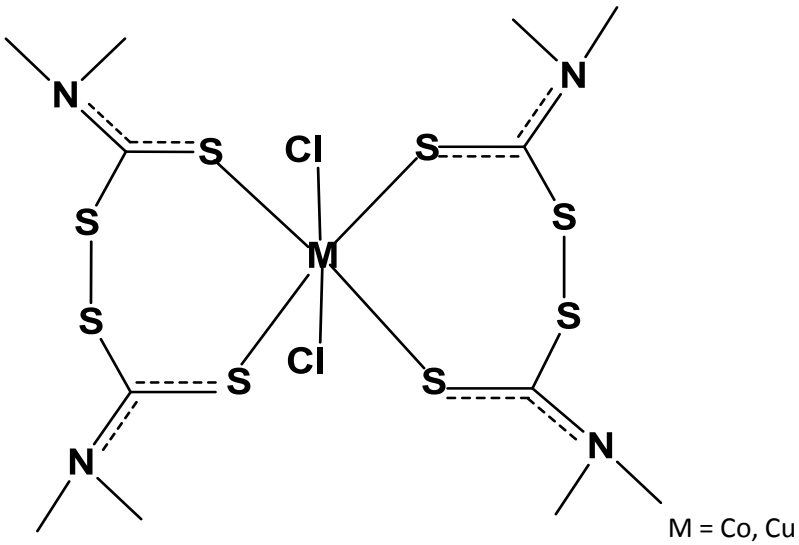

Figure 2.3: Chemical strucucture for bis(chloro,N,N,N',N'-tetramethylthiuram disulfide)cobalt(II)/copper(II).

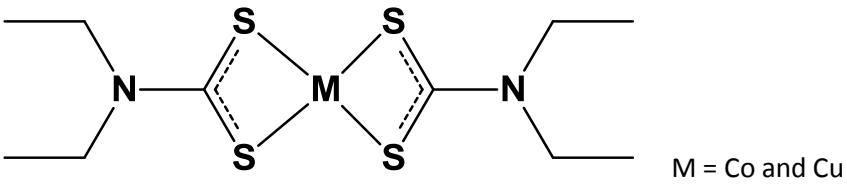

Figure 2.4: Chemical structure for bis(diethyldithiocarbamato)cobalt(II)/copper(II) complexes.

2.2 Experimental

2.2.1 Materials

Cobalt chloride hexahydrate(≥ 98 %), copper chloride(97 %), tetramethylthiuram disulfide(97 %) and sodium diethyldithiocarbamate(98 %), were used without further purification as purchased from Sigma Aldrich. The solvent such as ethanol(≥ 99.8 %), methanol(99.5 %)and deuterated chloroform (99.96 %) of analytical grade were also purchased from Sigma Aldrich. Distilled water was used as a solvent as well.

2.2.2 Instrumentation

(a) Thermogravimetry

The sample preparation for thermogravimetric analysis was done by weighing 10 mg of the complexes. These complexes were decomposed at temperature range of 50 to 800 °C. This analysis was performed on a Perkin Elmer Pyris 6 TGA under an inert atmosphere of dry nitrogen, and at a heating rate of 20 °C.Min^{-1}.

(b) NMR spectroscopy

In the preparation of the sample for the NMR, about 5 mg of the complex was dissolved in 5 ml of deuterated chloroform. The NMR spectra were recorded on a solid state NMRspectrometer [Bruker 300 MHz].

(c) FT-IR spectroscopy

Infrared spectra were recorded on FT-IR Perkin Elmer 400 spectrometer. Spectra were collected over the range from 400 to 4000 cm^{-1}.

(d) Microanalysis

Purity of the complexes was performed on a CARLO ERBA elemental analyzer for C, H, N, and S.

2.2.3 Preparation of the complexes

Complexes were prepared using two different methods, which are as follows: (I) Tetramethylthiuram disulfide complexes of copper sulfide were prepared by refluxing the mixture of the ligand and metal salts in methanol at 65 °C. (II) Metal salts and sodium diethyldithiocarbamatewere prepared using water as the solvent at room temperature in an open system.

(a) $[CoCl_2((CH_3)_2NCS(S)SC(S)N(CH_3)_2)_2]$ (I)

$[CoCl_2((CH_3)_2NCS(S)SC(S)N(CH_3)_2)_2]$(**I**)was synthesized from $CoCl_2{\cdot}6H_2O$ salts (1.00 g, 4.20 mmol) which were dissolved in hot methanol (50 ml). This solution was mixed with the solution of tetramethylthiuramdisulfide, which was prepared by dissolving tetramethylthiuram disulfide (2.02 g, 8.41 mmol) in hot methanol (50 ml). The mixture of these solutions was refluxed with constant stirring for 60 minutes. The formed dark green precipitates were filtered, washed with excess methanol and dried in open air environment. Percentage yield of 78 % (mass of the product was 2.00 g), m.p. 222 - 225°C. Anal Calc for $C_{12}H_{24}N_4Cl_2S_8Co$ (610.7166):.C, 23.42; H, 3.96; N, 9.17; S, 42.00. Found: C, 23.97; H, 3.71; N, 8.72; S, 42.21.IR spectra $\nu(cm^{-1})$: 2971.66(m), 2924.72(m), 1494.66(s), 1432.52(m), 1410.31(m),1371.55(s), 1231.30(s), 1147.02(s), 1131.91(s), 1051.63(m), 996.59(s), 958.94(s), 913.32(w), 852.01(s), 779.77(m), 574.83(s), 534.61(s).^{1}H NMR ($CDCl_3$) δ: 3.54(s, CH_3).

(b) $[Co(CH_3CH_2)_2NCS(S))_2]$ (II)

$[Co(CH_3CH_2)_2NCS(S))_2]$ (**II**)was synthesized by dissolving $CoCl_26H_2O$ (1.00 g, 4.21 mmol) in de-ionized water (25 ml). This solution was mixed with $NaS_2CN(C_2H_5)_2$ solution which was prepared by dissolving $NaS_2CN(C_2H_5)_2$ salts (1.90 g, 8.43 mmol). These solutions were mixed and stirred for 60 minutes at room temperature. The formed green precipitates were filtered, washed with excess de-ionized water and dried in open air environment. Percentage yield of 82% (mass of the product was 1.23 g), m.p. 258-261°C.Anal Calc. for $C_{10}H_{20}N_2S_4Co$ (355.479): C, 33.79; H, 5.67; N, 7.88; S, 36.08. Found: C, 33.31, H, 5.63; N, 7.19; S, 35.84. IR spectra $\nu(cm^{-1})$: 2973.02(m), 2929.23(m), 2868.69(w),1484.06(s), 1450.35(s), 1431.69(s), 1375.50(m), 1353.23(m), 1293.57(w), 1264.22(s), 1211.34(s), 1133.70(s), 1075.18(s),

998.96(s), 913.52(m), 850.82(m), 783.49(m), 518.61(s), 486.70(s). ^{1}H NMR ($CDCl_3$) δ: 1.19 (t, CH_3), 3.55, 3.75 (q, CH_2).

(c) [Cu($(CH_3)_2NCS(S)SC(S)N(CH_3)_2)_2$] (III)

[Cu($(CH_3)_2NCS(S)SC(S)N(CH_3)_2)_2$] (**III**) was synthesized from $CuCl_2$ salts (1.00 g, 7.44 mmol) which were dissolved in hot methanol (50 ml). This solution was mixed with the solution of tetramethylthiuram disulfide, which were prepared by dissolving tetramethylthiuram disulfide (3.58 g, 14.88 mmol) in hot methanol (50 ml). The mixture of these solutions was heated to reflux with constant stirring for 60 minutes. The formed dark brown precipitates were filtered, washed with excess methanol and dried in open air environment. Percentage yield of 72% (mass of the product was 3.57 g), m.p. 202–216°C.Anal Calc. for $C_{12}H_{24}N_4Cl_2S_8Cu$ (615.3296): C, 23.42; H, 3.93; N, 9.11; S, 41.69. Found: C, 22.97; H, 3.71; N, 8.82; S, 42.21. IR spectra ν(cm^{-1}): 2922.74(m), 2853.61(m), 1500.52(s), 1436.20(s), 1376.74(m), 1351.39(m), 1299.96(m), 1268.81(s), 1205.98(s), 1143.96(s), 1095.55(m), 1070.28(s), 995.13(s), 909.79(s), 845.76(s), 777.75(s).^{1}H NMR ($CDCl_3$) δ: 3.59(s, CH_3).

(d) [Cu($(CH_3CH_2)_2NCSS)_2$] (IV)

[Cu($(CH_3CH_2)_2NCSS)_2$] (**IV**) was synthesized by dissolving $CuCl_2$ (1.00 g, 7.44 mmol) in de-ionized water (25 ml). This solution was mixed with $NaS_2CN(C_2H_5)_2$ solution which was prepared by dissolving $NaS_2CN(C_2H_5)_2$ salts (3.35 g, 14.9 mmol). These solutions were mixed and stirred for 60 minutes at room temperature. The formed brown precipitates were filtered, washed with excess de-ionized water and dried in open air environment. Yield 68%

(mass of the product was 1.82 g), m.p 232-239°C. Anal Calc. $C_{10}H_{20}N_2S_4Cu$ (360.092): C, 33.36; H, 5.60; N, 7.78; S, 35.62. Found: C, 33.77, H, 5.42; N, 7.35; S, 35.63. IR spectra $\nu(cm^{-1})$: 2985.99(m), 2867.62(w), 1504.86(s), 1436.18(s), 1376.49(w), 1355.38(m), 1299.62(m), 1273.30(s), 1207.41(s), 1146.76(s), 1135.70(w), 1073.60(s), 996.76(s), 914.72(m), 846.97(s), 778.24(m), 607.67(m), 556.86(s).^{1}H NMR ($CDCl_3$) δ: 1.19 (t, CH_3), 3.54, 3.75 (q, CH_2).

2.3 Results and discussion

2.3.1 Synthesis of the complexes

Cobalt and copper complexes of tetramethylthiuram disulfide and diethyldithiocarbamate prepared were obtained in good isolated yields. Thermogravimetric analyses in conjunction with elemental analysis, melting point, FT-IR and NMR spectroscopy were used to characterize the complexes prepared. The complexes were prepared by dissolving tetramethylthiuram disulfide or diethylthioracarbamate ligand with an appropriate salt, in hot methanol, aqueous media, followed by refluxing. All the obtained complexes were air, stable.

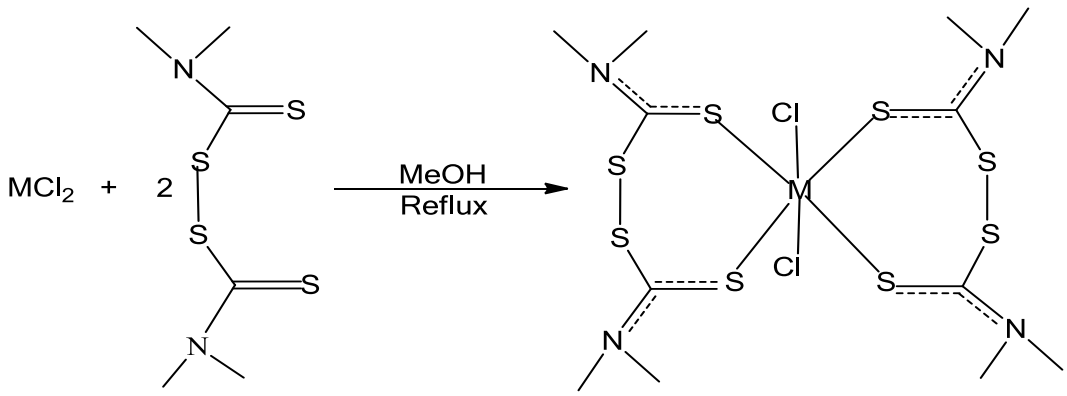

M = Co, Cu; MeOH = methanol

Scheme 2.1: Reaction of the ligand and metal salts to form a complex.

2.3.2 Spectroscopic studies

Both thiuram disulfide and dithiocabamate ligands are capable of forming bonds with the metal through sulfur atom. Thiuram disulfide and dithiocarbamate compounds are known to exhibit similar absorption bands in the 800 – 1500 cm^{-1} region [70]. Both ligands exhibit bands at 1500 – 1450, 1000 – 970 and 860 – 820 cm^{-1}, which are due to the contribution of ν(C=N) strong bands, ν(C=S) vibration and ν(C-S) weak bands respectively. Thiocarbamate act as both mono- and bi-dentate ligand. When it act as a bi-dentate, the ν(C=S) bands are normally in the 990 – 950 cm^{-1} range. However, for a mono-dentate behavior ν(C=S) band has doublet in 1000 ± 70 cm^{-1} region. Furthermore, ν(C=N) stretching frequency is increased for a bi-dentate in relation to the ligand. While the ν(C=N) stretching frequency for a mono-dentate is decreased. There are some remarkable features, which are related to the binding of the ligand to the metal. Table 2.3 shows infrared spectral values of selected band of interest of complexes (**I-IV**) and uncoordinated ligands (**V***, **VI***). All the complexes shows a relatively decrease in ν(C=S) stretching frequency, which resulted to an increase in ν(C=N) stretching frequency. This indicates a bi-dentate character of the ligands.

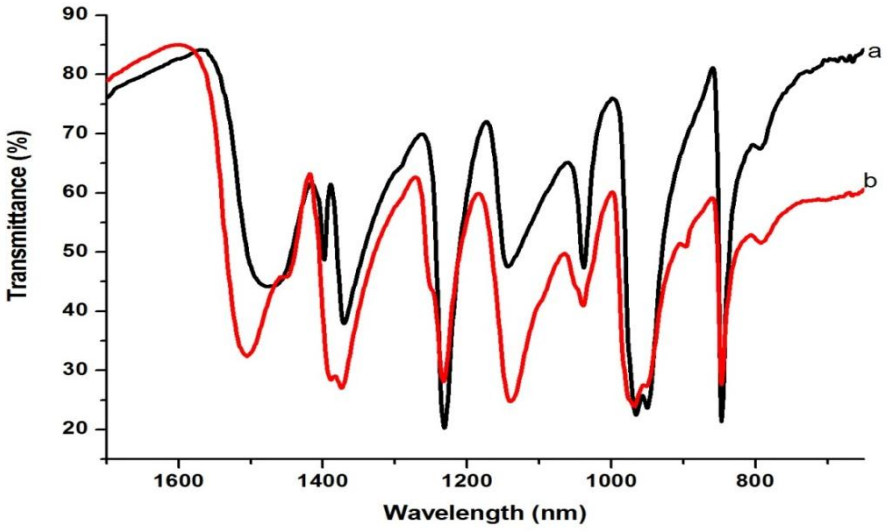

Figure 2.5: IR spectra for (a) $[(CH_3)_2NCSS_2SCN(CH_3)_2]$ and (b) its cobalt complex.

Table 2.1:

IR spectra for the complexes I – IV and the uncoordinated ligand						
Assignment	**I**	**II**	**III**	**IV**	**V***	**VI***
C=N Stretching	1494	1484	1504	1500	1485	1475
C=S Stretching	958	998	996	995	1037	1063
C-N Stretching	1211	1205	1232	1207	1240	1232
C-S	574	671	653	556	565	679

V* = $[(CH_3)_2NCSS_2SCN(CH_3)_2]$, **VI*** = $[(CH_3CH_2)_2NCSS^-]$

The ^1H NMR spectral data of the complexes were recorded at room temperature. Table 2.4 shows ^1H NMR spectral data for all the complexes. In tetramethylthiuram disulfide complexes (**I** and **III**), the methyl protons belonging to the CH_3 moiety exhibit downfield shift singlet at 3.54 and 3.59 ppm respectively. In diethyldithiocarbamate complexes (**II** and **IV**), the methyl protons belonging to the (CH_3) moiety exhibit downfield shifts at 1.19 ppm. However, methylene proton belonging to the (CH_2) moiety shows two signals at 3.55 and 375 ppm for complex (**II)**and a signals at 3.54 and 3.75 ppm for complex (**IV**), which originated from different positions (syn or anti). This appearance of two signals is associated to the barrier of rotation about the C-N band, which results in nitrogen substituent being magnetically non-equivalent [71]. The peaks at 7.20 is due to the chloroform which was used to dissolve the complexes, all the other peaks at around 7.5, 4.15, 2.29 and 1.5 ppm are due to the impurities of the solvent and the ligand used. The fact that these peaks were found in both ligandsof the complexes, this confirmed that these were impurities that are associated with the chemical used.

Table 2.2

*^{1}H NMR spectra for complexes **I** – **IV***

I	***II***	***III***	***IV***
3.54 (s, CH_3)	1.19(t, CH_3)	3.59(s, CH_3)	1.19(t, CH_3)
	3.55(q, CH_2)		3.54(q, CH_2)
	3.75(q, H_2)		3.75(q, H_2)

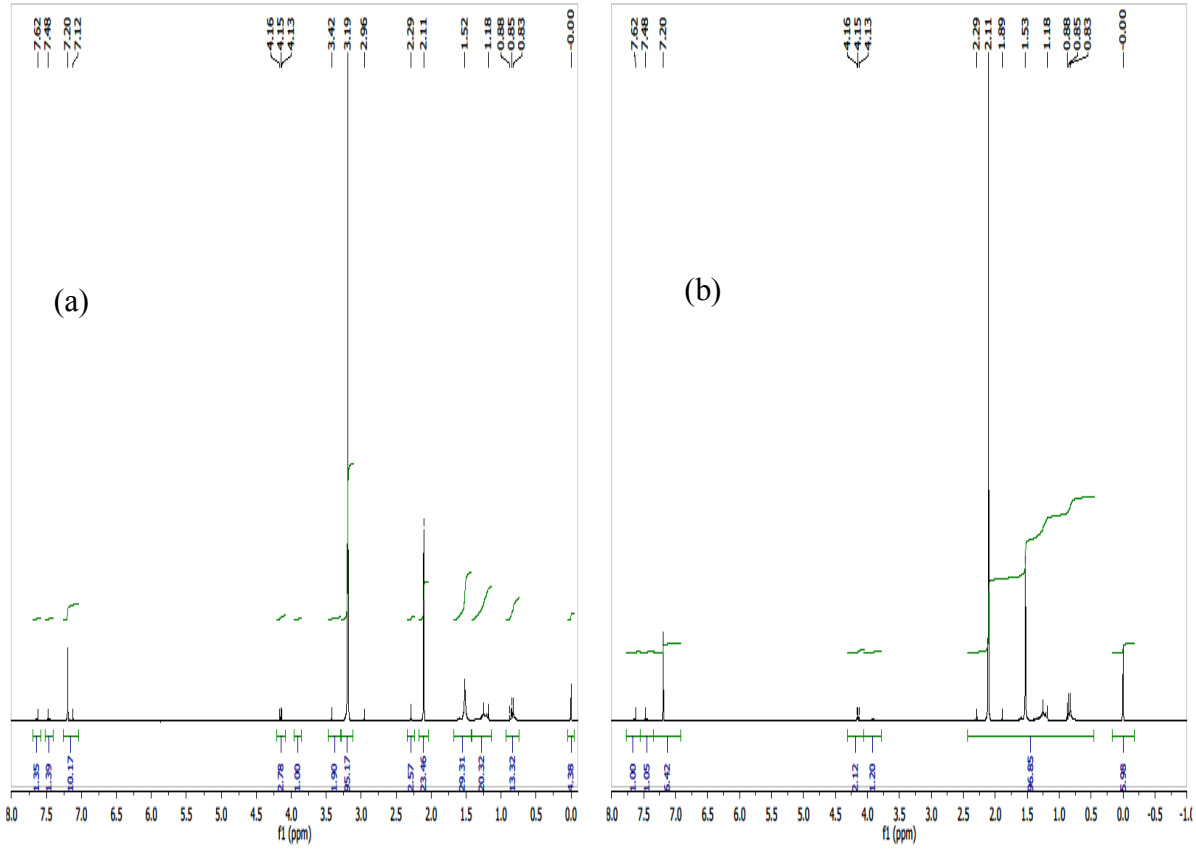

Figure 2.6: ^{1}H NMR spectra for (a) $CoCl_2[(CH_3)_2NCSS_2SCN(CH_3)_2]_2$ and (b) $[(CH_3)_2NCSS_2SCN(CH_3)_2]$

2.3.3 Thermogravimetric analysis

Figure 2.5: shows the TGA curves for cobalt and copper complexes. Complex **I** shows a single step decomposition between 293 – 414 °C with a final residue of 16.72%, which is in good agreement with a theoretical 14.90% of CoS. However, complex **II** decomposed in one step between 287 – 372 °C. The observed final residue was 21.72 %, which is comparable with theoretical of 25.60 % of CoS. Furthermore, complex III decomposed into three steps between 208 – 256 °C, 339 – 375 °C and 420 – 449 °C. The observed final residue was 19.61%, which is in good agreement with theoretical 20.75% of CuS_2. On the other hand, complex **IV** decomposed in one step between 221 – 350 °C, result with a final residue of 17.75%, which is in good agreement with 17.65% of CuS. Thermal decomposition of all complexes was between 100 – 400 °C, which is within range intended for the synthesis of metal sulfide nanoparticles.

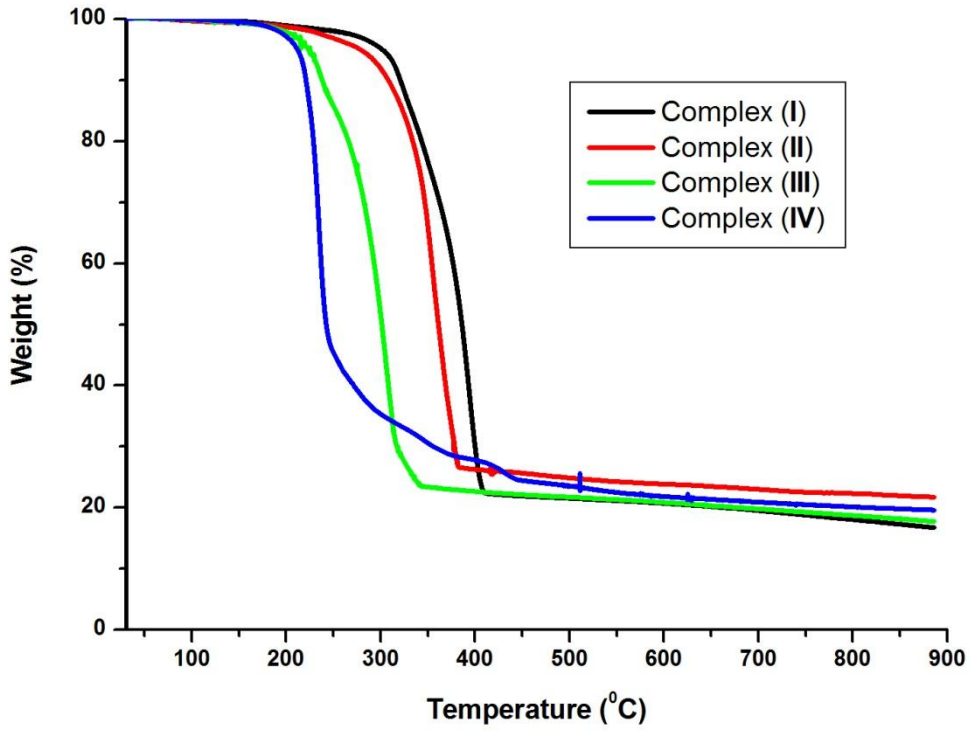

Figure 2.7: TGA curves of the complexes (**I**, **II**, **III** and **IV**).

2.4 Conclusions

All these complexes were successfully synthesized and characterized by a combination of spectroscopic techniques. Tetramethylthiuram disulfide and diethyldithiocarbamate complexes of cobalt and copper were synthesized for their use as precursors in the preparation of cobalt and copper sulfide nanoparticles. Techniques such as FT-IR, ^{1}H NMR, TGA, and microanalysis were used to characterize the complexes. The elemental analysis showed that most percentages of elements such as carbon, hydrogen and nitrogen were within the acceptable limits except sulfur. The possible reason could be due to contamination in the column of the instrument leading to unreliable values (higher than theoretical). The ^{1}H NMR for complexes prepared using thiuram ligands (**I** and **III**) single which is due to the methyl proton of CH_3 confirming that all CH_3 appeared to be in one position. However, the ^{1}H NMR of diethyldithiocarbamate complexes (**II** and **IV**) show two peaks of methylene proton belonging to the CH_2 moiety. This confirmed that these proton are no in the same position. The TGA curves clearly decomposed to form metal sulfide, hence this confirms that the all the complexes were potential useful for CoS and CuS nanoparticles.

CHAPTER THREE

SYNTHESIS AND CHARACTERIZATION OF COBALT SULFIDE NANOPARTICLES USING TETRAMETHYLTHIURAM DISULFIDE AND DIETHYLDITHIOCARBAMATE COMPLEXES OF COBALT

3.1 Background

Cobalt sulfides form a group of II-IV semiconductor materials, which are important because of their unique catalytic, electrical and magnetic properties. These compounds have considerable potential application in field such as electronic devices, hydro-desulfurization, hydro-dearomatization and in many industrial fields [88]. They are one of the most complex metal sulfides systems, with a number of phases and chemical composition. Their chemical composition have many phases such as Co_4S_3, Co_9S_8, CoS, $Co_{1-x}S$, Co_3S_4, Co_2S_3 and CoS_2[89].The diversity in the stoichiometry poses some challenge in controlling the morphologies of small-(particle). The challenges for controlled synthesis of cobalt sulfide can be caused by the stoichiometry of cobalt sulfide, which is much more complicated than that of cobalt oxide because of the coexistences of strong reducing cobalt ion and oxidizable sulfide ion. In addition, cobalt ion has a very strong affinity to oxygen. It is very difficult to exclude cobalt oxide or cobalt hydroxide impurities from the resultant materials. Another but not the least challenge is that the reaction temperature need to be well controlled because of the complicated phase diagram of cobalt sulfide [89]. This study focuses on the modulation of synthetic parameters in order to influence the size, structure, composition and arrangement of cobalt sulfide nanoparticles. The synthetic procedure followed was thermal decomposition of diethyldithiocarbamate and tetramethylthiuram disulfide complexes of cobalt in an inert environment in the presence of trioctylphosphine (solvent) and hexadecylamine (capping agent). The reaction condition such as concentration of the precursors, temperature of the reaction, and time growth of the nanoparticles werevaried in order to determine their influence.

3.2 Experimental section

3.2.1 Materials

Trioctylphosphine (97 %), hexadecylamine (90 %), toluene (99.8 %) and methanol (99.5 %) were purchased from Sigma Adrich and used without any purification.

3.2.2 Instrumentation

(a) Optical characterization

Absorption spectra of the particles were measure using a Perkin Elmer Lambda 20 UV-VIS Spectrophotometer. The samples were place in quartz cuvettes (1-cm path length) with toluene as the solvent. Emission spectra of the particles were recorded on a Perkin Elmer LS 45 photoluminescence (PL) spectrometer with a xenon lamp at room temperature. The samples were placed in glass cuvettes (1 cm) with toluene as solvent.

(b) X-ray diffraction analysis

X-ray diffraction (XRD) patterns on powdered samples were carried out in the 2θ on a D8 diffractometer. Samples were placed in silicon zero background sample holder. Measurements were taken using a glancing angle of incidence detector at an angle of 2°, for 2θ values over $20^{\circ} – 60^{\circ}$ in steps of 0.05° with a scan speed of $0.01\ ^{\circ}2\theta.s^{-1}$.

(c) Electron microscopy

The images were obtained using high-resolution transmission electron microscope (HRTEM Joel JEM-2100 microscope) operating at 200 kV with EDS analyzer. The samples were prepared by placing a drop of dilute solution of sample in toluene on to a copper grid. The sample was allowed to dry completely at room temperature.

3.2.3 Preparation of the nanoparticles

(a) Preparation of cobalt sulfide using complex I

Cobalt sulfide nanoparticles were synthesized at various concentrations of the complex, time of the reaction and temperature in about 5.0 g HDA. For the first part, different masses of the complex **I** (1.0, 0.5, 0.1 and 0.05 g) were dissolvedinto trioctyphosphine (TOP) (5 ml) separately. Each solution was injected into hot hexadecylamine (HDA) (5.0 g) which was heated and maintained at temperature of 130 °C under nitrogen atmosphere. This reaction was maintained at this temperature with constant stirring for 30 minutes. Then, the solution was cooled to 70 °C and an excess of methanol was added. The precipitate formed were isolated by a centrifuge, washed with methanol three times to remove some of the capping agent and dried in open air environment. For the second part of the experiment, the reaction was the same as the one of the first part except that the mass of complex **I** was 0.5 g and temperatures wasmaintained at 80, 130, 200, 250 °C for each reaction.For the third part of the experiment, the reaction was also the same as the one of first part except that the mass of complex **I** was 0.5g and aliquots were drawn at 5 minutes interval (5, 10, 15, 20, 25, 30 minutes).

(b) Preparation of cobalt sulfide using complex II

In preparation of cobalt sulfide using complex **II** as single source precursor, the reactions were similar to the one in 3.2.3 (a), except that for the first part masses of the complex **II** were 1.0, 0.5, 0.25, 0.125 g.

3.3 Results and discussions

3.3.1 Effect of concentration

The concentration of the precursor is major factor on both size and shape of the nanoparticles. The concentration of the precursor has a profound effect on the size with high concentration favouring large size [90]. The growth process of nanoparticles involves a delicate balance between kinetic and thermodynamic control. The concentration of the precursor affects the shape of the nanoparicle. The effect of the concentration on shape is quite complex, but it have been suggested that chemical potential of nanoparticle are related to the formation of nanoparticles with different size and morphology [91]. The chemical potential of the reaction is mainly determined by monomer concentrationat fixed temperature. The solvent also known as capping agent is an important component in the synthesis of the nanoparticles. In general, it serves two purposes. Evidently, its main purpose is to solubilise and disperse the nanocrystals and the reactants involved in the growth. The second task is to control the speed of the reaction. To do so, the solvent molecules need to bind and unbind dynamically on the surface of the growing crystals. Once a molecule detaches from the surface of the nanocrystal, new atomic species (monomers) can be incorporated into the nanocrystal, and thus it can grow. When referring to these characteristics of the solvent molecules, they are termed surface ligands, or surfactants. In a synthesis, the solvent can be a mixture of different species, including pure solvent and pure surfactants.

In general, the surfactant molecules exhibit two domains, one non-polar, generally a long alkyl chain, and a polar head group. The shape of the non-polar group as well as the binding strength of the polar group influences the growth dynamics. Briefly, the non-polar tail

biasesthe diffusion properties, whereas the polar head group mainly affects the binding efficiency.

(a) Nanoparticles prepared from complex I

Table 3.3.1 shows reaction conditions for the preparations of Co_xS_ynanoparticles by using various concentrations of complex **I**, while keeping all the other parameters the same. The amount of the precursor was varied.

Table3.3.1:

*Variation of concentration in the the preparation of Co_xS_y nanoparticlesfrom complex **I***

Surfactant (HDA) mass (g)	Complex**I** mass (g)	Temperature (°C)	Time (Minutes)
5.0	1.0	130	30
5.0	0.5	130	30
5.0	0.1	130	30
5.0	0.05	130	30

Cobalt sulfide is known to have an optical band gap of 1127.27nm with a cubic structure [92]. The absorption spectra of cobalt sulfide nanoparticles prepared at different concentrations of complex **I** (Table 3.3.1) are given in Figure 3.3.1(a-d). Cobalt sulfide nanoparticles prepared at high concentration (Figure 3.3.1(a) and (b)) show two major absorption peaks, an excitonic peak at 418 nm and a maximum peak at 329 nm. The spectra results for the particles prepared at low concentration (Figure 3.3.1(c) and (d)), reveals two peaks at 329 and 415 nm. The band gap of these particles is blue shifted from the bulk. Table 3.3.2clearly shows that as concentration of the precursor is decreased, the band gap also decreases. These results indicates that the size of the nanoparticles decrease with the decrease in concentration of the precursor.

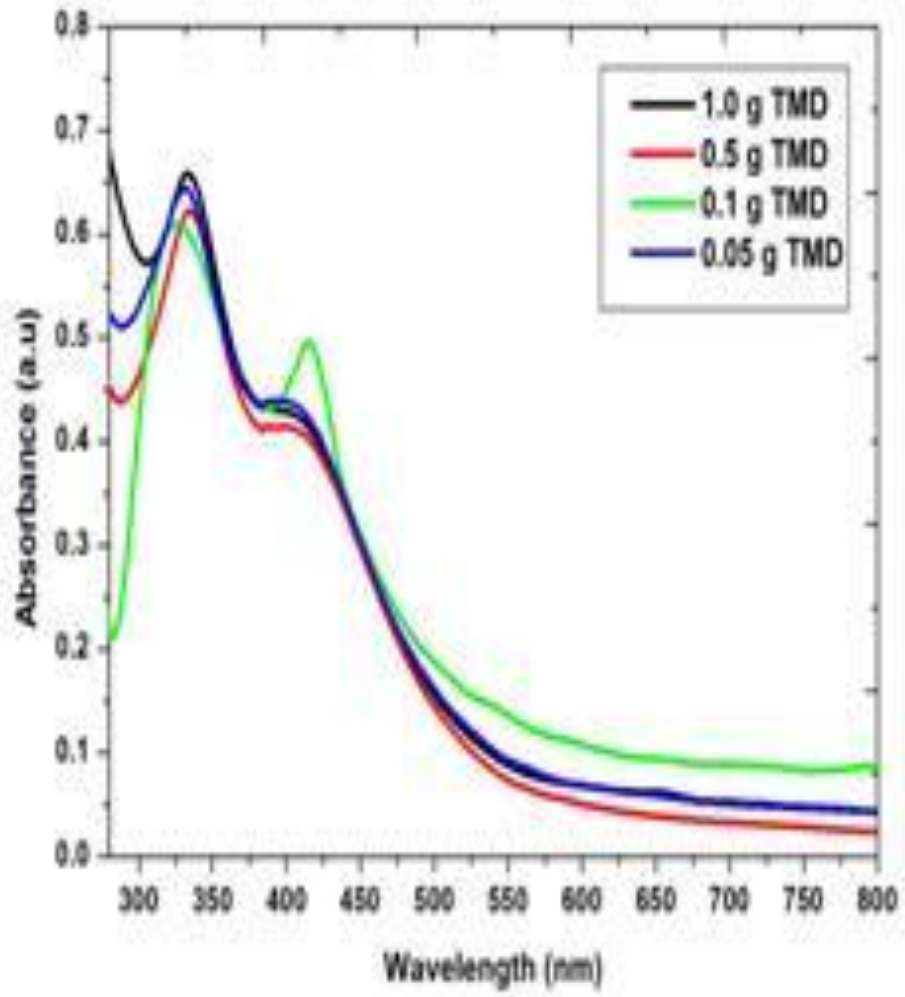

Figure 3.3.1: The absorption spectra of cobalt sulfide prepared at 130 °C for 30 minutes in 5.0 g HDA by using various amount of the complex : (a) 1.0, (b) 0.5, (c) 0.1 and (d) 0.05 g

The emission spectra of the samples prepared at various concentrations are given in Figure 3.3.2-(a-d). The emission maxima of the samples are red shifted from their respective band gap of the absorption spectra. The emission peaks for the sample prepared at low concentration have a narrow shape, which indicates the monodispersity and good passivation

of the particles. However, for the nanoparticle prepared at high concentration, the emission is very broad which indicate that the particles are polydispersed. The emission maximum shift to lower wavelength as the concentration of the precursor is decreased.

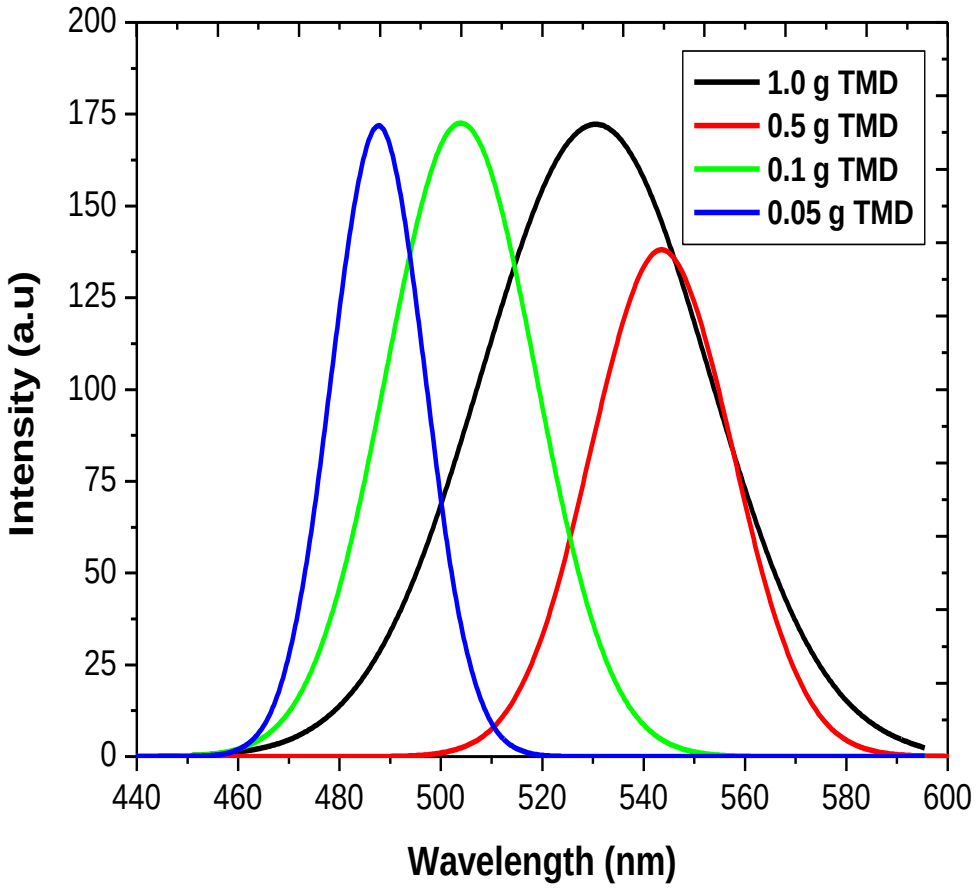

Figure 3.3.2 : The emission spectra of cobalt sulfide prepared at 130 °C for 30 minutes in 5.0 g HDA by using various amount of the complex : (a) 1.0, (b) 0.5, (c) 0.1 and (d) 0.05 g

Table 3.3.2:

Absorption band edges and emission maxima of the Co_xS_y nanoparticles prepared at 130 °C and 30 minutes using various amount of precursor in HDA.

Amount of precursor (g)	Absorption band edge (nm)	Emission maximum (nm)
1.0	543	565
0.5	524	547
0.1	486	506
0.05	459	483

The TEM images of the compound prepared at various concentrations are shown in Figure 3.3.3(a-d). The TEM of these nanoparticles show an increased in particle sizes as the concentration of complexes were increased. At high concentration of the precursor (1.0 g of complex **I**) (Figure 3.3.3(a)), the images were dominated by sphere with an average particle size of 26.03 ± 3.37 nm. When the concentration of the precursor was decreased to 0.5 g (Figure 3.3.3(b)), the images were found to be composed of sphere and rods with a length and width of 19.01 ± 2.75 and 4.35 ± 0.96 nm respectively. However, further decreasing the concentration of the precursor to 0.1 an 0.05 g (Figure 3.3.3(c) and (d)), the images were found to be dominated by spheres with an average particle size of 11.96 ± 2.4 and 6.44 ± 0.94 nm respectively. The particle size trend conforms with the decrease from the highest to the lowest concentration promoted by the amount of precursor provided in the nucleation and growth of particles.

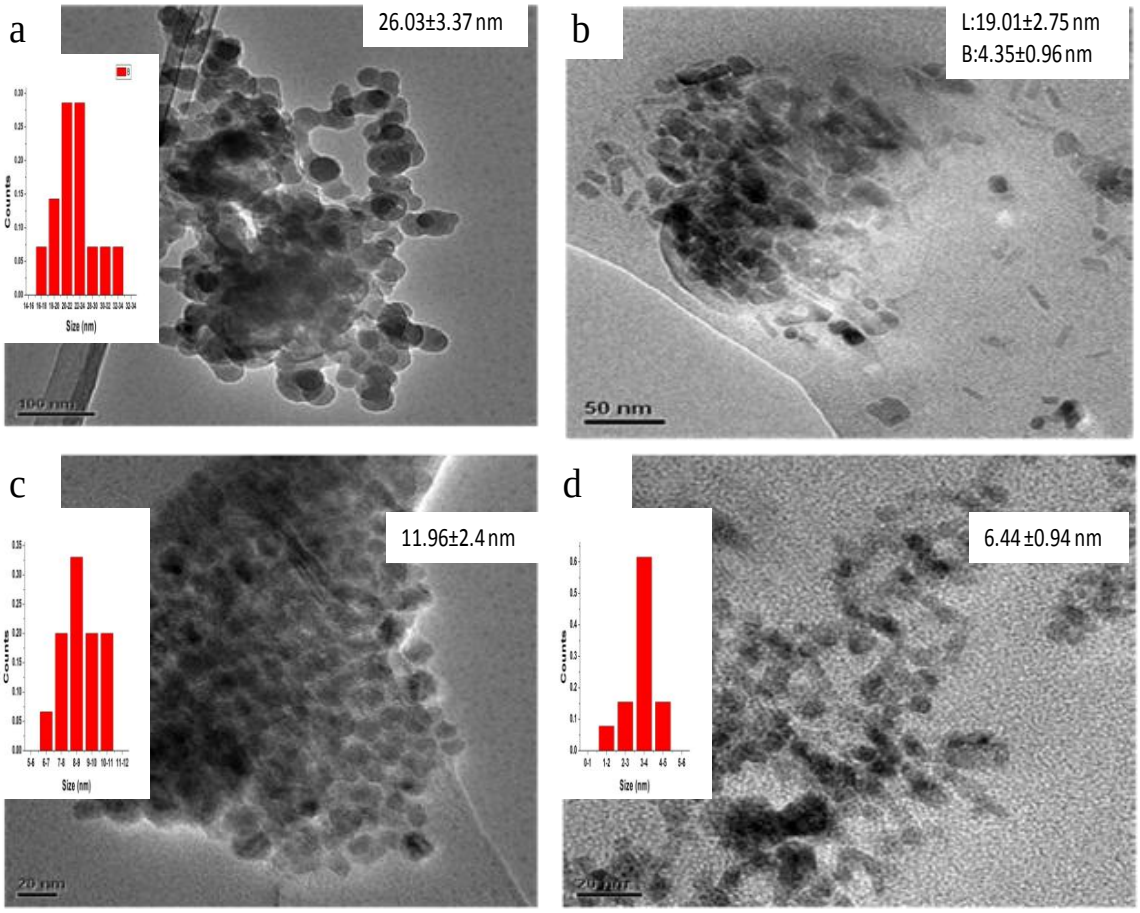

Figure 3.3.3: TEM images of cobalt sulfide prepared at 130 °C for 30 minutes in 5.0 g HDA by using various amount of the complex : (a) 1.0, (b) 0.5, (c) 0.1 and (d) 0.05 g

Figure 3.3.4shows the XRD patterns of the nanoparticles prepared at various concentration of precursor. Figure 3.3.4(a-d) shows four predominant peaks due to Co_3S_4 face-cantered cubic with 2θ values 19.19, 23.82, 45.45 and 65. 02. These diffraction peaks can be indexed to a cubic phase of Co_3S_4, which matches well with the standard XRD pattern (ICSD No. 024212)[92]. The other peaks are due to hexadecylamine, which was used as the capping molecules. At low concentration, the peaks of the hexadecylamine were more pronounce as compared to the one of the nanoparticles.

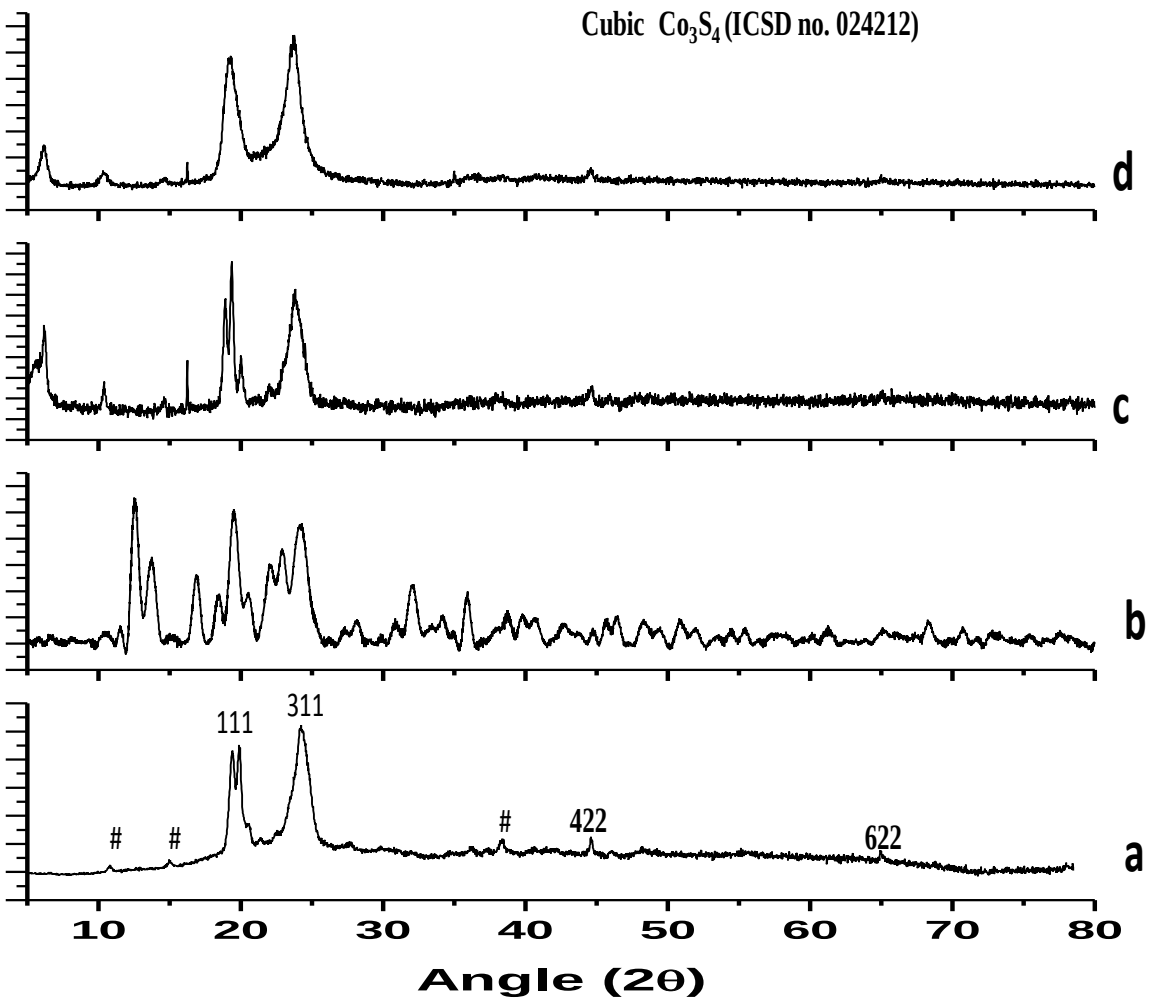

Figure 3.3.4: XRD patterns of cobalt sulfide nanoparticles prepared at 130 °C for 30 minutes in 5.0 g HDA by using various amount of the complex : (a) 1.0, (b) 0.5, (c) 0.1 and (d) 0.05 g.

3.3.1 (b) Nanoparticles prepared from complex II

Table 3.3.2 shows reaction conditions for the preparations of $Co_xS_y$by using various concentrations of complex **II**, while keeping all the other parameters the same. The amount of the complex was varied from 0.125 g to 1.0 g in a similar amount of 5.0 g of hexadecylamine.

Table 3.3.3:

*Variation of the amount of complex **II** for the preparation of Co_xS_y nanoparticles*

Surfactant (HDA) mass (g)	Complex **II** mass (g)	Temperature °C	Time minutes
5.0	1.0	130	30
5.0	0.5	130	30
5.0	0.25	130	30
5.0	0.125	130	30

The absorption spectra of cobalt sulfide nanoparticles prepared at different concentrations of complex **II** (Table 3.3.2) are shown in Figure 3.3.5(a-d). The spectra show two major absorption peaks, excitonic peak at 406.25 nm and a maximum peak at 330 nm for nanoparticles prepared at both 1.0 and 0.5 g of the precursor concentration (Figure 3.3.5(a) and (b)). However, for nanoparticles prepared at low concentration (0.25 and 0.125 g), the spectra show three major peaks. The spectra revealed the first excitonic peak at 475 nm, second peak at 406.25 nm and third peak at 330 nm for both concentrations (Figure 3.3.5(c) and (d)). The band edges of these nanoparticles were found to be 543.75, 522.75, 508.5 and 505 nm for particles prepared at 0.1, 0.5, 0.25 and 0.125 g of the precursor concentration. The particle size trend conforms with the decrease from the highest to the lowest concentration promoted by the amount of precursor provided in the nucleation and growth of particles.

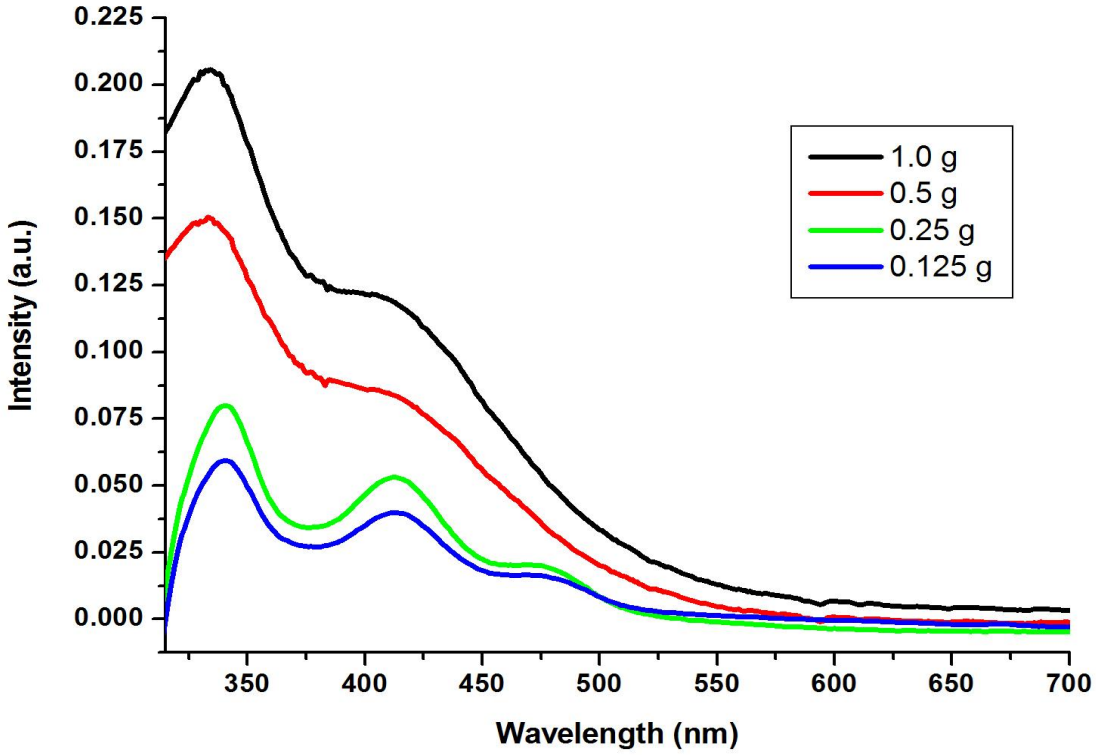

Figure 3.3.5: The absorption spectra of cobalt sulfide prepared at 130 °C for 30 minutes in 5.0 g HDA by using various amount of the complex : (a) 1.0, (b) 0.5, (c) 0.25 and (d) 0.125 g

Figure 3.3.6shows the XRD patterns of the nanoparticles prepared at various concentration of precursor (Table 3.3.2). Figure 3.3.6(a-b) shows five major peaks which are characterized by the (101), (102), (110), (200) and (202) reflections of hexagonal $Co_{1-x}S$ (JCPDS file card No. 42-0826)[91]. The pattern show that the peaks are less pronounced at low precursor concentration as indicated in Figure 3.3.6(b). This is expected as the yield becomes very low as the concentration of the precursor was decreased.

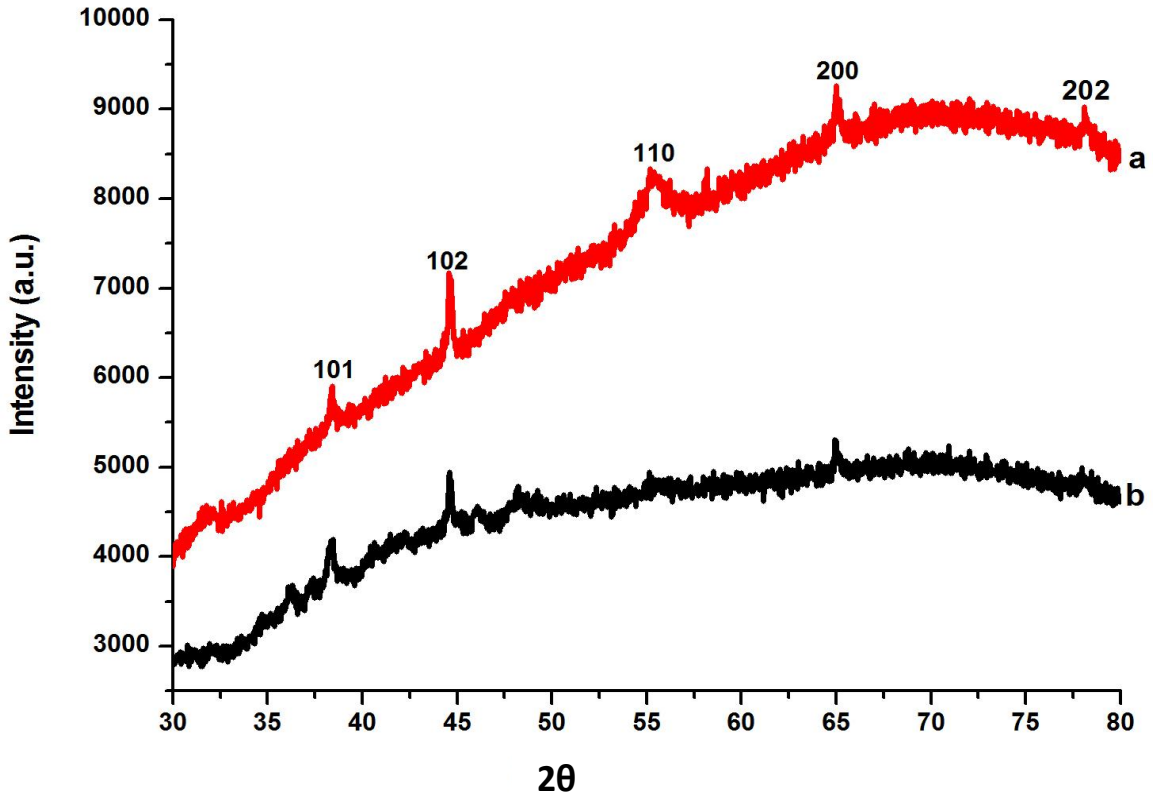

Figure 3.3.6: XRD pattern of $Co_{1-x}S$ nanoparticles prepared at 130 °C for 30 minutes and various amount of the complex II in 5.0 g HDA (a) 1.0 g and (b) 0.125 g.

The TEM images of the compound prepared at various concentrations are shown in Figure 3.3.7(a-d). All the images were composed of irregular spheres, with particle size becoming smaller as the concentration of the precursor was decreased. The average particles were found to be 10.11 ± 1.7, 7.09 ± 1.6, 5.3 ± 0.63 and 2.83 ± 0.83 nm for 1.0, 0.5, 0.25 and 0.125 g of the precursor. This trend is expected, as it is well know that high concentration generate a large number of nuclei, which in turn leads to the formation of large particles by Ostwald ripening. However, low concentration generate few nuclei, which in turn leads to the formation of small particles by the process Ostwald ripening. These results are in good agreement with absorption spectra results as shown in Figure 3.3.5(a- d).

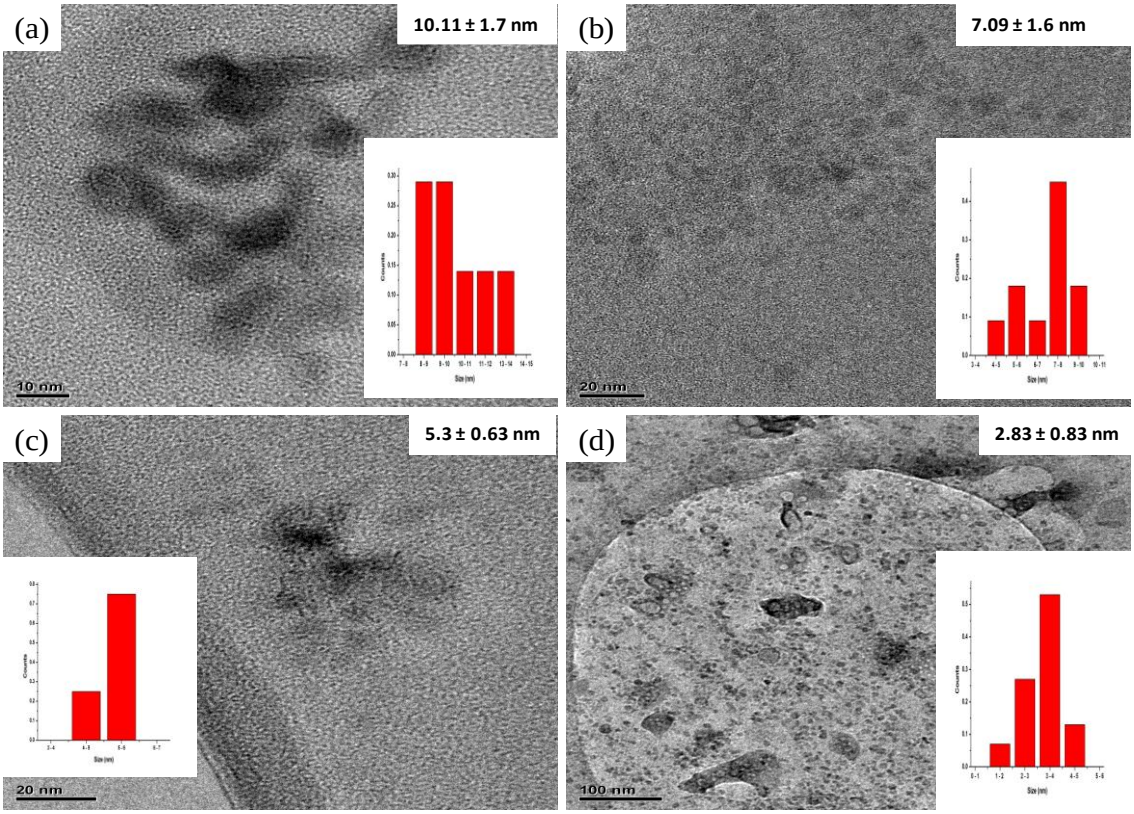

Figure 3.3.7: TEM images of cobalt sulfide prepared at 130 °C for 30 minutes and various amount of the complex in 5.0 g HDA (a) 1.0 g, (b) 0.5 g, (c) 0.25 g, (d) 0.125 g.

3.3.2 Effect of temperature

Temperature is one of the major factors that contribute significantly on size, shape, and phase of the nanoparticle synthesis. The temperature of the reaction has an effect on particle size with higher temperature favouring large size [93]. The reaction temperature affects the shape of the nanoparticles due to the competition between kinetic and thermodynamic regime [90]. Crystallographic phase of the initial seed is one the most critical factors during the nucleation process. Sometimes, the seed have a variety of crystallographic phases, but the stable phase is highly dependent on its environment, most commonly temperature. However, the control of temperature during the nucleation process can result to a crystalline phase of one compound being more favourable over the others [94].

3.3.2 (a) Nanoparticles prepared from complex I

Table 3.3.4 shows reaction conditions for the preparation of Co_xS_y nanoparticles by using different temperature of the reaction and keeping all the other reaction conditions the same.

Table 3.3.4:

*Variation of temperature used for the preparation of Co_xS_y nanoparticlesusing complex **I***

Surfactant (HDA) mass (g)	Complex **I** mass (g)	Temperature °C	Time minutes
5.0	0.5	80	30
5.0	0.5	130	30
5.0	0.5	200	30
5.0	0.5	250	30

The absorption spectra of cobalt sulfide nanoparticles prepared by varying the temperature of the reaction (as outline Table 3.3.3) are shown in Figure 3.3.8(a-d). All the spectra show two major absorption peaks. An excitonic peak at 412.5 nm and a maximum peak at 337.5 nm for nanoparticles prepared at 80 °C (Figure 3.3.8(a)). However, for nanoparticles prepared at 130 °C the spectra show an excitonic peak at 400 nm and a maximum peak at 337.5 nm (Figure 3.3.8(b)). Furthermore, an increase in reaction temperature to 200 °C show an absorption spectra with an excitonic peak at 310 nm, and a maximum peak at 273 nm (figure 3.3.8(c)). The band edges of these nanoparticles were found to be 525, 500 and 343.75 nm for particles prepared at 80, 130 and 200 °C.

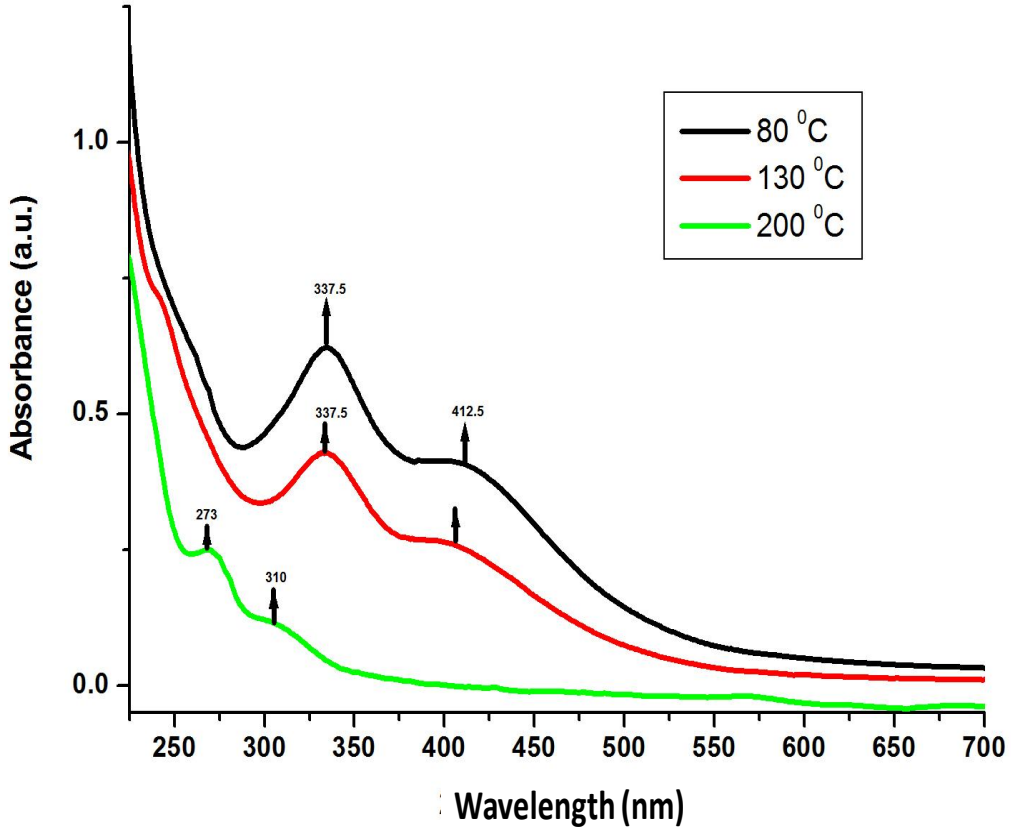

Figure 3.3.8: Absorption spectra of cobalt sulfide prepared by using 0.5 g of the complex, 5.0 g of HDA, for 30 minutes at different temperature (a) 80, (b) 130 and (c) 200 °C.

The TEM images of the Co_xS_y nanoparticles prepared by varying the temperature of the reaction are shown in Figure 3.3.9(a-d). All the images were composed of irregular spheres, with particle size becoming smaller as the temperature of the reaction was increased. The average particles were found to be 8.5 ± 1.1, 7.5 ± 0.72, 5.4 ± 0.53 and 3.3 ± 0.63 nm for 80, 130, 200 and 250 °C, respectively. This trend is in good agreement with absorption spectra results as shown in Figure 3.3.8(a- d). This observed trend could be due the nanoparticles change from one phase to another as the temperature was increase. The sizes of the particle for the new composition were decrease as opposed to the other phase.

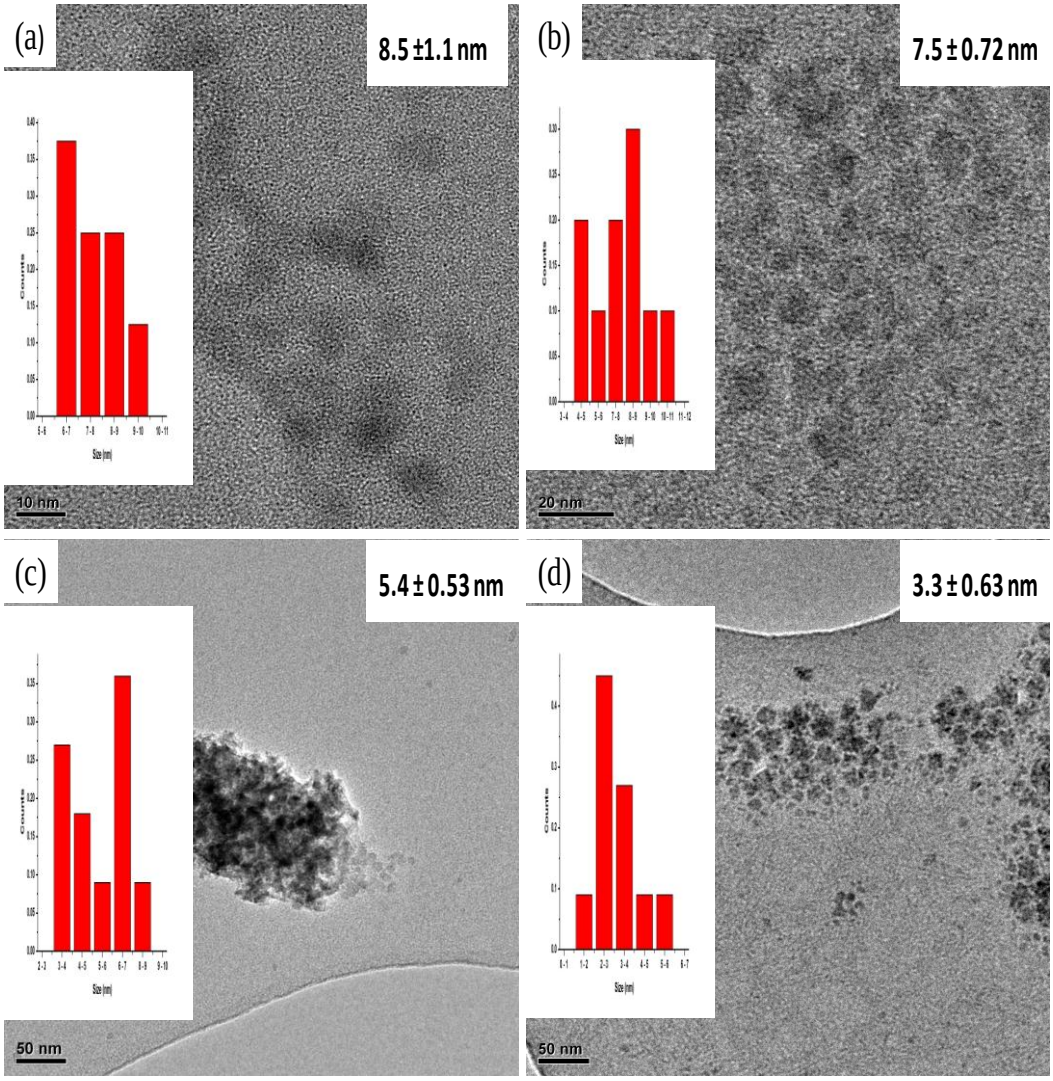

Figure 3.3.9: TEM images of cobalt sulfide prepared by using 0.5 g of the complex, 5.0 g of HDA, for 30 minutes at different temperature (a) 80, (b) 130, (c) 200, and (d) 250 °C.

3.3.2 (b) Nanoparticles prepared from complex II

Table 3.3.5 shows reaction conditions for the preparations of Co_xS_y by using different temperature of the reaction and keeping all the other reaction conditions the same.

Table 3.3.5:

*Variation of temperature used for the preparation of Co_xS_y nanoparticles prepared using complex **II***

Surfactant (HDA) mass (g)	Complex **II** mass (g)	Temperature °C	Time minutes
5.0	0.5	80	30
5.0	0.5	130	30
5.0	0.5	200	30
5.0	0.5	250	30

The absorption spectra of cobalt sulfide nanoparticles prepared by varying the temperature of the reaction (as outline Table 3.3.4) are shown in Figure 3.3.10(a-c). The absorption spectra for nanoparticles prepared at 80 °C show three major peaks, an excitonic peak at 398 nm, 364.2 nm and maximum peak at 328 nm. However, nanoparticles prepare at 200 °C show a peak at 286.2. Furthermore, nanoparticles prepared at 250 °C an excitonic peak at 328.4 nm. The band edges of these nanoparticles were found to be 456.2, 450.2, and 373.4 nm for particles prepared at 80, 200, and 250 °C.

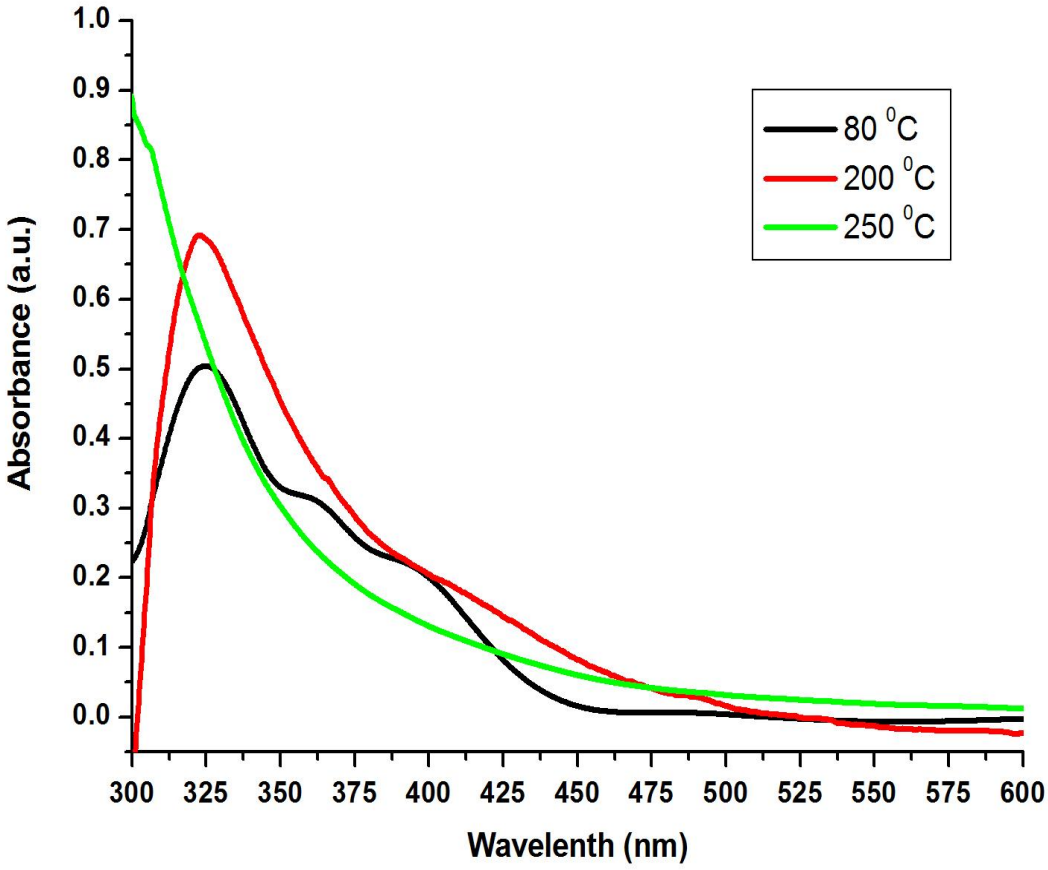

Figure 3.3.10: Absorption spectra of cobalt sulfide prepared by using 0.5 g of the complex, 5.0 g of HDA, for 30 minutes at different temperature (a) 80, (b) 200, and (c) 250 °C.

The TEM images of the Co_xS_y nanoparticles prepared by varying the temperature of the reaction are shown in Figure 3.3.11(a-d). All the images were composed of irregular spheres, with particle size becoming smaller as the temperature of the reaction was increased Figure 3.3.11((b) and (c)). The nanoparticles prepared at 80 and 250 °C, were agglomerated and not clear. This could be due to more capping molecule, but it seems as if there are small particles within those big molecules.

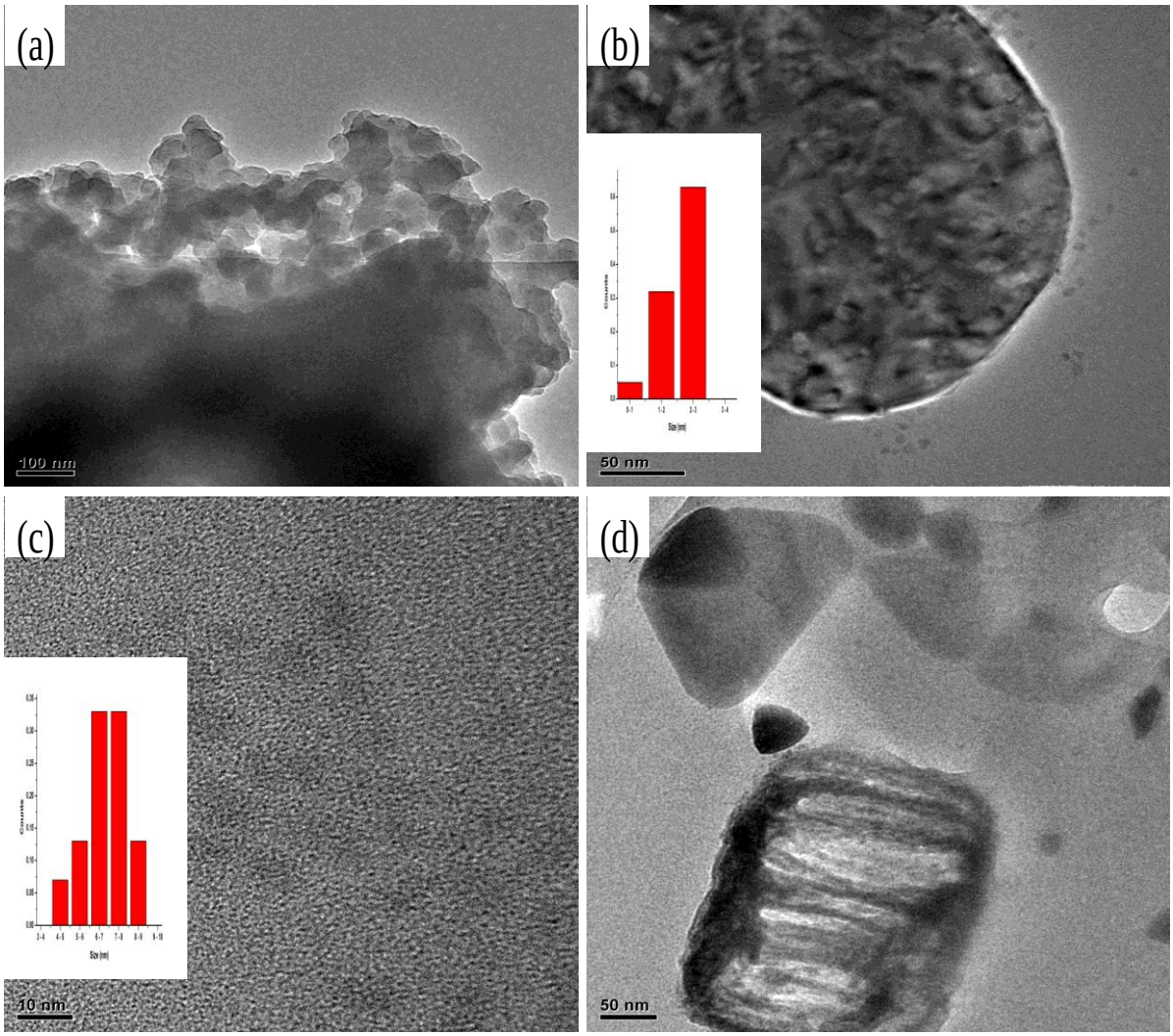

Figure 3.3.11: TEM images of cobalt sulfide nanoparticles prepared at various temp, (a) 80, (b) 130, (c) 200 and (d) 250 °C using complex II.

3.3.3 Effect of time

The time of the reaction is major factor in nanoparticles. The time has a significant effect in both size and shape, but less effect on the phase of the nanoparticle. The time has a profound effect on the size with long time favouring large particles size [91]. The effect of time on the morphology is a bit complex, different morphologies were observed with variation in time of the reaction [91]. The formation of different structure with different reaction times can be

explained by Ostwald ripening process [32]. During a reaction, a large number of nuclei are formed in a short time through Ostwald ripening process. As the reaction proceeds, the aggregate continuously grows in size and density. In succession, the particles with small size dissolve and recrystallize because of their higher surface free energy when compared to with that of the larger ones.

3.3.3(a) Nanoparticles prepared from complex I

Table 3.3.5 shows reaction conditions for the preparations of Co_xS_y by drawing out aliquots at 5 minutes while all the other reaction conditions were kept the same.

Table 3.3.6:

*Variation of time for the preparation of Co_xS_y nanoparticlesusing complex **I***

Surfactant (HDA) mass (g)	Complex**I** mass (g)	Temperature °C	Time minutes
5.0	0.5	130	5
5.0	0.5	130	10
5.0	0.5	130	15
5.0	0.5	130	20
5.0	0.5	130	25
5.0	0.5	130	30

Figure 3.3.12 show the absorption spectra of cobalt sulfide nanoparticles prepared by drawing out aliquots at 5 minutes intervals. The spectra show two major absorption peak at 410 and a maximum at 332 nm for nanoparticle prepared at 5, 10, 25 and 30 minutes time of the reaction. However, nanoparticles prepared at 15 and 20 minute show excitonic peak at 405 nm and major peaks at 330 and 328 nm respectively. The band edges of the nanoparticles prepared at 5, 10, 15, 20, 25 and 30 minutes were estimated to be 532, 542, 539, 526, 550 and

546 nm. The observed trend reveals and increase in particles size as the time was increase with the exception of the particles prepared at 15 and 20 minutes. This could be due to the two internal optical transition or presence of two populations [95].

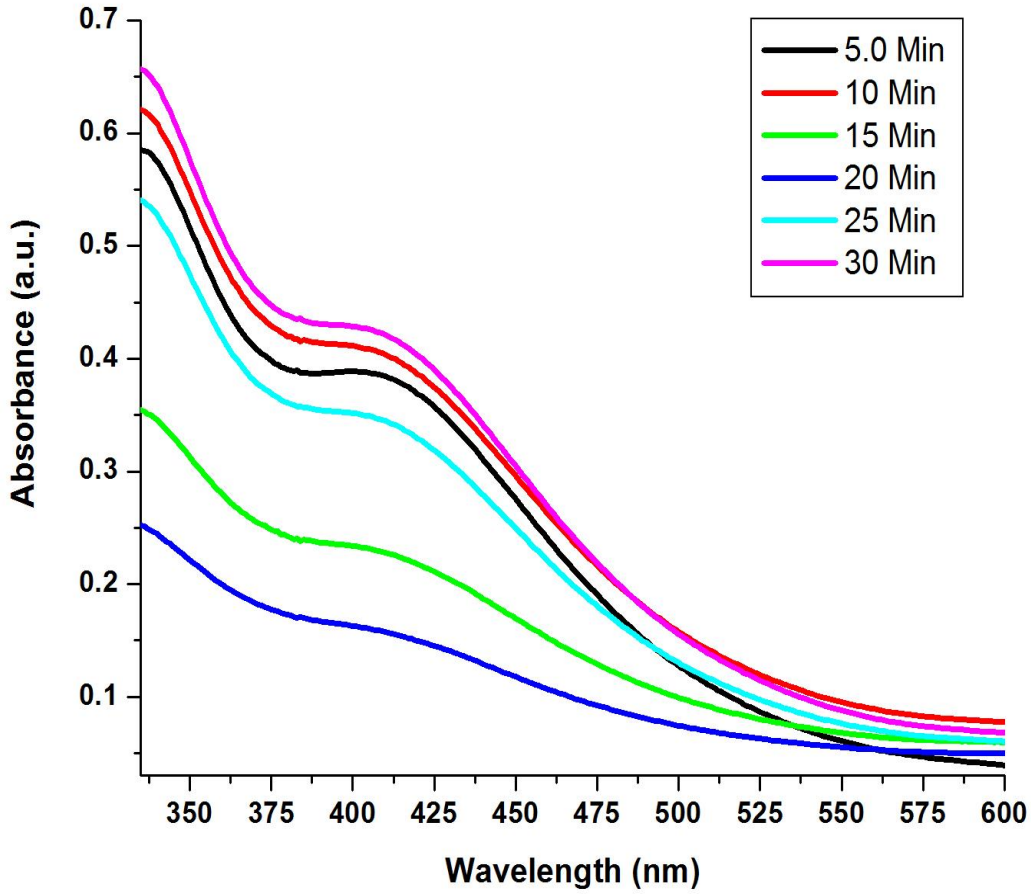

Figure 3.3.12: Absorption spectra of cobalt sulfide prepared using 0.5 g of the complex in HDA (5.0 g), 130 °C and at various time interval of 5 min (5 – 30).

Figure 3.3.13shows the XRD patterns of the nanoparticles prepared by drawing out aliquots at 5 minutes. These diffraction peaks can be indexed to a cubic phase of Co_3S_4, which matches well with the standard XRD pattern (ICSD No. 024212)[96]. The other peaks are due to hexadecylamine, which was used as the capping molecules. This results confirm that the time

of the reaction have less or no significance on the stoichiometry of the reaction. The broad peaks signify small particles sizes.

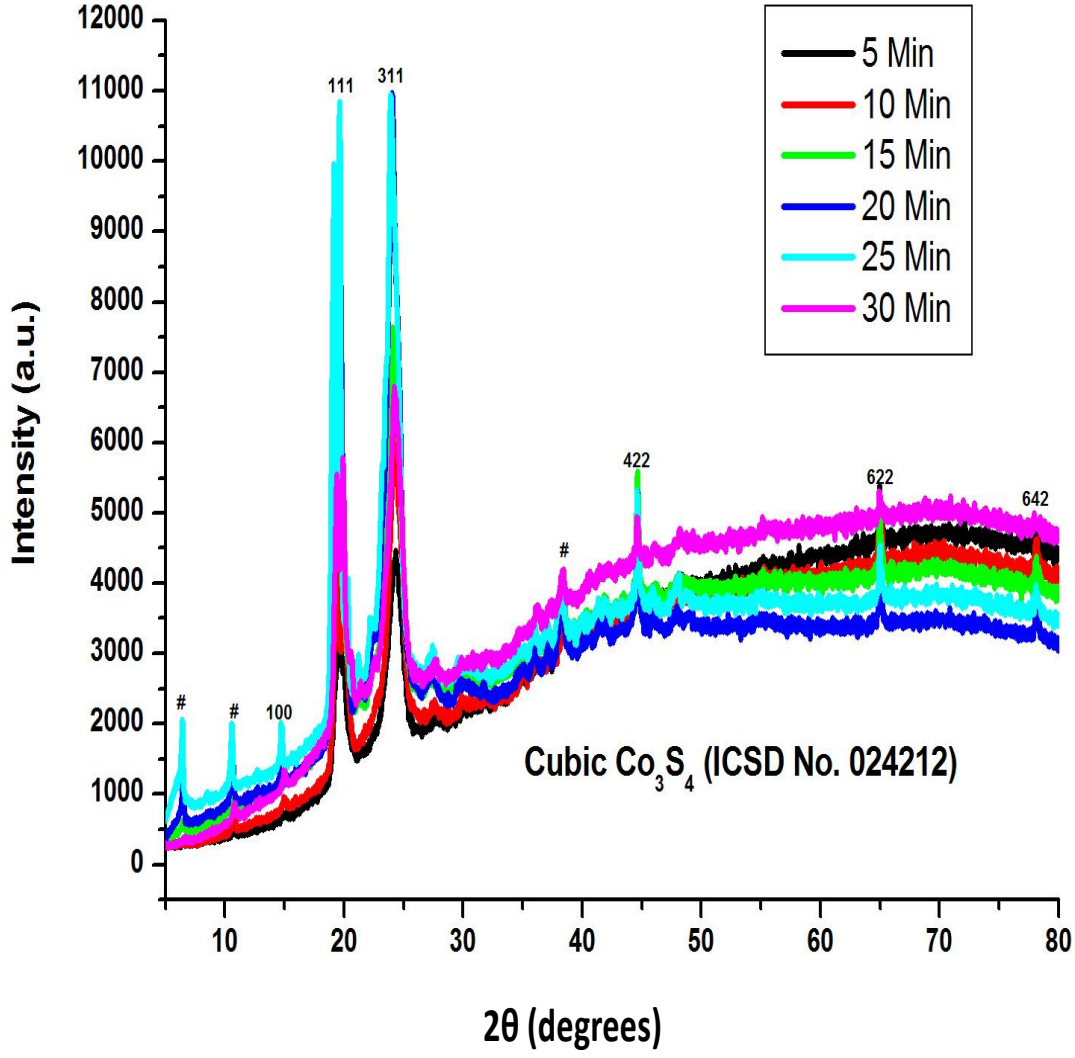

Figure 3.3.13: XRD pattern of cobalt sulfide prepared using 0.5 g of the complex in HDA (5.0 g), 130 °C and at various time interval of 5 min (5 – 30).

3.3.3 (b) Nanoparticles prepared using complex II

Table 3.3.6 shows reaction conditions for the preparations of $Co_xS_y$by drawing out aliquots at 5 minutes while all the other reaction conditions were kept the same.

Table 3.3.7:

*Variation of time for the preparation of Co_xS_y nanoparticlesusing complex **II***

Surfactant (HDA) mass (g)	Complex **II** mass (g)	Temperature °C	Time minutes
5.0	0.5	130	5
5.0	0.5	130	10
5.0	0.5	130	15
5.0	0.5	130	20
5.0	0.5	130	25
5.0	0.5	130	30

Figure 3.3.14 show the absorption spectra of cobalt sulfide nanoparticle prepare at various time of the reactions. All the spectra prepared at various time of the reactions show major peak at 275 nm. The band edges for nanoparticles prepared by drawing out aliquots at 5, 10, 15, 25 and 30 minutes interval were estimated to be 305 nm. The band edges are associated to the particle size of the nanoparticles, which gradually increases with reaction time. The XRD pattern were found to be the same as the one in section 3.3.3(a)

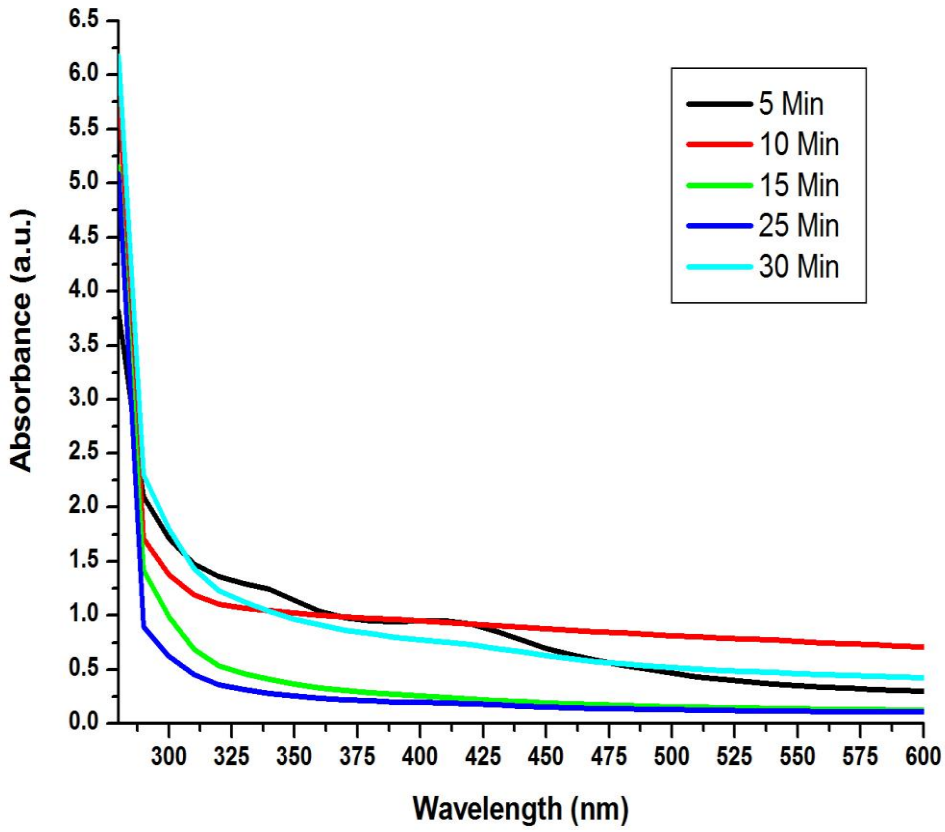

Figure 3.3.14: Absorption spectra of cobalt sulfide nanoparticles prepared using 0.5 g of HDA at 130 °C by varying time from 5 to 30 minutes

3.4 Conclusions

Cobalt sulfide nanoparticles were successfully synthesized by thermal decomposition of diethyldithiocarbamate and tetramethylthiuram disulfide complexes (**I** and **II**) in the presence of hexadecylamine capping agent. Optical properties revealed that the study of concentration on particles havemore effect on the size of the nanoparticles. This was confirmed by the decrease in the band edge and emission maximum of the nanoparticle prepared by decreasing the concentration of the precursors. The TEM results show that the nanoparticles prepared were dominated by irregular sphere with average particle size of 29–3 nm. The results depict

that size of the nanoparticles is more dependent on the concentration of the complex of the reaction. The XRD results showed that the nanoparticles prepared by using complex I was cubic phase of Co_3S_4, however were complex II used the results was confirmed to hexagonal phase of $Co_{1-x}S$.

The temperatures of the reaction have a significant effect on the rate of the reaction that will affect the size and shape of the nanoparticles. This effect was confirmed by absorption spectra of nanoparticles prepared at various temperatures of the reactions. The spectra shows that absorption maximum and band edge shift to lower wavelength as the temperature of reaction was progressively increased. This trend is associated to the decrease in particles size of the prepared nanoparticles. TEM images further confirmed that the particles size of the prepared nanoparticles was progressively decreased as the temperature was increased. Irregular spheres with an average particle of 10–4 nm dominated the images.

Time taken for the reaction to be completed is one of the most important parameter of the reaction. A series of nanoparticles were prepared by drawing aliquots at different time interval. The absorption spectra for nanoparticle prepared at 5 minutes interval showed that nanoparticles developed into stages as time elapsed. The variation in time showed less or no effect on the stoichiometry of the nanoparticles as this was revealed by XRD pattern of the prepare nanoparticles. The XRD results confirmed cubic phase of Co_3S_4 for nanoparticles prepared at various time interval.

CHAPTER FOUR

SYNTHESIS AND CHARACTERIZATION OF COPPER SULFIDE NANOPARTICLES USING TETRAMETHYLTHIURAM DISULFIDE AND DIETHYLDITHIOCARBAMATE COMPLEXES OF COPPER

4.1 Background

Copper complexes based on thiocarbamates were easily prepared by refluxing and characterized by a combination of IR, NMR spectroscopy as well as elemental analysis. The complexes were found to be relatively stable, crystalline product with good yields. The bonding of the ligand through sulfur atom/s to the metal copper provides a useful feature for thermolytic products of metal sulfide. When the reaction is performed under controlled conditions the nucleation and growth of particles can be achieved. Dithiocarbamates tends to bind to the metals through the two sulfur atoms in a similar way to the thiuram ligand. Both are bidentate ligands. As observed in the TGA curve (Figure 2.3) the copper complexes decomposed gradually to produce the percentage of the component remaining that conforms to the copper sulfide for the dithiocarbamate and copper residue in the thiuram complex. The formation of copper sulfide from thiuram complex is not thermally stable and eventually converts into copper. In this chapter the conditions, temperature, time and the amount of the precursor used are investigated in the synthesis of copper sulfide nanoparticles. The capping molecule used was hexadecylamine and other conditions were varied as per factor under consideration. The conditions were varied to ensure that the stoichiometry of copper sulfide was investigated from the effect of temperature, concentration and time as to how each is likely to influence the stoichiometry of copper sulfide nanoparticles.

Copper sulfide nanoparticles have different stoichiometry that includes CuS, $Cu_{1.96}S$, $Cu_{1.94}S$, $Cu_{1.9}S$, $Cu_{1.8}S$, Cu_9S_5, $Cu_{7.2}S_4$, Cu_7S_4 and CuS_2 [95]. Copper sulfide nanoparticles are known for the excellent properties as semiconductor material. These compounds are can be used as p-type semiconductors in solar cells, as optical filters, and superionic materials [97].

This study focuses on the modulation of synthetic parameters in order to influence the size, structure, composition and arrangement of copper sulfide nanoparticles. The synthetic procedure followed was thermal decomposition of diethyldithiocarbamate and tetramethylthiuram disulfide complexes of copper in an inert environment in the presence of trioctylphosphine (solvent) and hexadecylamine (capping agent). The reaction condition such as concentration of the precursors, temperature of the reaction, and time growth of the nanoparticles are responsible for the final products.

4.2 Experimental

4.2.1 Materials

The material used is the same as the one outlined in Chapter Three Section 3.2.1.

4.2.2 Instrumentation

The entire instrument used for the characterization of copper sulfide nanoparticles has been outlined in Chapter Three Section 3.2.2.

4.2.3 Preparation of the nanoparticles

(a) Preparation of copper sulfide using complex III

Copper sulfide nanoparticles were synthesized at various concentrations of complex, time of the reaction and temperature in about 5.0 g HDA. For the first part, different masses of the complex **III** (1.0, 0.5, 0.25 and 0.125 g) were dissolved into trioctyphosphine (TOP) (5 ml) separately. Each solution was injected into hot hexadecylamine (HDA) (5.0 g) which was heated and maintained at temperature of 130 °C under nitrogen atmosphere. This reaction was maintained at this temperature with constant starring for 30 minutes. Then, the solution was

cooled to 70 °C and an excess of methanol was added. The precipitate formed were isolated by centrifugation, washed with methanol three times to remove some of the capping agent and dried in open air environment.

For the second part of the experiment, the reaction was the same as the one of the first except that the mass of complex **III** was 0.5 g, time of the reaction was 30 minutes and temperatures was kept at 80, 130, 200, 250 °C for each reaction.

For the third part of the experiment, the reaction was also the similar to the one of first part except that the mass of the complex **III** was 0.5 g, temperature was kept at 130 °C and aliquots were drawn at 5 minutes interval (5, 10, 15, 20, 25, 30 minutes).

(b) Preparation of copper sulfide using complex IV

In preparation of copper sulfide using complex **IV** as single-source precursor with all the conditions were the same as the one outlined in section 4.2.3 (a).

4.3 Results and discussions

The reaction parameter such as concentration of the precursor, temperature of the reaction and time of the reaction showed a profound effect on the size, morphology and stoichiometry of the reaction.

4.3.1 Effect of concentration

The effect of the concentration of the precursor on the preparation of the nanoparticles has been outline in Chapter Three Section 3.3.1.

(a) Nanoparticles prepared from complex III

Table 4.3.1 shows the reaction parameters for the preparation of Cu_xS_ynanoparticlesby using various concentrations of complex **III**, while no other parameters were changed.

Table 4.3.1 :

*Variation of concentration in the the preparation of Cu_xS_y nanoparticlesfrom complex **III***

Surfactant (HDA) mass (g)	Complex **III** mass (g)	Temperature °C	Time minutes
5.0	1.0	130	30
5.0	0.5	130	30
5.0	0.1	130	30
5.0	0.05	130	30

Copper sulfide is known to have an optical band gap of 1078.26 nm [98]. The absorption spectra of copper sulfide nanoparticles prepared at different concentrations of complex **III** (Table 4.3.1) are shown in Figure 4.3.1(a-d). Copper sulfide nanoparticles prepared at high concentration (1.0 g) show a major absorption peak at 330 nm and a band edge of 450 nm. However, when the concentration of the precursor was decreased to 0.5 g, the spectra show an excitonic peak at 380 nm and a band edge of 448 nm. Furthermore, when the concentration of the precursor was decreased to 0.25 g, the spectra show a maximum excitonic peak at 380 nm and a band edge of 446 nm. When the concentration of the precursor was decreased to 0.125 g, the absorption spectra show an excitonic peak at 290 and a band edge of 310 nm. The particle size trend conforms with the decrease from the highest to the lowest concentration promoted by the amount of precursor provided in the nucleation and growth of particles. This resulted to an increase in the band gap energy of the nanoparticles.

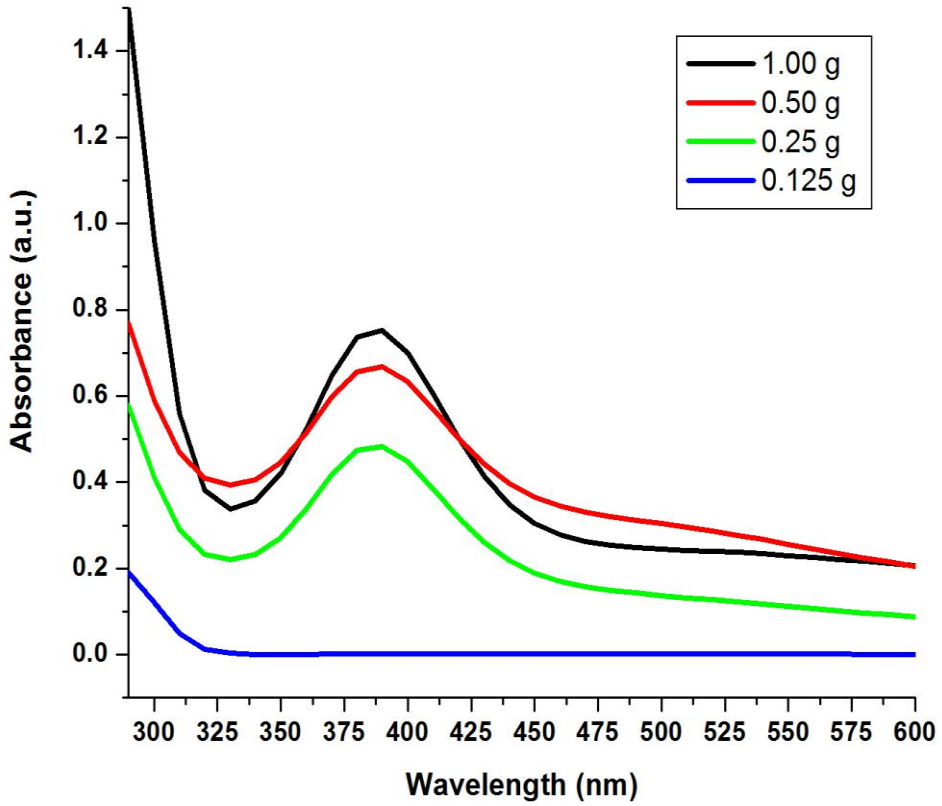

Figure 4.3.1: The absorption spectra of copper sulfide prepared at 130 °C for 30 minutes in 5.0 g HDA by using various amount of the complex : (a) 1.0, (b) 0.5, (c) 0.25 and (d) 0.125 g

The XRD patterns of the nanoparticles prepared at various concentration of precursor were shown in Figure 4.3.2(a-d). The pattern show five major peaks at 32.3°, 31.7°, 46.3°,48.6° and 54.1° which can be indexed to orthorhombic $Cu_{1.97}S$ [JCPDS file card no. 20-0365][98]. The peak become less visible as the concentration of the precursor was decrease that is due to the yield decreasing with concentration.These results show that the variation in concentration does not affect the stoichiometry of the prepared nanoparticles.

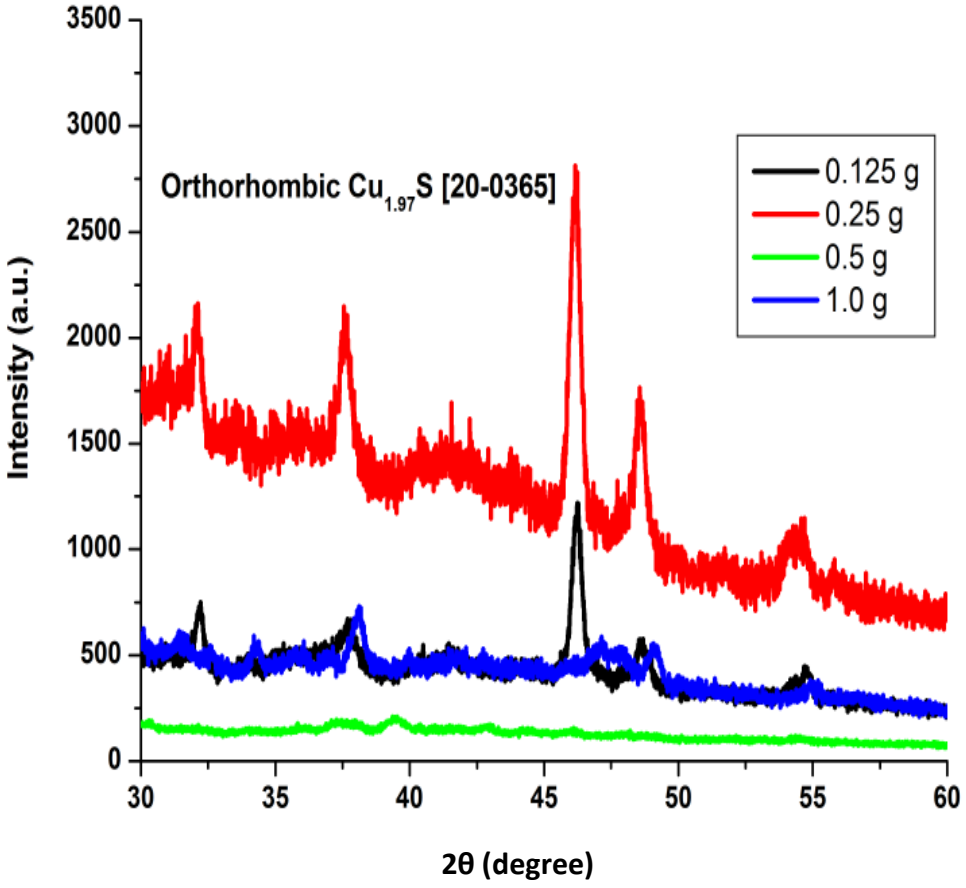

Figure 4.3.2: XRD pattern of copper sulfide prepared at 130 °C for 30 minutes in 5.0 g HDA by using various amount of the complex : (a) 1.0, (b) 0.5, (c) 0.25 and (d) 0.125 g

Figure 4.3.3 (a-d) shows the TEM images of the copper sulfide nanoparticles prepared at various concentrations. The images were dominated by spheres, with an average particle size of 8.42 ± 2.15, 7.26 ± 1.21, 5.77 ± 1.13 and 2.49 ± 0.52 nm. The TEM results show that the particle size was decreasing with concentration. This trend is in good agreement with the literature, high concentration generate a large number of nuclei, which in turn leads to the formation of large particles by Ostwald ripening. However, low concentration generate few nuclei, which in turn leads to the formation of small particles by the process Ostwald ripening.

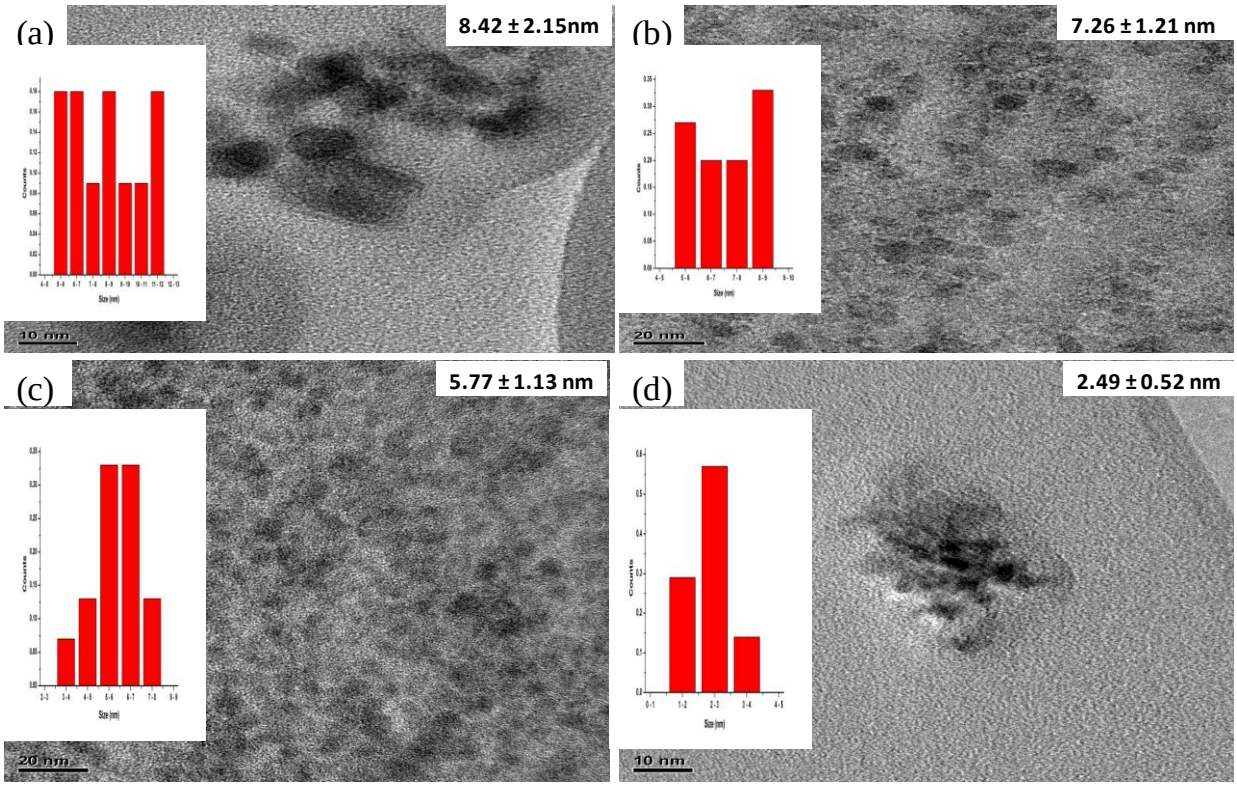

Figure 4.3.3: The XRD patterns of copper sulfide prepared at 130 °C for 30 minutes in 5.0 g HDA by using various amount of **the complex : (a) 1.0, (b) 0.5, (c) 0.25 and (d) 0.125 g**

4.3.1 (b) Nanoparticles prepared from complex IV

Table 4.3.2 shows reaction conditions for the preparations of $Cu_xS_y$by using various concentrations of complex **IV**, while no other parameters were changed.The amount of the complex was varied from 0.125 g to 1.0 g in a similar amount of 5.0 g of hexadecylamine.

Table 4.3.2

*Variation of the amount of complex **IV** for the preparation of Cu_xS_y nanoparticles*

Surfactant (HDA) mass (g)	Complex **IV** mass (g)	Temperature °C	Time minutes
5.0	1.0	130	30
5.0	0.5	130	30
5.0	0.25	130	30
5.0	0.125	130	30

The absorption spectra of copper sulfide nanoparticles prepared at different concentrations of complex **IV** (Table 4.3.2) are shown in Figure 4.3.4(a-d). All the spectra show two major absorption peaks, an excitonic peak at 290 nm and a maximum peak at 380 nm. The band edges of these nanoparticles were found to be 480, 470, 460 and 450 nm for particles prepared at 0.1, 0.5, 0.25 and 0.125 g of the precursor concentration. The particle size trend conforms with the decrease from the highest to the lowest concentration promoted by the amount of precursor provided in the nucleation and growth of particles.

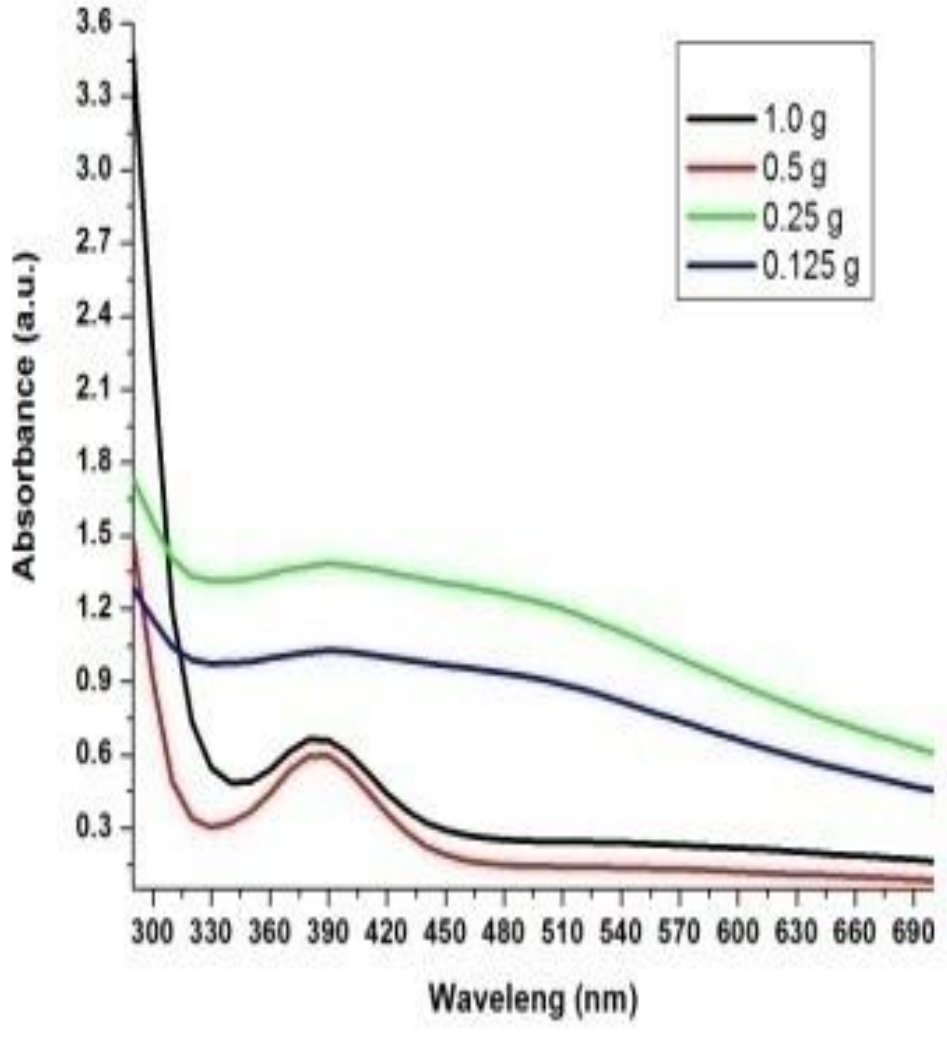

Figure 4.3.4: The absorption spectra of copper sulfide prepared at 130 °C for 30 minutes in 5.0 g HDA by using various amount of the complex : (a) 1.0, (b) 0.5, (c) 0.25 and (d) 0.125 g

The XRD patterns of the nanoparticles prepared at various concentration of precursor are shown in Figure 4.3.5(a-d). The pattern show five major peaks at 32.3°, 37.7°, 46.3°,48.6° and 54.1° which can be indexed to orthorhombic $Cu_{1.97}S$ [JCPDS file card no. 20-0365][98]. The peak become less visible as the concentration of the precursor was decrease which is due

to the yield decreasing with concentration. The results show that the variations in concentration have a little effect on the phase composition.

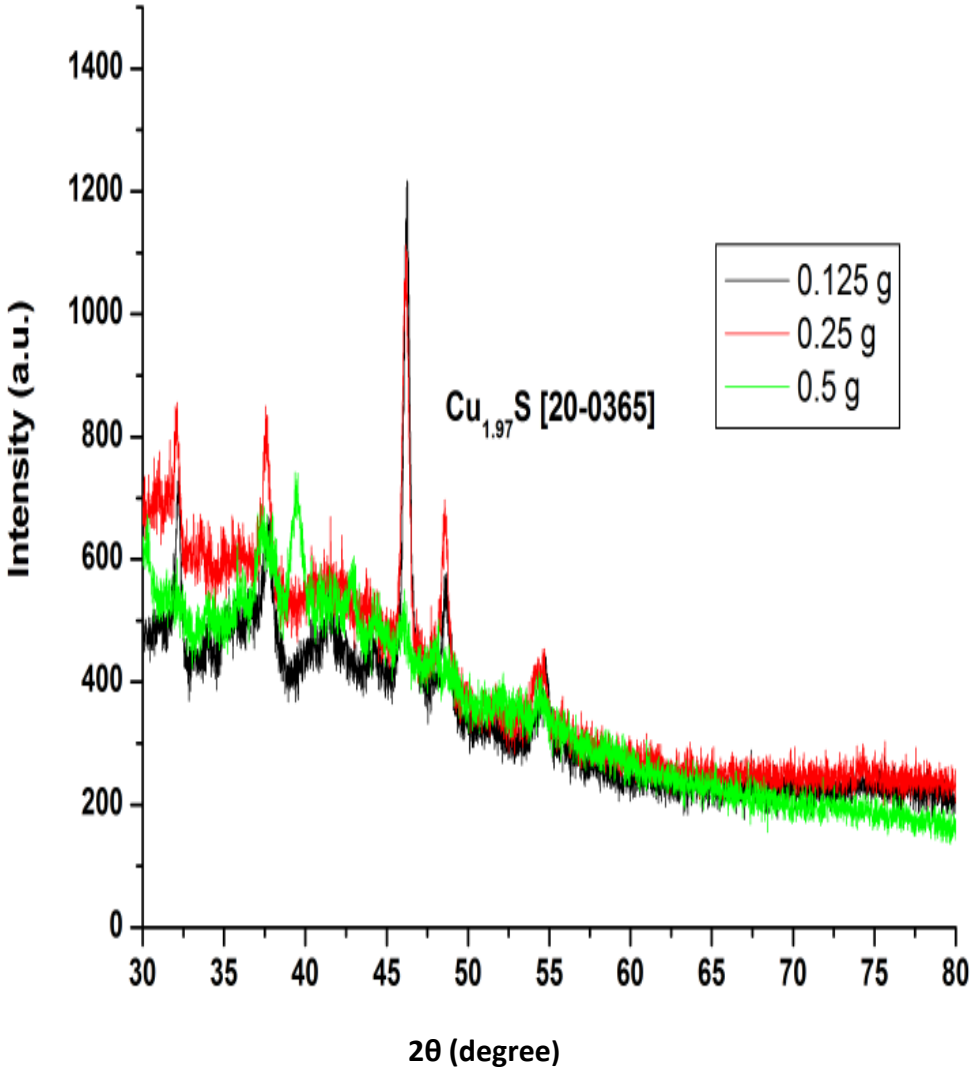

Figure 4.3.5: XRD pattern of copper sulfide prepared at 130 °C for 30 minutes in 5.0 g HDA by using various amount of the complex : (a) 1.0, (b) 0.5, (c) 0.25 and (d) 0.125 g

Figure 4.3.6 (a-d) show the TEM images of the copper sulfide nanoparticles prepared by varying the concentration of the precursor. The images of the prepared nanoparticles were

dominated by spheres, with particle size decreasing as the concentration of the precursor was decreased. The average particles were found to be 7.76 ± 2.04, 5.38 ± 0.34, 4.59 ± 1.01 and 3.40 ± 0.84 nm. The observed trend could explained by Ostwald ripening. It is widely known that high concentration generates a large number of nuclei, which leads to the formation of large particle size. However, low concentration generate few nuclei, which in turn leads to the formation of small particles by the process Ostwald ripening. These results are in good agreement with absorption spectra results as shown in Figure 4.3.4(a- d).

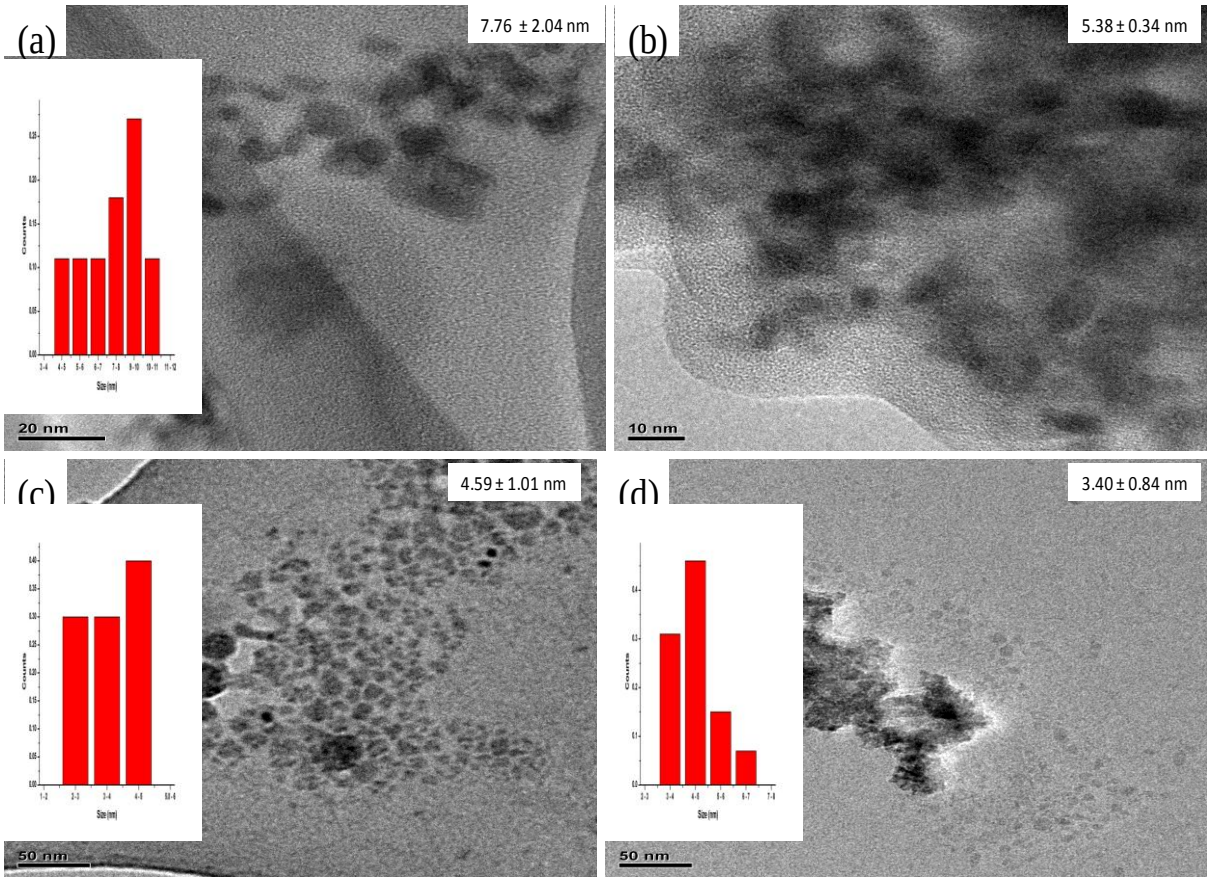

Figure 4.3.6: TEM image of copper sulfide prepared at 130 °C for 30 minutes in 5.0 g HDA by using various of the complex IV: (a) 1.0, (b) 0.5, (c) 0.25 and (d) 0.125 g

4.3.2 Effect of temperature

The role of temperature in the reaction hasbeen outlined in Chapter Three Section 3.3.2. The temperature in the synthesis of the nanoparticles has more effect on the thermodynamic growth of the nanoparticles.

4.3.2 (a) Nanoparticles prepared from complex III

Table 4.3.3 shows reaction conditions for the preparations of Cu_xS_y by using different temperature of the reaction and keeping all the other reaction conditions constant.

Table 4.3.3:

*Variation of temperature used for the preparation of Cu_xS_y nanoparticlesusing complex **III***

Surfactant (HDA) mass (g)	Complex **III** mass (g)	Temperature °C	Time minutes
5.0	0.5	80	30
5.0	0.5	130	30
5.0	0.5	200	30
5.0	0.5	250	30

Figure 4.3.7(a-d) show the absorption spectra of copper sulfide nanoparticles prepared at various temperature of the reaction. For the nanoparticles prepared at 80 °C, the spectra show an excitonic peak at 380 nm and a maximum peak at 280 nm. However, when the temperature was increased to 130 °C, we observed an excitonic peak at 380 nm and maximum peak at 290 nm. For nanoparticles prepared at high temperature (200 and 250 °C), the spectra show a maximum peak at 280 nm. The band edges were found to be 450, 460, 350, 340 nm for the nanoparticles prepared at 80, 130, 200 and 250 °C respectively. This is in contrast to the trend

observe when the temperature of reaction is increase. This might be because nanoparticles changing the phases as the temperatures were increased.

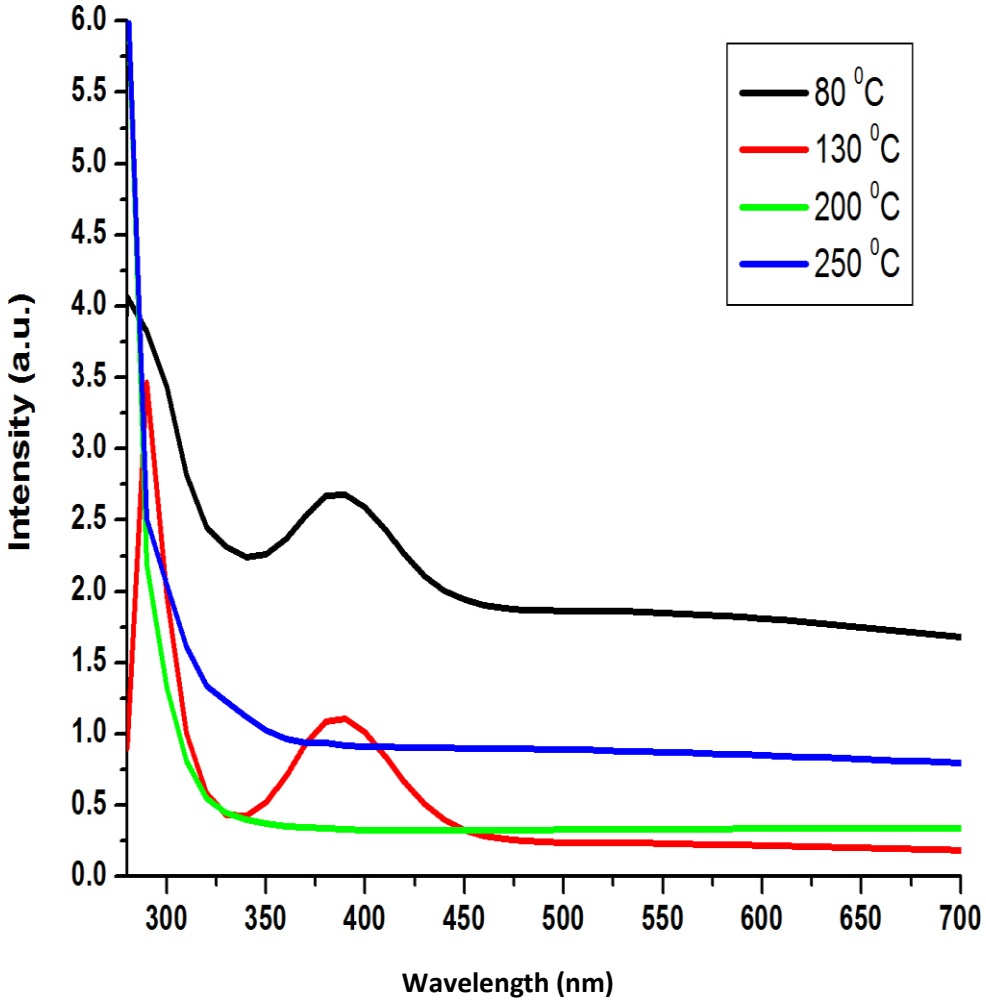

Figure 4.3.7: Absorption spectra of copper sulfide prepared by using 0.5 g of the complex, 5.0 g of HDA, for 30 minutes at different temperature (a) 80, (b) 130, (c) 200 and (d) 250 °C

The XRD patterns for nanoparticles prepared by varying the temperature of the reaction are given in Figure 4.3.8(a-d). For the nanoparticles prepared at low temperatures (80 °C), show XRD pattern which were indexed to be $Cu_{1.8}S$ [JCPDS file card no. 47-1748] [98]. For nanoparticles prepared at high temperatures (130, 200, 250 °C), the XRD pattern were found to be due to orthorhombic $Cu_{1.97}S$ [JCPDS file card no. 20-0365][98].

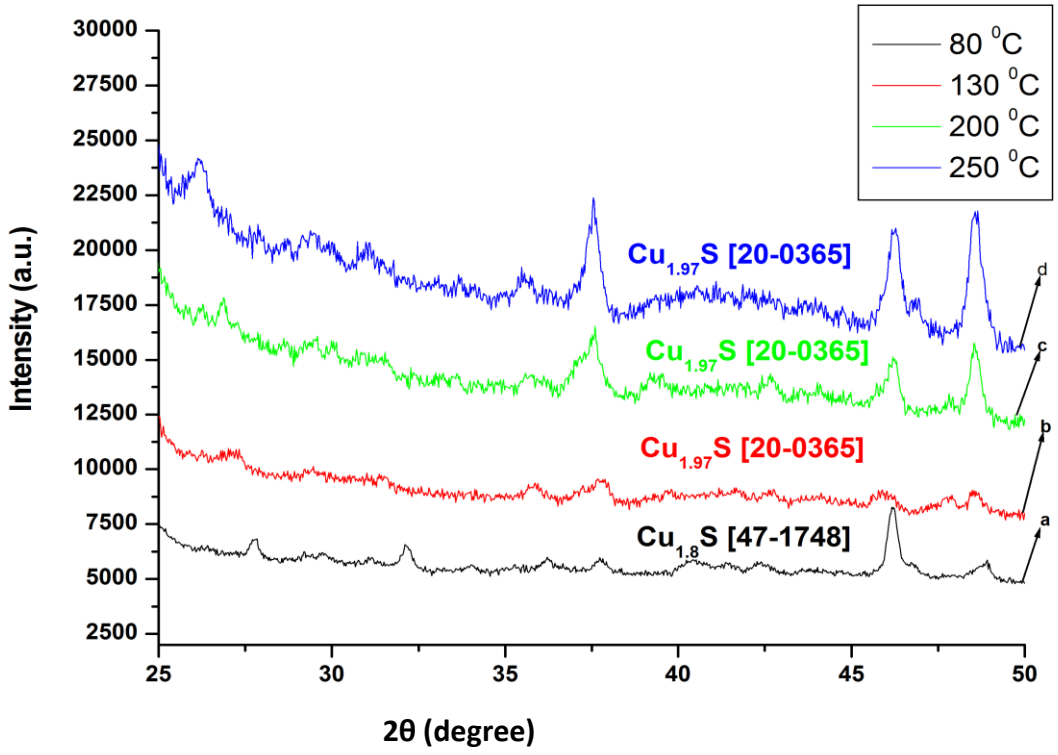

Figure 4.3.8: XRD pattern copper sulfide prepared by using 0.5 g of the complex, 5.0 g of HDA, for 30 minutes at different temperature (a) 80, (b) 130 and (c) 200 and (d) 250 °C

Figure 4.3.9(a-d) show the TEM images of nanoparticles prepared by varying the temperature of the reaction. The nanoparticles prepared at low temperatures (80, 130 °C) show irregular

spheres with an average particle size of 5.31 ± 0.91 nm and 7.72 ± 1.90 nm respectively. However, for nanoparticles prepared at relatively high temperatures (200 ℃), the TEM image show agglomerated triangular shape nanoparticles. At high temperature 250 ℃, the image of the nanoparticles was found to be dominated by hexagonal shaped nanoparticles.

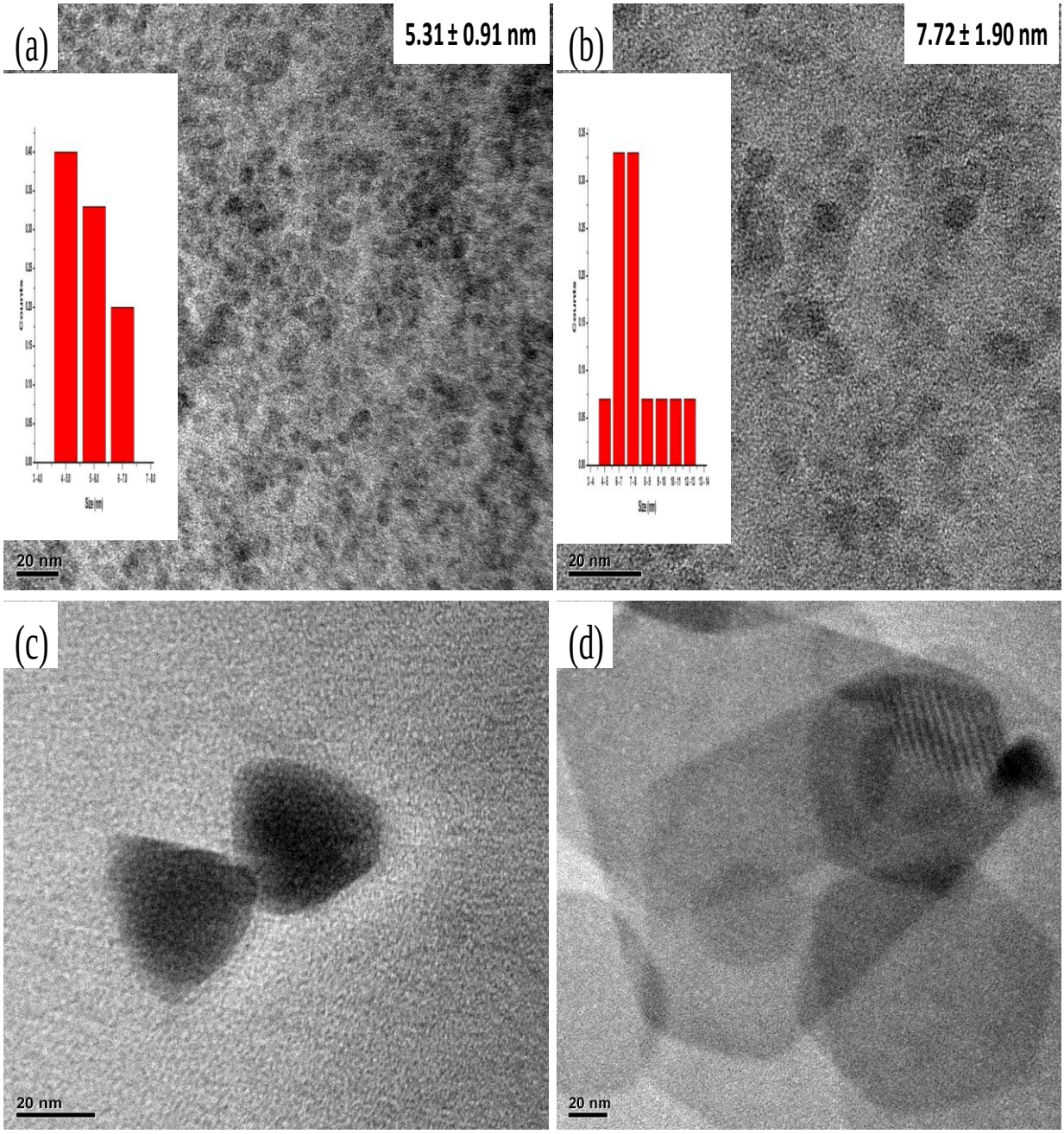

Figure 4.3.9: TEM images of copper sulfide prepared by using 0.5 g of the complex, 5.0 g of HDA, for 30 minutes at different temperature (a) 80 °C, (b) 130 °C, (c) 200 °C, and (d) 250 °C.

4.3.2 (b) Nanoparticles prepared from complex IV

Table 4.3.4 shows reaction conditions for the preparations of Cu_xS_y by using different temperature of the reaction and keeping all the other reaction conditions constant.

Table 4.3.4

*Variation of temperature used for the preparation of Cu_xS_y nanoparticles prepared using complex **IV***

Surfactant (HDA) mass (g)	Complex **IV** mass (g)	Temperature °C	Time minutes
5.0	0.5	80	30
5.0	0.5	130	30
5.0	0.5	200	30
5.0	0.5	250	30

The absorption spectra of copper sulfide nanoparticles prepare at various temperature of the reaction are given in Figure 4.3.10(a-c). The band edges were found to be 330, 340, 350, 390 nm for the nanoparticles prepared at 80, 130, 200 and 250 °C respectively. This observed trend is due to nanoparticles becoming bigger as the temperature is increased. This result show that the increase in temperature resulted in the formation of large particles, which are more stable by Ostwald, ripening process. The temperatures affect thesize, shape and the composition of the nanoparticles. This is expected as the rate of reaction change dramatically with temperature.

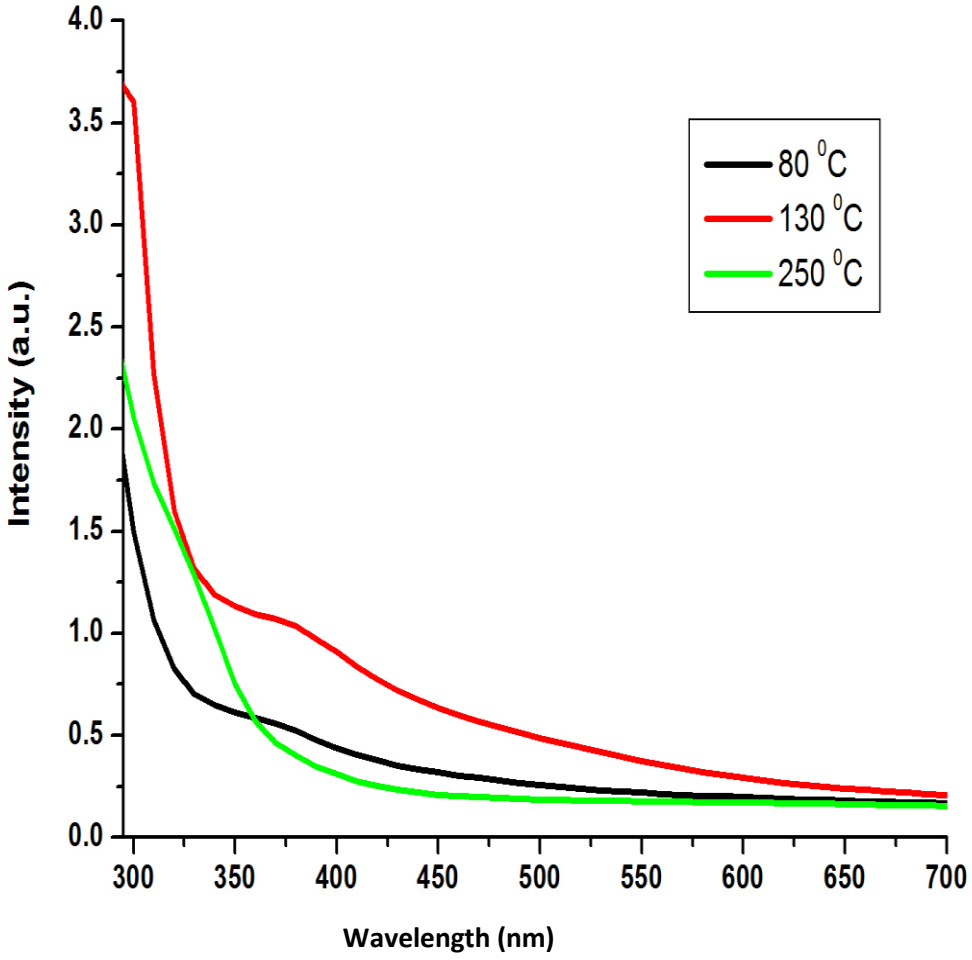

Figure 4.3.10: Absorption spectra of copper sulfide prepared by using 0.5 g of the complex, 5.0 g of HDA, for 30 minutes at different temperature (a) 80, (b) 130 and (c) 250 °C.

The XRD patterns of the nanoparticles prepared at various temperatures of the reactions are shown in Figure 4.3.11(a-d). The pattern show five major peaks at 32.3°, 31.7°, 46.3°,48.6° and 54.1° which can be indexed to orthorhombic $Cu_{1.97}S$ [JCPDS file card no. 20-0365] [98]. The peak become more visible as the temperature of the reaction was increased. This due to the nanoparticles form crystals at high temperatures.

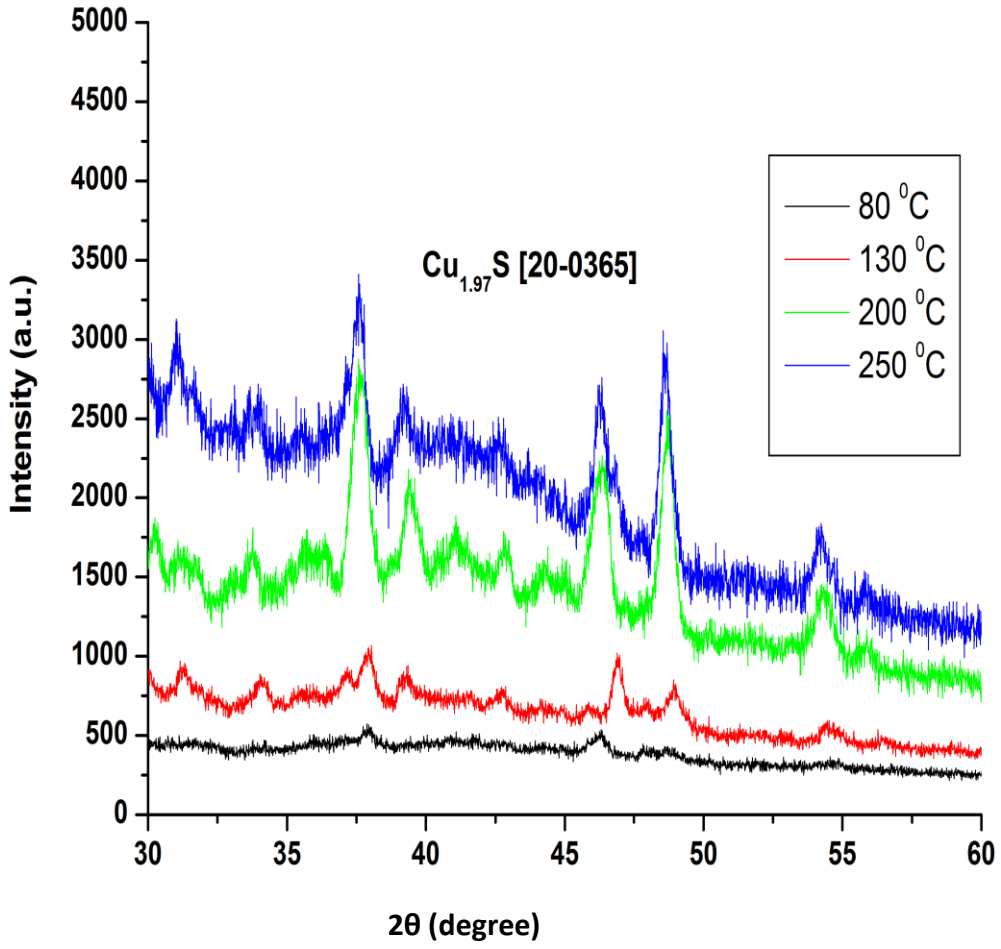

Figure 4.3.11: XRD pattern of copper sulfide prepared by using 0.5 g of the complex, 5.0 g of HDA, for 30 minutes at different temperature (a) 80, (b) 130 , (c) 200 , (d) 250 °C.

The TEM images of the compound prepared at various temperatures are shown in Figure 4.3.12(a-d). For the nanoparticles prepared at low temperature (80, 130 °C), the TEM image show irregular nanoshere which are agglomerated. However, at 200 °C the image were composed of a mixture of hexagonal and triangular nanoparticle with increased size. Furthermore, when the temperature was increased to 250 °C, the images were dominated by hexagonal shaped nanoparticles.

4.3.3 Effect of time

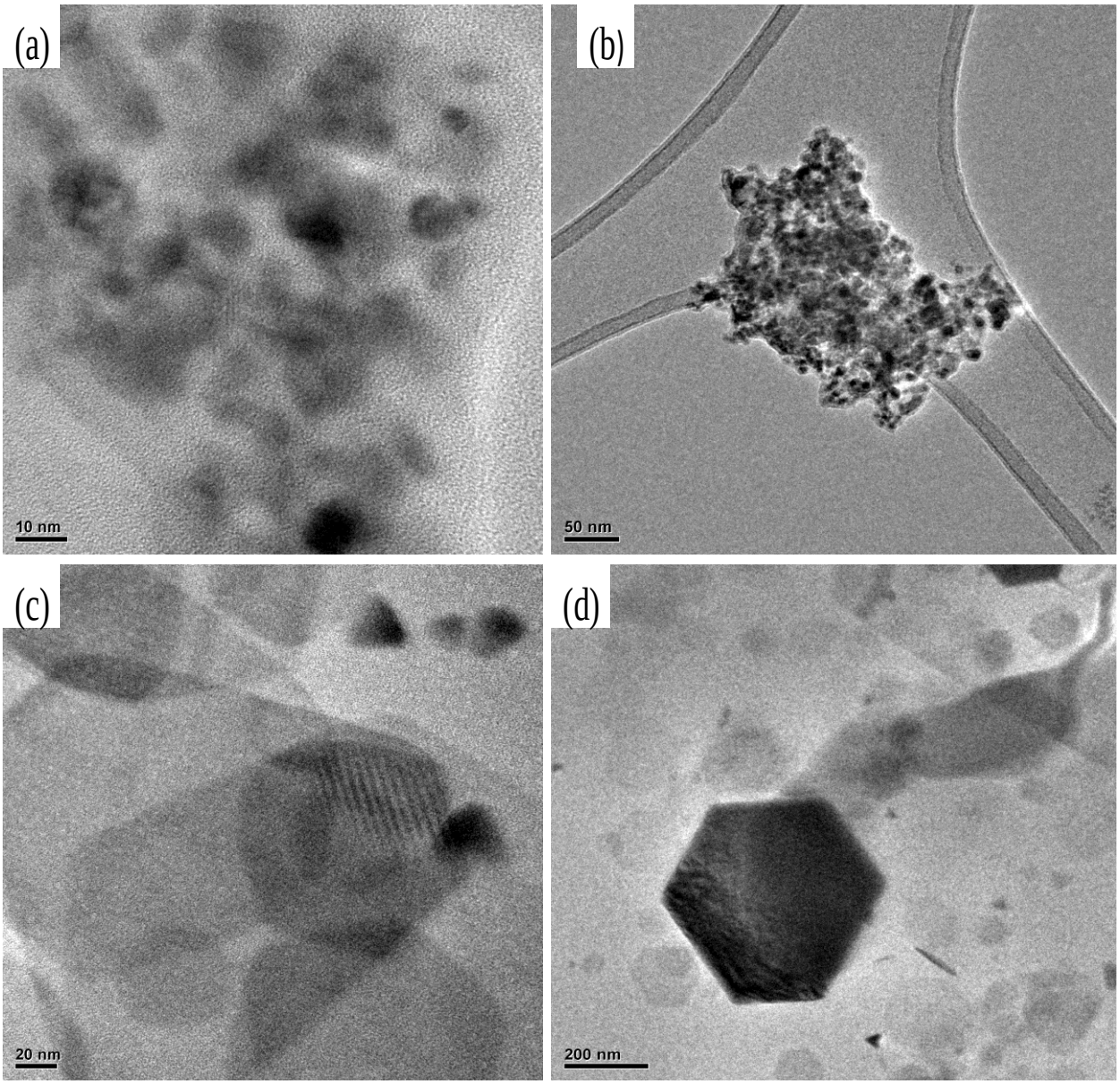

Figure 4.3.12: TEM images of copper sulfide prepared by using 0.5 g of the complex, 5.0 g of HDA, for 30 minutes at different temperature (a) 80 °C, (b) 130 °C, (c) 200 °C, and (d) 250 °C.

The effect of time in reaction has outlined in section 3.3.3. The literature has reported that prolonged time yields larger particle size due to the ostward ripening process [95]. During a typical reaction procedure, a large number of nuclei are formed in a short time through Ostwald ripening process. As the reaction is prolonged, the aggregate continuously grows in size and density to form preferred morphology through the interaction between the capping molecules and the particles by Van der Waals force and intermolecular hydrogen bonds.

4.3.3 (a) Nanoparticles prepared from complex III

Table 4.3.5 shows reaction conditions for the preparations of $Cu_xS_y$by drawing out aliquots at 5 minutes while all the other reaction conditions were kept the same.

Table 4.3.5:

*Variation of time for the preparation of Cu_xS_y nanoparticlesusing complex **III***

Surfactant (HDA) mass (g)	Complex **III** mass (g)	Temperature °C	Time minutes
5.0	0.5	130	5
5.0	0.5	130	10
5.0	0.5	130	15
5.0	0.5	130	20
5.0	0.5	130	25
5.0	0.5	130	30

Figure 4.3.13 show the absorption spectra of copper sulfide nanoparticles prepared by drawing out aliquots at various time interval (5 – 30) minutes. The spectra show an excitonic peak at 270 nm for nanoparticles prepared at 5 and 10 minutes intervals. However, when the reaction was prolonged (15 – 30) minutes, the excitonic peaks were found to be at 290 nm.

The nanoparticles prepared at 5 an 10 minutes show a band edge at 310 and 315 nm respectively. However, all the nanoparticles (15, 20, 25 and 30 minutes) show a band edge at 325 nm. This trend is consistent with the Ostwald ripening process. These results depict that at short time interval, small nanoparticles are formed by small nuclei. However, as the reaction is prolonged, the small nanoparticles dissolve to form large particles, which are more stable, and the process is called Ostwald ripening.

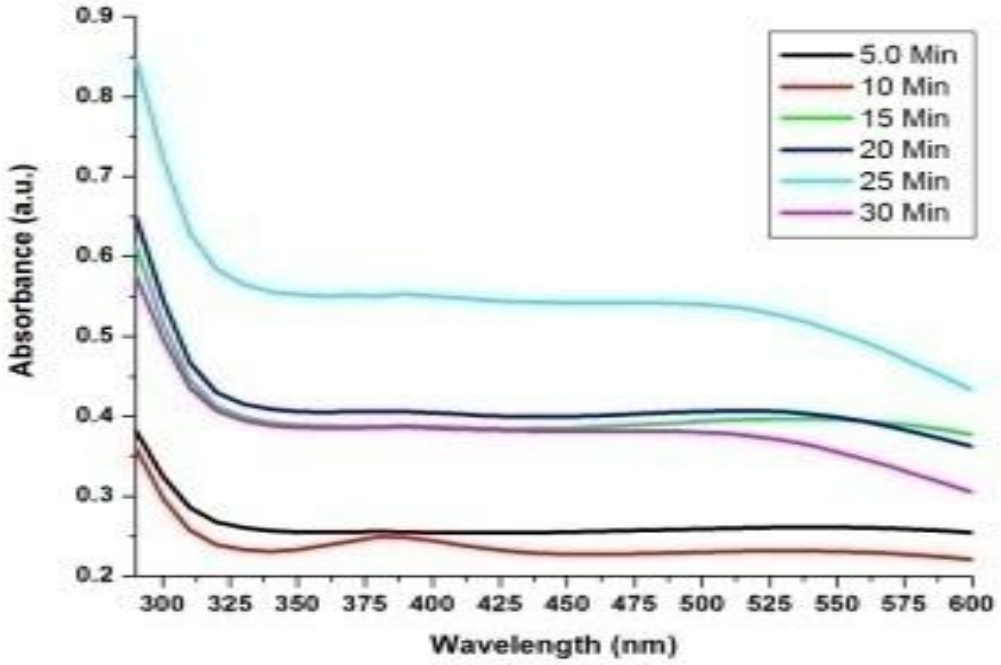

Figure 4.3.13: Absorption spectra of copper sulfide nanoparticles prepared using 0.5 g of the comnplex in 5.0 g HDA, 130 °C and at various time interval (5 – 30 minute)

The XRD pattern of copper sulfide nanoparticles prepared by drawing out aliquots at various time interval (5 – 30) minutes are given figure 4.3.14. The XRD pattern show five major peaks at 32.3°, 31.7°, 46.3°, 48.6° and 54.1° which can be indexed to orthorhombic $Cu_{1.97}S$ [JCPDS file card no. 20-0365] [98]. These results showed that the variation in time of the

reaction has less or no effect on the stoichiometry of the nanoparticles. Hence, although the time of the reaction was varied, the results show no changes in the phase composition of the prepared nanoparticles.

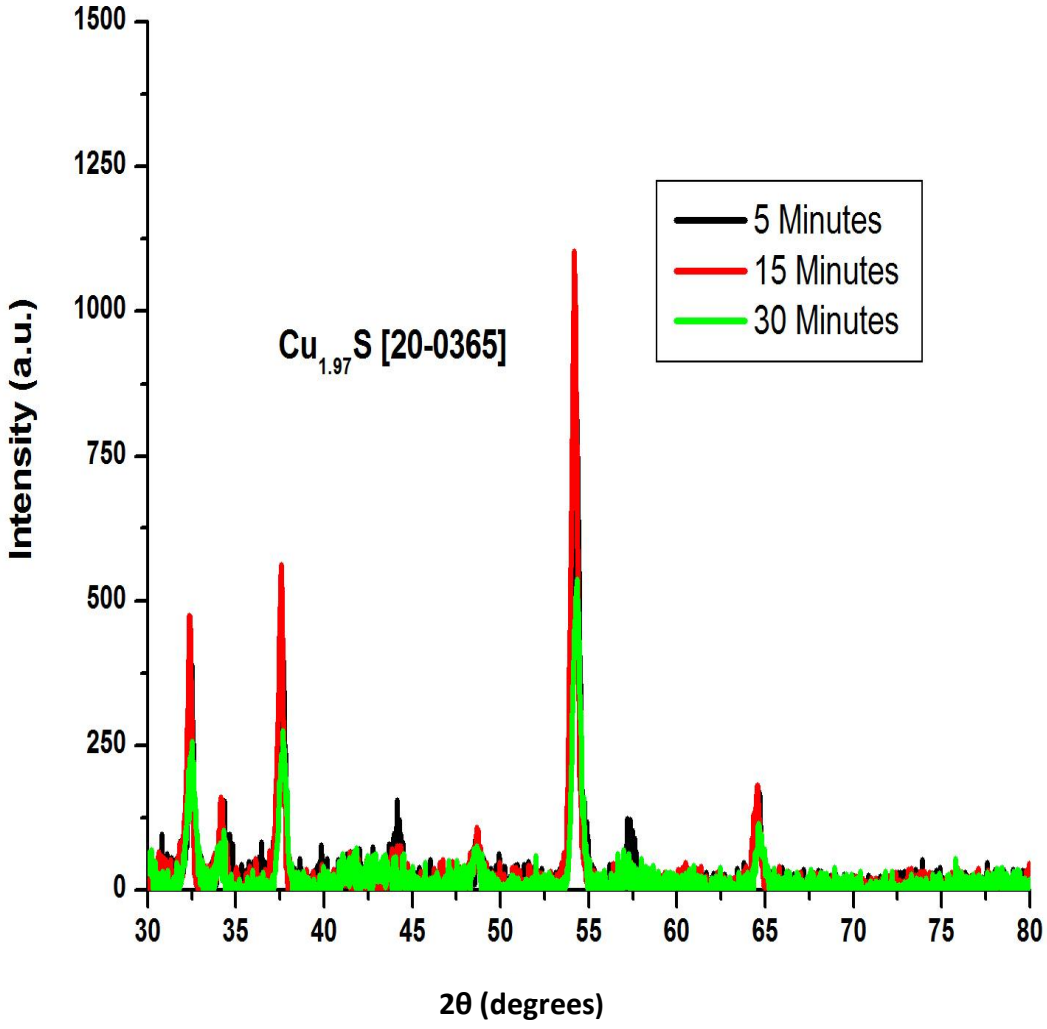

Figure 4.3.14: XRD pattern of copper sulfide nanoparticles prepared using 0.5 g of the comnplex in 5.0 g HDA, 130 °C and at various time interval (5 – 30 minute)

4.3.3 (b) Nanoparticles prepared using complex IV

Table 4.3.6 shows reaction conditions for the preparations of $Cu_xS_y$by drawing out aliquots at 5 minutes while all the other reaction conditions were kept the same.

Table 4.3.6:

*Variation of time for the preparation of Co_xS_y nanoparticlesusing complex **IV***

Surfactant (HDA) mass (g)	Complex **IV** mass (g)	Temperature °C	Time minutes
5.0	0.5	130	5
5.0	0.5	130	10
5.0	0.5	130	15
5.0	0.5	130	20
5.0	0.5	130	25
5.0	0.5	130	30

Figure 4.3.15 show the absorption spectra of copper sulfide nanoparticles prepared by drawing out aliquots at various time interval (5 – 30) minutes. The spectra revealed an excitonic at 280 nm and a band edge at 310 nm for nanoparticles prepared at 5 minutes. However, for nanoparticles prepared at 10 minutes, the spectra show an excitonic peak at 282.5 and a band edge at 314 nm. When the reaction was prolonged for time (15, 20, 25 and 30 minutes), the absorption spectra show a major peak at 287.5 nm. The band edge for nanoparticles prepared at 15, 20, 25 and 30 minutes were found at 317, 317, 317 and 320 nm respectively. This result is in good agreement with Ostwald ripening.

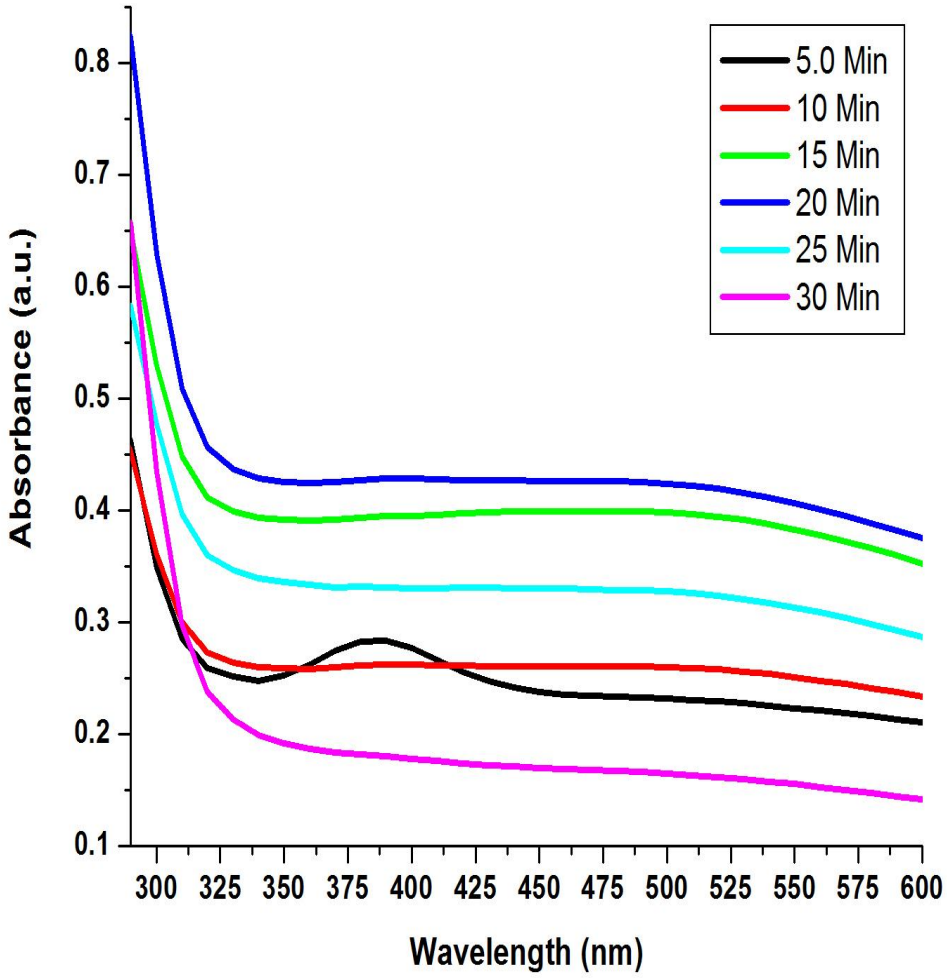

Figure 4.3.15: Absorption spectra of copper sulfide nanoparticles prepared using 0.5 g of the complex IV, in 5.0 g HAD, 130 °C and at various time interval (5 – 30 minutes)

4.4 Conclusion

Copper sulfide nanoparticles were successfully synthesized by thermal decomposition of diethylditocarbamate and tetramethylthiuram disulfide complexes (**III** and **IV**) in the presence of hexadecylamine capping agent. Optical properties revealed that the study of concentration on particles havemore effect on the size of the nanoparticles. This was confirmed by the

decrease in the band edge and emission maximum of the nanoparticle prepared by decreasing the concentration of the precursors. The TEM results show that the nanoparticle prepared were dominated by irregular sphere with average particle size of 2 – 30 nm. The results depict that size of the nanoparticles is more dependent on the concentration of the complex of the reaction. The XRD results show a cubic phase of $Cu_{1.97}S$ nanoparticles prepared by using complex **III** and complex **IV**.

The temperature of the reaction plays a very important role in controlling the reaction. The effect of temperature was investigated by duplicating the reaction at various temperatures at the same reaction conditions. The absorption spectra showed an increase in absorption maxima and band gap as the temperature was increased. This increase in absorption maxima and band gap is associated to an increase in particle size as the temperature was increased. The XRD pattern further confirmed that prepared nanoparticles were composed of mixture of $Cu_{1.8}S$ and orthorhombic $Cu_{1.97}S$ phases.

Time is very importantgift in life and is constantly changing. Any progress in life is measured in relation to time.Time of the reaction is an important parameter that has a profound effect on the reaction. The effect of time on the reaction was investigated by drawing out aliquots at 5 minutes interval of the reaction. The absorption spectra showed a decrease in absorption maxima and band gap. A decrease in absorption maxima and band gap is associated to a decrease in particle size of the prepared nanoparticles. The XRD pattern confirmed an orthorhombic $Cu_{1.97}S$ for nanoparticles prepared at various time intervals. These results confirmed that the variation in time has no observable effect on the stoichiometry of the prepared nanoparticle.

CHAPTER FIVE

CONCLUSION AND FUTURE WORK

5.1 Conclusion

Cobalt and copper sulfide nanoaparticles were successfully synthesized from cobalt and copper complexes of tetramethylthiuram disulfide (I, III) and diethyldithiocarbamate (II, IV). The effects of amount of the complexes, temperature of the reaction and time of the reaction on the growth of the cobalt and copper sulfide nanoparticles were investigated. The instigation of the concentration yield results that depicted that with decrease for precursor, the band edge decreases from their bulk. Hence, the band edges of the nanoparticles were blue shifted significantly to the bulk as the amount of the precursors were progressively decreased. This is related to the particles of the nanoparticles being decrease as amount of the precursor was decrease. This resulted to a decrease in the energy gap between valence and conduction band. The XRD pattern confirmed that the amount of the precursor has little or no significant effect on the composition of the nanoparticles as there was only one phase observed as the amount of the precursor was varied. The TEM images also confirmed the size and the shape of the nanoparticles. The TEM images showed a significant decrease in particle size as the amount of the precursor was decreased with various morphologies as the amount of the precursor were varied. The capping molecule and the amount of the precursor have a profound effect on the growth of the nanoparticles.

The effect of temperature was investigated by varying the temperatures of the reactions. The temperature was observed to be affecting size, morphology and the composition of the growth of the nanoparticles. The investigation of the temperature yield results that revealed the decrease in band edges of the copper sulfide nanoparticles prepared by gradually increasing the temperature of the reaction. This suggests that the particles size of the nanoparticles is decreasing in size with an increase in temperature of the reactions. This contradicts the literature, which reveals an increase in particles size with temperature [90]. This might be due to complex being relatively stable at this temperature range of this synthesis. The TEM

images confirmed irregular spheres with particle sizes decreasing with an increase in temperature. These nanoparticles could not dry out, hance the XRD technique could not be used to confirm the composition. However, copper sulfide nanoparticles show an increase in size with temperature. This was confirmed by an increase in band edge of the nanoparticles as the temperature of the reactions was increased. This is expected as the rate of the reaction increases with temperatures. The TEM images show showed irregular sphere, which to triangular and finally hexagonal images as the temperature is gradually increased. The XRD pattern confirmed a pattern of a mixture of $Cu_{1.8}S$ and orthorhombic $Cu_{1.97}S$.

The effect of time was also investigated by drawing out aliquots at 5 minutes interval. The time of the reaction is one of the most significant factors in the synthesis of the nanoparticles. The instigation of the time of the reaction yield results that depicted that with increase in time of the reaction, the band edge increases, but relatively at short wavelength to the bulk. Hence, the band edges of the nanoparticles were blue shifted significantly to the bulk. The results show that with an increase in the time of the reaction, the nanoparticles increases in their size through Ostwald ripening. The XRD patterns show one composition regardless of the variation in time of the reaction. These results confirmed the time of the reaction have little or no effect on composition of the nanoparticles.

5.2 Future works

Base on the conclusions of this study there are still some things one can study further in order to understand the effect of the conditions:

1. The investigation of the capping molecule on the growth of these nanoparticles and what is the role does it play for this preferred results.

2. Investigate the effect temperature at above 300 °C using the same complexes of cobalt, why could not dry out and understand the stoichiometry at various temperatures.

3. And also to observe the TEM images of these nanoparticles at various time intervals, how much do they increase at the selected intervals.

4. Improve the quality of the synthesized materials.

5.3 REFERENCES

1. Faraday, M., *Philos. Trans. R. Soc. London*. 147 (**1857**) 145.
2. Brus, L. E., J. Chem. Phys. 80 (**1984**) 4403.
3. Rao, C. N. R., Kulkarni, G. U., Thomas, P. J., Edwards, P. P., Chem. Eur. J. 29 (**2002**) 27.
4. Klimov, V. T., Semicinductorsaand metalnanocrystals. Synthesis, electronic and optical, Marcel Dekker, Inc, (**2004**).
5. Jorge, P., Martins, M. A., Trindade, T., Santos, J. L., Farahi, F. *Sensors* 7 (**2007**) 3489.
6. Murray, C. B., Kagan, C. R., Bawendi, M. G., *Annu. Rev. Mater. Sci*. 30 (**2000**) 545.
7. Murray, C. B., Sun, S., Gaschler, W., Doyle, H., Betley, T. A., Kagan C. R., *IBM J. Res. Dev*. 45 (**2001**) 47.
8. Rossetti, R., Ellison, J. L., Gibson, J. M., Brus, L. J., *J. Chem. Phys*. 80 (**1984**) 4464.
9. Henglein, A., *Chem Rev*. 89 (**1989**) 1861.
10. Weller, H., Koch, U., Gutierrez, M., Henglein, A., Ber. Bunsen-Ges. *Phys. Chem*. 91 (**1987**) 88.
11. Talapin, D. V., Rogach, A. L., Kornowski, A., Haase, M., Weller, H., *Nano. Lett*. 1 (**2001**) 207.
12. Hässelbarth, A., Eychmuller, A., Eichberger.R, Giersig, M., Mews, A., Weller, H., *J. Phys. Chem.* 97 (**1993**) 5333.
13. Zhou, H. S., Honma, I., Komiyama, H., Haus, J. W. *J. Phys. Chem*. 97 (**1993**) 895.
14. Zhou, H. S., Sasahara, H., Honma, I., Komiyama, H., Haus, J. W., *Chem. Mater*. 6 (**1994**) 1534.
15. Eychmüller, A., Hässelbarth, A., Weller, H., *J. Lumin*. 53 (**1992**) 113.
16. Kortan, A. R., Hull, R., Opila, R. L. Bawendi, M. G., Steigerwald, M. L., Carroll, P.J., Brus L.E., *J. Am. Chem. Soc.* 112 (**1990**) 1327.

17. Hoener, C. F., Allan, K. A., Bard, A. J., Campion, A., Fox, M. A., Mallouk, T. E., Webber, S. E., White, J. M., *J. Phys. Chem.* 96 (**1992**) 3812.

18. Mews, A., Eychmuller, A., Giersig, M., Schoob, D., Weller, H., *J. Phys. Chem*. 98 (**1994**) 934.

19. Wang, Y., Herron, N., *J. Phys. Chem*. 91 (**1987**) 257.

20. Cassagneau, T., Hix, G. B., Jones, D. J., Maireles-Torres, P., Romari, M., Roziere, J., *J. Mater. Chem.* 4 (**1994**) 189.

21. Abe, T., Tachibana, Y., Uematsu, T., Iwamoto, M., J. *Chem. Soc., Chem. Commun*. (**1995**) 1617.

22. Korgel, B. A., Monbouquette, G., *J. Phys. Chem.* 100 (**1996**) 346.

23. Choi, K. M., Shea, K. J., *J. Phys. Chem*. 98 (**1994**) 3207.

24. Nirmal, M., Murray, C. B., Bawendi, M. G., *Phys. Rev. B* 50 (**1994**) 2293.

25. Shinojima, H., Yumoto, J., Uesugi, N., Omi, S., Asahara, Y., *Appl. Phys. Lett*. 55 (**1989**) 1519.

26. Steigerwald, M. L., Alivisatos, A. P., Gibson, J. M., Harris, T. D., Kortan, R., Muller, A. J., *J. Am. Chem. Soc*. 110 (**1988**) 3046.

27. Stuczynski, S. M., Brennan, J. G., Steigerwald, M. L., *Inorg. Chem*. 28 (**1989**) 4431.

28. Wong, K. K. W., Mann, S., *Adv. Mater*. 8 (**1996**) 928.

29. Thayer, A. M., Steigerwald, M. L., Duncan, T. M., Douglass, D. C., *Phys. Rev. Lett*. 60 (**1988**) 2673.

30. Mohapatra, M.,Anand.*International Journal of Engineering, Science and Technology*. 2(**2010**) 127.

31. Mitroova, Z., Melnikova, L., Kovac, J., Vavra, I., Timko, M. *Nano Con.* 9 (**2011**) 21.

32. Murray, C. B., Norris, D. J., Bawendi, M. G., *J. Am. Chem. Soc.* 115 (**1993**) 8706.

33. Aliv, H. T., Shiang, J. J., Kadavanich, A. V., *J. Phys. Chem*. 99 (**1995**) 1741.

34. Manna, L., Scher, E. C., Alivisatos, A. P., *J. Am. Chem. Soc*. 122 (**2000**) 12700.

35. Dabbousi, B. O., Rodriguez-Viejo, J., Mikulec, F. V., *J. Phys. Chem. B* 101 (**1997**) 9463.

36. Trindade, T., O'Brien, P., Zhang, X-M., Motevalli, M., *J. Mater. Chem*. 7 (**1997**) 1011.

37. Trindade, T., Monteiro, O. C., O'Brien, P., Motevalli, M., *Polyhedron* 18 (**1999**) 1171.

38. Lee, S.-M., Ju, Y.-w., Cho, S.-N.,Cheon, J., *J. Am. Chem. Soc*. 124 (**2002**) 11244.

39. Cumberland, S. L., Hanif, K. M., Javier, A., Khitrov, G. A., Strouse, G. F., Woessner, S. M., Yun, C. S., *Chem. Mater*. 14 (**2002)** 1576.

40. Malik, M. A., O'Brien, P., Revaprasadu, N., *Chem. Mater*. 14 (**2002**) 2004.

41. Peng, Z. A., Peng, X., *J. Am. Chem. Soc*. 123 (**2001**) 183.

42. Trindade, T.,*Curr. Opin. Solid State Mater. Sci*. **(2002**) 347.

43. Guzelian, A. A., Banin, U., Kadavanich, A. V., Alivisatos, A. P., *Appl. Phys. Lett*. 69 (**1996)** 1432.

44. Treece, R. E., Macala, G. S., Rao, L., Franke, D., Eckert, H., Kaner, R.B., *Inorg. Chem.* 32 (**1993**) 2745.

45. Kher, S. S., Wells, R. L., *Chem. Mater*. 6 (**1994**) 2056.

46. Wells, R. L., Aubuchon, S. R., Kher, S. S., Lube, M. S., White, P. S., *Chem. Mater*. 7 (**1995**) 793.

47. Uchida, H., Curtis, C. J., Nozik, A. J., *J. Phys. Chem*. 95 (**1991**) 5382.

48. Byrne, E. K., Parkanyi, L. K., Theopold, H., *Science.* 241 (**1988**) 332.

49. Douglas, T., Teopold, K. H., *Inorg. Chem.* 30 (**1991**) 594.

50. Goel, S. C., Chiang, M. Y., Buhro, W. E., *J. Am. Chem. Soc*. 112 (**1990**) 5636.

51. Klinowski, J., Barrie, P. J., *Recent Advances in Zeolite Science. Elsevier, Amsterdam* (**1990).**

52. Zhan, J. H., Yang, X. G., Zhang, W. X.,Wang, D. W.; Xie, Y; Qian, Y. T., *J.Mater. Res*., 15 (**2000)** 629.

53. Gautam, U. K., Rajamathi, M., Meldrum, F.C., Morgan, P., Seshadri, R.,*J. Chem. Soc., Chem. Commun*., (**2001**) 629.

54. Wang, W., Yan, P., Liu, F., Xie, Y., Geng, Y., Qian, Y., *J.Mater. Chem*., 8 (**1998)** 2321.

55. Li, B., Xie, Y., Huang, J., Qian, Y., *Adv. Mater*., 11 (**1999**) 1456.

56. Xiao, J., Xie, Y., Xiong, Y., Tang, R., Qian, Y., *J. Mater. Chem*., 11 (**2001**) 1417.

57. Komarneni, S., D'Arigo, M. C., Leonelli, C.,Pellacani, G. C., Katsuki, H., *J. Am. Ceram. Soc*., 81 (**1998**) 3041.

58. Yoffe, A. D. *Adv. Phys.* 42 (**1993**) 173.

59. Srouji, F.; Afzaal, M.; Waters, J.; O`Brein, P., *Chem. Vap. Deposition*. 11 (**2005**) 91.

60. Kemmler, M.; Lazell, M.; O`Brein, P.; Otway, D. J.; Park, J-H.; Walsh, J. R., *Journal of Materials Science: Materials in electronics*.13 (**2002**) 531.

61. Trindade, T., O'Brien, P., *Adv. Mater*. 8 (**1996**) 161.

62. Brus, L. E. *J., Chem. Phys.* 79 (**1983**) 5566.

63. Service, R. F., *Science* 271 (**1996**) 920.

64. Weisbuch, C., Vinter, B., *Acedemic Press, San Diego, U.S.A*. (**1991**).

65. Colvin, V. L., Schlamp, M. C., Alivisatos, A. P., *Nature* 370 (**1994**) 354.

66. Brus, L., *Appl. Phys. A* 53 (**1991**) 465.

67. Peyghambarian, N., Hanamura, E., Koch, S. W., Masumoto, Y. and Wright, E. M., *Institute of Physics Publishing, Bristol, U.K*. (**1996**) 395.

68. Hodes, G., Albu-Yaron, A., Decker, F., Motisuke, P., *Phys. Rev. B* 36 (**1987**) 4215.

69. Weller, H., *Ngew. Chem. Int. Ed. Engl.* 32 (**1993**) 41.

70. Thorn, G. D., Ludwig R. A., *Amsterdam, Elsevier Publishing* Co. (**1962**).

71. Ivanov, A. V., Antzutkin, O. N., *Top Curr Chem.* 246 (**2005**) 271.

72. Shaheen, F., Badshah, A., De Vos, D., Mirva, B., Journal *of Organometallic Chemistry*. 692 (**2007**) 3019.

73. Pandeya, K. B., Singh, R., Mathur, P. K., Singh. R. P., *Transition Met. Chem*. 11 (**1986**)340.

74. Macias, B., Villa, M. V., Rodrı´guez-Gallego, M. R., *Transition Met. Chem.* 20 (**1995**) 347.

75. Macias, B., Criado, J. J., Villa, M. V., Rodrı´guez, J. L., Castillo, M., *Polyhedron* 12 (**1993**) 2791.

76. Golding, R. M., Rae, A. D., Ralph, B. J., Sulligoi, L., *Inorg. Chem.*10 (**1974**) 2499.

77. Ewart, D. K., Hughes, M. N., *Adv. Inorg. Chem.* 36 (**1991**) 103.

78. Radanovic, D. J.; Matovic, Z. D.; Mileyic, V. D., *Transition Met.Chem*. 21 (**1996**) 169.

79. Baba, I.; Farina, Y.; Kassim, K.; Othman, A. H.; Razak, I. A.; Fun, H. K.; Ng, S. W., .*Act Crystallogr., Sect. E* 57 (**2001**) 55.

80. O'Brien, P.; Walsh, J. R.; Watson, I. M.; Hart, L.; Silva, S. R. P., *J. Cryst. Growth.* 167 (**1996**) 133.

81. Nair, P.; Revaprasadu, N.; Radhakrishnan, T.; Kolawole, G. A., *J. Mater. Chem.* 11 (**2001**) 1555.

82. Cleverty, J. A. M.; Morrison, N., *J.Chem. Sot., Dalton Trans.* (**1976**) 2169.

83. Barrientos, C. F.; Contreras, J. G., *An. Quim.*75 (**1979**) 245.

84. Brinkhoff, H. C.; Dautzenberg, J. M. A., *Rec. Trav. Chim*. 91 (**1972**) 117.

85. Contreras, J. G.; Gnecco, J. A.; Carbacho, H. V., *J. Coord. Chem.* 19 (**1989**) 371.

86. Steggerda, J. J.; Cras, J. A.; Willemse, J., *Rec. Trav. Chim*. 100 (**1981**) 41.

87. Ojima, I.; Onishi, T.; Iwamoto, T.; Inamoto, N.; Tamaru, K., *Inorg. Nucl. Chem. Lett.* 6 (**1970**) 65.

88. Ramasamy, K.; Maneerprakorn, W.; Malik, M. A.; O`Brien, P., *Phil. Trans. R. Soc. A.* 368 (**2010**) 4249.

89. Bao, S.-J.; Li, C. M.; Guo, C.-X.; Qiao, Y., *J. Power Source.*180 (**2008**) 676.

90. Cheng, Z., Wang, S., Wang, Q., Geng, B., *Cryst. Eng. Comm*. 12 (**2010**) 144.

91. Ramasamy, K., Maneerprakorn, W., Malik, M. A., O`Brien, P., *Phil. Trans. R. Soc.* A. 368(**2010**) 4249.

92. Bao, S.-J.; Li, Y., Li, C. M.; Bao, Q.; Lu, Q., Guo, J. *J. Crystal Growth and Design.*.8 (**2008**) 3745.

93. Moloto, N., Revaprasadu, N., Musetha, P. L., Moloto, M. J.,Journal of Nanoscience and Nanotechnology. 9 (**2008**)1.

94. Lee, S-M., Cho, S-N., Cheon, J., *Adv. Mater*. 15 (**2003**) 441.

95. Moloto, N., Moloto, M. J., Conville, N. J., Ray, S. S, *Journal of Crystal Growth.* 324 (**2011**) 41.

96. Lou, W., Chen, M., Wang, X., Liu, W., *J. Phys. Chem. C*. 111 (**2007**) 9658.

97. Wu, C., Yu, S-H., Chen, S., Liu, G., Liu, B., *J. Mater. Chem*. 16 (**2006**) 3326.

98. Zao, Y., Pan, H., Lou, Y., Qiu, X., Zhu, J., Burda, C. *J. Am. Chem. Soc*. 131 (**2009**) 4253.